TRIBOLOGICAL COMPARISON OF MATERIALS

By

Bing Shi

RECOMMENDED:

Thomas Kuh

E. Mianne Rehard

Lawrence K Duffy

Advisory Committee Co-chair

Advisory Committee Co-chair

Tom Clausen

Chair, Department of Chemistry and Biochemistry

APPROVED:

John Bradwon

Dean, College of Natural Science and Mathematics

Susan M. Henrichs

Dean of the Graduate School

December 15, 2004

Date

TRIBOLOGICAL COMPARISON OF MATERIALS

A

THESIS

Presented to the Faculty

Of the University of Alaska Fairbanks

In Partial Fulfillment of the Requirements

For the Degree of

DOCTOR OF PHILOSOPHY

By

Bing Shi, M.S.

Fairbanks, Alaska

December 2004

Abstract

Approximately 600,000 total joint replacement surgeries are performed each year in the United States. Current artificial joint implants are mainly metal-on-plastic. The synthetic biomaterials undergo degradation through fatigue and corrosive wear from load-bearing and the aqueous ionic environment of the human body. Deposits of inorganic salts can scratch weight-bearing surfaces, making artificial joints stiff and awkward. The excessive wear debris from polyethylene leads to osteolysis and potential loosening of the prosthesis. The lifetime for well-designed artificial joints is at most 10 to 15 years. A patient can usually have two total joint replacements during her/his lifetime. Durability is limited by the body's reaction to wear debris of the artificial joints. Wear of the artificial joints should be reduced.

A focus of this thesis is the tribological performance of bearing materials for Total Replacement Artificial Joints (TRAJ). An additional focus is the scaffolds for cell growth from both a tissue engineering and tribological perspective. The tribological properties of materials including Diamond-like Carbon (DLC) coated materials were tested for TRAJ implants. The DLC coatings are chemically inert, impervious to acid and saline media, and are mechanically hard. Carbon-based materials are highly biocompatible. A new alternative to total joints implantation is tissue engineering. Tissue engineering is the replacement of living tissue with tissue that is designed and constructed to meet the needs of the individual patient. Cells were cultured onto the artificial materials, including metals, ceramics, and polymers, and the frictional properties of these materials were investigated to develop a synthetic alternative to orthopedic transplants.

Results showed that DLC coated materials had low friction and wear, which are desirable tribological properties for artificial joint material. Cells grew on some of the artificial matrix materials, depending on the surface chemistry, wettability, morphology, microstructure etc. The dry, lubricated, and cell culture friction tests showed that bovine serum albumin solution and culture media performed as lubricants. Frictional properties varied. Glass and TR-2 (PET, polyethylene terephthalate) showed good cell culture results and low friction. Both are suitable materials, both as artificial joint implant coatings and as substrates for preparing total joint implants via tissue engineering.

TABLE OF CONTENTS

LIST OF FIGURES

LIST OF TABLES

LIST OF APPENDICES

ACKNOWLEDGEMENTS

Although my name is on this thesis, it would not have been written had it not been for the support and encouragement of many people. I would like to start by expressing my gratitude to my committee members: Drs Lawrence Duffy, Hong Liang, Thomas Kuhn, and Dianne Rekow for all of their encouragement, mentorship, and patience. I am grateful for Dr. Duffy's support and the guidance. Your optimism has been a windfall for me. I am always amazed by your mentorship. Many thanks to Dr. Liang for giving me the chance to work on such a challenging research, supporting, and guiding my research down the most productive paths. Your devotion to research is what I admire. Dr. Kuhn, you have been a tremendous source of knowledge and mentorship. I thank you for your encouraging words, support, and professional guidance. I thank Dr. Rekow for the guidance of providing me the advices on the biomaterials, and on the thesis writing. Your experience of the research in the similar area has been such a useful source for me. I also would like to acknowledge the Department Chairs: Drs Thomas Clausen, Douglas Goering, and Jonah Lee for giving me the opportunity to study in your departments.

Results shown in the part of the study on Total Replacement of Artificial Joints are derived from work performed at Argonne National Laboratory. Argonne is operated by The University of Chicago for the U.S. Department of Energy under contract W-31-109-Eng-38. I would like to thank Drs George Fenske, Ali Erdemir, Oyelayo Ajayi, Robert Erck, and all the other individuals in the Tribology Section of Argonne National Lab. I want to thank Dr. Yong Yue and Kraipat Cheekachorn too. Without you I could not finished my job in Argonne.

I acknowledge Dr. John Keller, Dr. Ken Severin, Quinton Costello (Rest in Peace), Tim Howe, Sheila Chapin, Emily Reiter, Marlys Schneider, Sarah Hall, all the students in material science group, and all the staff at the interlibrary loan department. I would also like to thank Neal and Lisa Matson for helping me whenever and whatever I need. A friend in need is a friend indeed.

Thanks to my family, especially to my mother. You are the reason I am. I love you.

There are many other individuals who have helped me in large and small ways I did not list their names here. I hope they know how much I appreciate their help.

Chapter 1

Introduction

1.1 Overview of bioengineering

The cost of treating patients with organ or tissue failure accounts for approximately 50 percent of total health-care costs in the United States annually (Langer et al. 1993). Approximately 600,000 total joint replacement surgeries, including more than 120,000 artificial hip joints, are performed each year in the United States. It is estimated that 85 to 95% of these will still be functioning after ten years (McLaughlin 1994; Ritter et al. 1995). Artificial joint replacement is needed when the cartilage that lines the joint deteriorates, resulting in bones grinding against each other causing pain (Figure 1.1). Non-surgical treatments, such as anti-inflammatory drugs, walking aids, and support braces do not offer relief.

Joint replacement surgery is most commonly performed for hips, knees, and shoulders (Figure 1.2), although toe, finger, and elbow joints have been successfully replaced. Most artificial joint replacements are designed to remove the diseased areas of the joint and replace them with metal-plastic implants designed specifically to restore that joint's function and stability.
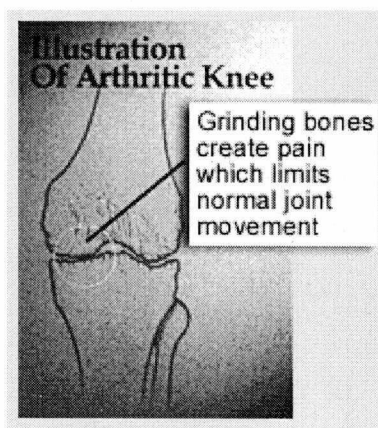
Figure 1.1 Knee joint deterioration

(Biomet 2001)
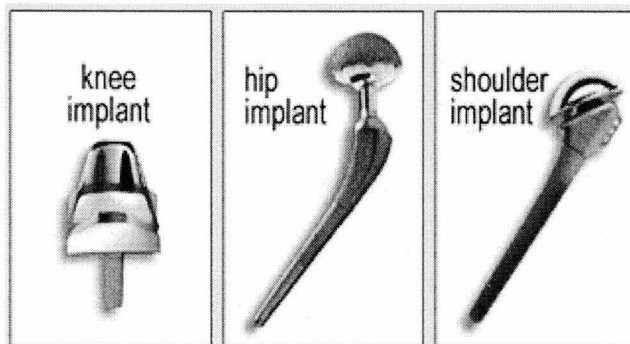
Figure 1.2 Joint replacements

(Biomet 2001)

The materials used in artificial joints, such as stainless steel, titanium alloy, polymers, and ceramic composites, undergo degradation through fatigue and corrosive wear from load-bearing and the aqueous ionic environment of the human body. At the same time, deposits of inorganic salts can scratch weight-bearing surfaces, making artificial joints stiff and awkward. The increasing life expectancy of an aging population, and the need to surgically treat arthritis in increasing numbers of young patients, are placing greater demands on the durability of artificial joints. At present the lifetime for well-designed artificial joints like hip joints is at most 10 to 15 years. A patient will usually have two total joint replacements during his/her lifetime, each requiring further revision and losing of some of their own remaining sound bone.

Scientists conduct research to improve the quality of artificial joints by 1) designing new materials; 2) designing appropriate microstructure of materials; 3) designing appropriate shape and morphology; and 3) investigating the synovial fluid's effects on artificial joints and durability (Ritter et al. 1995; Long et al. 1998; Wang et al. 1997; Dicarlo et al.1992; Kossovsky 1991; Collier et al. 1991; Shi et al. 2003). Over the past several years, studies have also been carried out to examine possible connections among tribology, the mechanism of normal joint function, and joint degeneration such as seen with osteoarthritis (Stachowiak et al.; 1994; Furey et al.1997).

A new alternative to total joint implantation is becoming available. Tissue engineering is the replacement of living tissue with tissue that is designed and constructed to meet the needs of the individual patient (Vacanti et al. 1999). Tissue engineering integrates the fields of biomaterials, cell biology, biochemistry, and clinical medicine. The goal is to create substitutes that functionally repair damaged or diseased tissues and organs.

Tissue culture is used to develop a synthetic alternative to orthopedic transplants, such as bone, ligament, and cartilage. Once implanted, the presence of cells and growth factors initiate bone regeneration throughout the pore network. As regeneration continues, the polymer matrix will be slowly resorbed by the body and the implant site will be filled with newly regenerated tissue. Several examples are illustrated: engineered bone (Figure 1.3), engineered ligament

(Figure 1.4), engineered cartilage (Figure 1.5), and cell culture (Figure 1.6). In studies examining cell growth on these matrices, osteoblast cell lines have been utilized, as well as bone cells isolated from rat calvaria to create model systems for cell growth on bio-erodible materials. Figure 1.6 shows osteoblasts growing on the surface of the microsphere matrix. It is interesting to note that the cells are growing in a circumferential pattern due to the structure of the matrix.
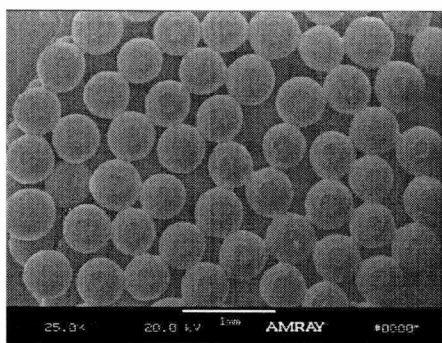
Figure 1.3 Tissue engineered bone

(Laurencin 2001)
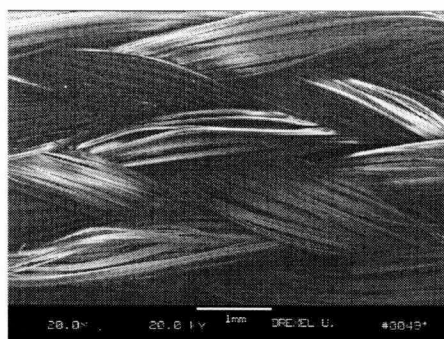
Figure 1.4 Tissue engineered ligament

(Laurencin 2001)
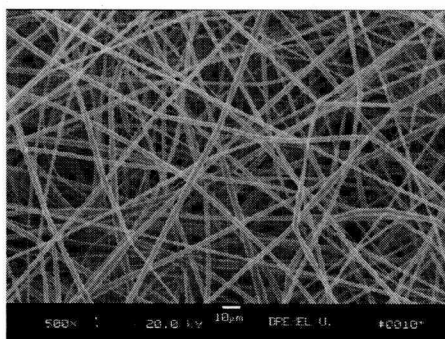
Figure 1.5 Tissue engineered cartilage

(Laurencin 2001)
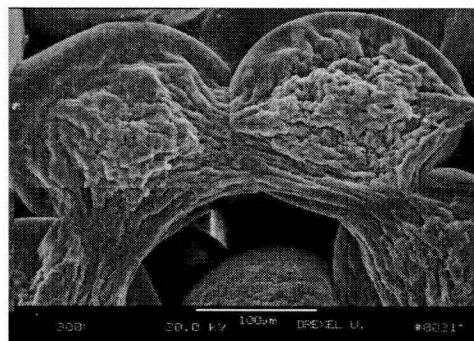
Figure 1.6 Cell culture

(Laurencin 2001)

Once the biomaterials have been developed and are accepted by the human body, patients will not need major surgery to change total artificial joints. Instead, they will just need a minor

surgery for implantation of a small piece of polymer inside the deteriorated area and will no longer need to change the artificial joints every 10-15 years. Patients will also save money because the lifetime of artificial joints will be longer.

These advances are important for an aging population. More organs, joints, and other critical body parts will wear out and need to be replaced if people are to maintain their quality of life. Biomaterials will play a major role in replacing or improving the function of every major body system (skeletal, circulatory, nervous, etc.). Some common implants used already include orthopedic devices such as total knee and hip joint replacements, spinal implants, and bone fixators; cardiac implants such as artificial heart valves and pacemakers; soft tissue implants such as breast implants and injectable collagen for soft tissue augmentation; and dental implants to replace teeth/root systems and bony tissue in the oral cavity. Biomaterials and implant research will continue to concentrate on serving the needs of medical device manufacturers and recipients. Development of technologies will meet those needs through the design of materials with strength, suitable shape, function, and behavior. Future biomaterials should incorporate biological factors (such as bone growth) directly into an implant's surface to improve biocompatibility and bioactivity. New projects will be directed at materials development for improved mechanical integrity, corrosion resistance, and biocompatibility.

1.2 Tribology and biotribology

Tribology is the study of friction, wear, and lubrication. It is the science of interacting surfaces in relative motion. It is an interdisciplinary subject that involves physics, chemistry, material science, mathematics, mechanics, and rheology. Tribology was first defined by a United Kingdom government committee in 1966 as the 'science and technology of interacting surfaces in relative motion and practices related thereto' (Dowson 1979). Friction, wear, and lubrication has been studied for a long time. Chinese pictographs dating back to the middle of the second millennium BC show wheeled chariots. Pottery wheels using fired porcelain cups as bearings

appeared in China about 1500 BC, and by 400 BC Chinese bearing technology had developed sophisticated lubricated bronze bearings for use on war chariots (Williams 1994).

1.2.1 Friction

Friction is defined as the resistance to motion that occurs when attempting to slide one surface over another in contact with it (Andersen 2004). Static friction is the value of the limiting friction just before slipping occurs. Kinetic friction is the value of the limiting friction after slipping has occurred.

The first published scientific study of friction (Amontons 1699) revealed certain 'laws' of friction (Figure 1.7) which still form the basis for the analysis of many sliding contacts (Torrance 2004).
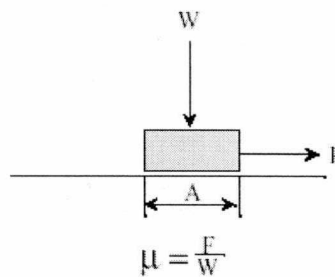
Figure 1.7 Amontons' laws of friction (Amontons 1699)

For dry friction, 1) the force of friction is directly proportional to the applied load (Amontons 1st Law); 2) the force of friction is independent of the apparent area of contact (Amontons 2nd Law); and 3) kinetic friction is independent of the sliding velocity (Coulomb's Law).

For fluid film lubrication friction, Reynolds' steady state equation is used

$$F \propto \frac{v\eta}{D}$$

The frictional (drag) force, F, is proportional to both the sliding velocity, v, and the bulk fluid viscosity, η, and inversely proportional to the film lubricant thickness, D. The

hydrodynamic theory breaks down below a critical thickness threshold that is expressed in the Stribeck-Curve (Figure 1.8). There are three regions in the Stribeck-Curve: boundary lubrication (BL), mixed lubrication (ML) and elasto-hydrodynamic lubrication (EHL). Under boundary lubrication, dry contact is excluded from boundary lubrication. Characteristic for boundary lubrication is the absence of hydrodynamic pressure. One hundred percent of the loading is carried by the asperities in the contact area, protected by adsorbed molecules of the lubricant and/or a thin oxide layer. Mixed lubrication is the intermediate region between boundary lubrication and hydrodynamic lubrication. A hydrodynamic pressure is built up in the lubricant when the speed increases. Characteristic of mixed lubrication is that the loading is carried by a combination of the hydrodynamic pressure and the contact pressure between the asperities of both surfaces. Under EHL, the hydrodynamic pressure increases such that the surface asperities are completely separated by a lubricant film. Characteristic for hydrodynamic lubrication is that the load and hydrodynamic pressure are in equilibrium (Overney 2004).
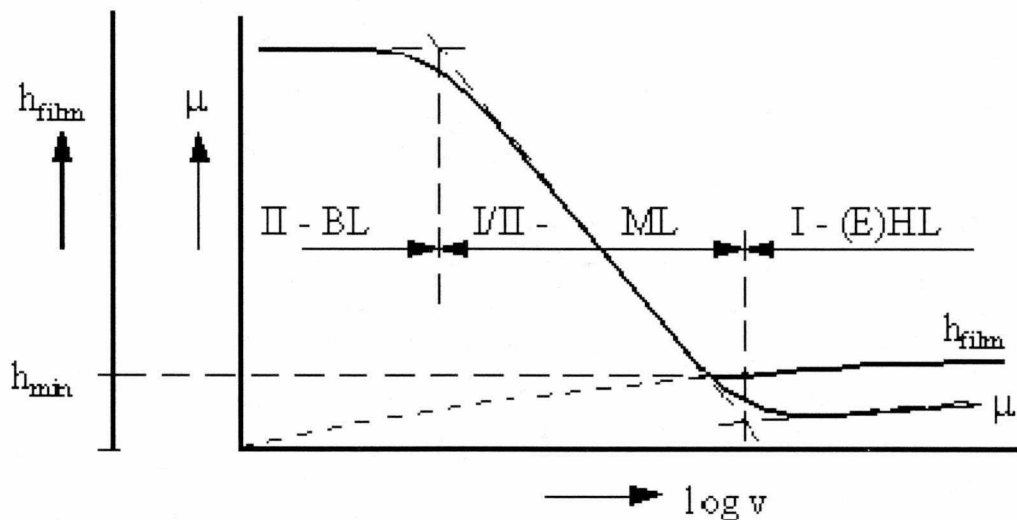
Figure 1.8 Stribeck-Curve (Overney 2004)

I, Elasto-Hydrodynamic Lubrication; I/II, ML; II: boundary lubrication

The coefficient of friction (μ) is the ratio of the limiting friction to the normal reaction between the sliding surfaces, $\mu = F/W$ where F=friction force and W=the normal load. It is constant for a given pair of surfaces.

1.2.2 Wear

Wear is defined as the damage to a surface that generally involves progressive loss of material and is due to relative motion between that surface and a contacting substance or substances. Plastic shear deformation of a surface is one sign of wear. This is typically followed by shear fraction, which leads to a scale-like topography. Wear can also be accompanied by a number of other surface damage modes such as extrusion, chip formation, tearing, brittle fracture, etc. (Ekberg 1997).

The main mechanisms of wear between the surface and interface are 1) abrasive wear which occurs when asperities of a rough, hard surface or hard particles slide on a softer surface and damage the interface by plastic deformation or fracture; 2) adhesive wear which occurs when two nominally flat solid bodies are in sliding contact; 3) fatigue wear which occurs when repeated loading and unloading circles are applied to the materials and induce the formation of subface or surface cracks, which finally will result in the breakup of the surface; 4) chemical and corrosive wear which occurs when sliding takes place in a corrosive environment; 5) impact wear by erosion, which occurs due to jets and streams of solid particles, liquid droplets, and implosion of bubbles formed in the liquid and by percussion from repetitive solid body impacts; and   6) fretting wear and fretting corrosion which occur where low-amplitude oscillatory motion in the tangential direction takes place between contacting surfaces which are nominally at rest (Bhushan 2002; Anonymous 1955; Hurricks 1970; Waterhouse 1981; Waterhouse 1992). Combinations of these mechanisms are involved for biological systems such as articular cartilage (Furey 1986).

1.2.3 Lubrication

Lubrication is the introduction of a substance between the contact surfaces of moving parts to reduce friction and to dissipate heat. A lubricant may be oil, grease, graphite, or any

substance-gas, liquid, semisolid, or solid - that permits free action of mechanical devices and prevents damage by abrasion and 'seizing' of metal or other components through unequal expansion caused by heat. In machining, process lubrication also functions as a coolant to forestall heat-caused deformities. The lubricant regimes are listed in the order of decreasing lubricant film thickness (Table 1.1, Torrance 2004).

Table 1.1 Regimes of Lubrication (Torrance, 2004)

Type of Lubrication	Film thickness	Film formed by	Features
Hydrodynamic lubrication	1 - 100 mm	Oil dragged	Moderate-high speed Conformal contact.
Hydrostatic lubrication	1 - 100 mm	Oil pumped into contact.	Any speed Conformal contact.
Elastohydrodynamic lubrication	0.1 - 1 mm	Oil dragged into contact.	Moderate-high speed Concentrated contact.
Boundary lubrication	1 - 100 nm	Oil reacts, or absorbs, & debris	Low speed/ High load.
Dry friction	0 – 1 mm	No oil. (oxide, debris)	

The study of tribology leads to the development of strategies to save energy and reduce friction between most parts of machines or heads and disks. Tribology is not only important to industry, it also affects day-to-day life. In some other situations, such as the friction between an icy road and a wheel of a vehicle, the floor and a shoe, and the bare foot and the surface of the tub, a higher friction is desired. In other situations friction should be controlled within a range, such as in a polishing process or with the strings of a musical instrument. Each movement of the human body is full of friction, even before one starts to move. Static friction must be overcome to start the movement.

An addition to the traditional research on tribology, microtribology/nanotribology research and biotribology research are growing areas of interest. Increasingly, tribology research is focused on the wear of dental materials and the friction in joints and artificial joints.

1.2.4 Biotribology

When tribology is used to study a biological system, it is called biotribology. Biotribology investigates tribology of materials in artificial hip and knee joints, the mechanism of lubrication and wear, the methods of *in vitro* simulation and testing, biocompatibility and biological reactions to wear products. It contributes to standardizing of *in vitro* testing and simulation, novel low wearing designs, and developing biomaterials for bearing surfaces in total artificial joints.

Biotribology is a new field in the discipline of tribology. It describes the study of friction, wear, and lubrication in biological systems such as synovial joints (the human hip and knee, jaw, and spine). Tribology of biomaterials is the study of how materials work and fail in a living body, which aims to gather information about friction, adhesion, lubrication, and wear of biological systems and to apply this knowledge to develop products. Compared with traditional tribology, biotribology is more complex since it includes other fields such as biophysics, biochemistry, biomaterials, biomechanics, and pathology.

Nature produces the best system in tribology in the healthy human body. An example is that the friction coefficient of the knee joint is as low as 0.002. The friction coefficient of ice on ice is 0.03. Natural tribological systems have served as models for the artificial ones. Artificial tribosystems of humans have been investigated for more than 150 years. Tribological process in a movable joint involves the friction and wear of the contacting surfaces, such as the articular cartilage, and the lubrication by the surrounding medium such as synovial fluid. Higher friction will cause the local temperature to increase slightly. Lower friction in the joint is expected to protect the joints and also make the movement easier. Lower wear of the cartilage is very important. Once there is serious wear, further deterioration results in osteoarthritis, a non-inflam

arthritis (Tracey 2002, Mow et al. 1980). Wear debris can illicit the body's inflammatory response, creating inflammatory arthritis and/or bone resorption. Since osteolysis, dissolution or degeneration of bone tissue through disease, with artificial joint use is due to wear debris, elimination of wear debris would be beneficial. More recent biotribology topics of active study have included the wear of human dental tissues and restorative materials, the tribological behavior of synovial joints and their replacement, the lubrication by plasma of red blood cells in narrow capillaries, the wear of replacement heart valves, the wear of screws and plates in and on bone in fracture repair, the tribology of skin and the friction of hair, biosensors, and artificial fingers.

1.3 Biomaterials

1.3.1 Introduction

A biomaterial is a natural or synthetic material such as a polymer or metal that is suitable for introduction into living tissue, especially as part of a medical device such as an artificial heart valve or joint. Any natural or synthetic material that interfaces with living tissue or biological fluids may be classified as a biomaterial (Williams, 1987). Biomaterials are used to restore form and function. Many metals, ceramics, and polymers are being used, especially in the joint replacements without being biodegradable. With only very few exceptions, biomaterials are synthetic and intended to be permanent implants that substitute for diseased or traumatized tissues (Stupp 2001). Dr. Stupp (2001) pointed out that the main objective in biomaterials research has become the design of materials that can interact specifically with the biological environment for a given purpose. Some biomaterials are considered as temporary 'anchoring scaffolds' on which specific types of cells can colonize and elaborate three-dimensional tissues. The objective of many is to regenerate the missing or dysfunctional tissues by providing a biodegradable substrate. Others materials, such as ceramics, polymers, and metals used in artificial joint replacements, restore the functions but do not generate tissues. Another objective is to use materials as vehicles to deliver large and small molecules to specific tissues in order to restore normal physiological

function. Biomaterials improve the quality of life for an ever increasing number of people each year. This increasing demand arises from an aging population with higher quality of life expectations.

1.3.2 Classifications

Biomedical materials can be divided roughly into three main types governed by the tissue response. Inert (more strictly, nearly inert) materials which elicit minimal or no tissue response; active materials which encourage bonding to surrounding tissue with new bone growth being stimulated; and degradable, or resorbable materials which are incorporated into the surrounding tissue or may even dissolve completely over a period of time. Metals are typically inert, ceramics may be inert, active or resorbable, and polymers may be inert or resorbable (Azom.com et. al. 2004).

Biomaterials can be polymers, metals, inorganic compounds, ceramics, and their composites. Progress has been made in the development of biomaterials due to advances in molecular and cell biology over the past two decades. Early studies dealt with the selection and characterization of well-established synthetic materials. Selected materials were used to fabricate implants for use in medicine and they were also used as restorative materials in dentistry. Some biomaterials that have been studied for tribological use are listed in Table 1.2 (Long et al. 1998; Gilbert et al. 1997; Gilbert et al. 1995; Goldberg et al. 1997; Sarikaya et al. 1999).

1.3.3 Properties

In general biomaterials must be biocompatible. Some additional characteristics, such as proper mechanical behavior and feasibility for manufacturing are also required (Table 1.3, Hoeppner et al. 1994).

In vitro studies simulate the biological environment for conditions of load, contact, corrosion, fatigue, creep, and wear. Animal *in-vivo* tests using implants show the biological response elicited by materials in various tissues as well as load, contact, corrosion, fatigue, creep, and wear.

Table 1.2 Summary of Biomaterials Used in Medical Implants

Material	Application	Major Properties Description
Metal: Brass, Stainless Steel, Nickel Plated, Nickel Plated Steel, Zinc Plated Steel	Insert	Wear, corrosion, and fatigue resistance
Alloy: Titanium Alloys, Titanium Aluminum Vanadium Alloy, Cobalt Chromium Alloy, Cobalt Chromium Molybdenum Alloy	Total joint replacement	Wear and corrosion resistance
Inorganic: Diamond-Like Carbon (DLC)	Biocompatible coatings	Reducing friction and increasing wear resistance
Ceramics: Al_2O_3, ZrO_2, Si_3N_4, SiC, B_4C, quartz, bioglass(Na_2O-CaO-SiO_2-P_2O_5), sintered hydroxyapatite ($Ca_{10}(PO_4)_6(OH)_2$)	Bone joint coating	Wear and corrosion resistance
Polymers: UHMWPE	Joint socket	Wear, abrasion and corrosion resistance
Polytetraflouroethylene (PTFE)	Interpositional implant temporomandibular	Low friction coefficient
Polyglycolic acid	Joint (Jaw) Joint bone	Elastic with less wear
Polyurethane (PU)	Leaflet heart valve	Highly biocompatible, high strength, and dynamic ranges of breathability
Methacrylate	Bone cements and dental restoratives	Wear, abrasion and corrosive resistance
Polyethylene terephthalate fibers	Artificial blood vessels	
Composites: Specialized silicone polymers	Bone joint	Wear, corrosion, and fatigue resistance

Specific mechanisms involved in osteoblast response to implant surfaces are of great interest in bone repair -- one of the most useful medical applications of biomaterials. Studies of mechanisms such as phospholipid strategies for biomineralization, photopolymerizable biomaterials, materials for gene delivery, and self-assembling polymer membranes and colloids are ongoing (Stupp 2001). There are intensive efforts to develop self-assembling biomaterials and the biosynthesis of materials using genetically modified organisms. In the field of biomineralization other strategies are being explored that could lead to the development of biomimetic materials for tissue repair.

Table 1.3 Factors of Material Design of Implants (Hoeppner et al. 1994)

Requirements of implants		
Compatibility	Mechanical Properties	Manufacturing

*Tissue Reactions
*Changes in Properties
  **mechanical
  **physical
  **chemical
*Degradation leads to
  **local deleterious
  changes
  **harmful systemic
  effects
	*Elasticity
	*Yield strength
	*Ductility
	*Toughness
	*Time dependent
	*Deformation
	*Creep
	*Ultimate strength
	*Fatigue strength
	*Hardness
	*Wear resistance
		*Fabrication methods
		*Consistency and conformity to all
		  requirements
		*Quality of raw materials
		*Superior techniques to obtain
		  excellent surface finish or texture
		*Capability of materials to get safe
		  and efficient sterilization
		*Cost of product

1.3.4 Applications

The range of applications of biomaterials is vast. They can be used in 1) orthopedic applications such as pins, plates, femoral stems, joint replacements, bone spacer and bone

bonding; 2) dental applications such as tooth implants, coatings on implants and to fill large bone voids resulting from disease or trauma, and restoring tooth structure (fillings), crowns and dentures; 3) cardiovascular applications such as heart valves and pace maker leads; 4) cosmetic surgery such as breast augmentation; and 5) external applications, such as casts, braces, contact lenses, etc. In the future, biomaterials may include materials based on stem-cell technology that have the potential for 'natural' replacement of tissues and organs, but this technology is a distant and somewhat uncertain prospect (SRI Consulting Business Intelligence 2004).

1.4 Tissue engineering

All procedures that restore missing tissue in patients require some type of replacement structure for the area of defect or injury. These devices have traditionally been totally artificial substitutes (joints), non-living processed tissue (heart valves), or tissue taken from another site from the patients themselves or from other patients (transplantation) (Langer et al. 1999). Now a new alternative, tissue engineering, is becoming available: the replacement of living tissue that is designed and constructed to meet the needs of the individual patient (Vacanti et al. 1999). Tissue engineering is an interdisciplinary field that applies the principles of engineering and the life sciences toward the development of biological substitutes that restore, maintain, or improve tissue function (Skalak et al. 1988; Nerem, 1991). Tissue engineering may also provide an alternative to organ and tissue transplantation, which suffer from a limitation of supply. The purpose of tissue engineering is to transplant cells onto a biocompatible, biodegradable scaffold that provides an appropriate environment to induce 3-dimensional tissue growth. This construct can be implanted and should create tissue that functions, remodels, and grows like native tissue (Sodian et al. 2000; Mooney 1993). This results from a non-inflammatory cell seeded onto open, porous, exogenous extracellular matrices fabricated from biocompatible materials.

There are examples of this approach stretching over 70 years. A mouse tumor cell line was encased in a polymer membrane and inserted into the abdominal cavity of a pig in 1933 (Bisceglie 1933). For clinical use, Chick et al. (1975) reported their results of encapsulating

pancreatic-islet cells in semi-permeable membrane to aid glucose control in patients with diabetes mellitus. Replacement of the skin with cells in collagen gels or collagen-glycosaminoglycan composites to guide regeneration were attempted in the early 1980's (Bell et al. 1981; Burke et al. 1981). Three general strategies have been adopted for the creation of new tissue: 1) Isolated cells or cell substitutes; 2) Tissue-inducing substances; and 3) Cells placed on or within matrices (Langer et al. 1993). Langer and Vacanti (1999) discussed the replacement of ectodermal tissue such as nervous system, cornea, and skin; endodermal tissue such as liver, pancreas, and tubular structures; and mesodermal-derived tissue such as cartilage, bone, muscle, and blood vessels.

For clinical applications, the cells are generally derived from the patients themselves, from close relatives, or other individuals. In choosing the cells, there are must be consideration of ethical issues. Recent studies showed that stem cells derived from human embryonic blastocysts can be proliferated through multiple generations and made to differentiate into the appropriate cell type (Thomson et al. 1998). Other current research is learning how to control the permanent differentiation of stem-cell populations into the desired cell types such as cartilage, bone, liver, or some other cell type. Another approach is to create cells that could be used as 'universal donors'. Large-scale cell culture systems will be important to growth sufficient cells *in vitro* (Hu et al. 1991). Alternatively, stem cells reside in the blood and can be distributed through a scaffold and held in place (until they begin to differentiate) in a bloodclot.

The materials used in tissue engineering are also a major area of study. Materials used in tissue-engineering need to meet the nutritional and biological needs of the cells. They must have good mechanical characteristics. Geometries must be considered while the devices are fabricated so as to maintain the structure during new tissue formation. Natural materials such as collagen, hydroxyapatite, or alginate are advantageous in that they are compatible macromolecules that facilitate cell attachment or maintenance of differentiated function. Natural materials may be the actual in-vivo extracellular matrix components for cells and as such would possess natural interactive properties such as cell adhesiveness. Synthetic degradable polymers such as lactic-

glycolic acid or polyacrylonitrile-polyvinyl chloride and some ceramics were used as templates for cells to form permanent new tissues (Vacanti et al. 1988). Highly porous structures may be crucial to the success of tissue engineer (Mikos et al. 1993). Systems designed with highly porous structures meet the needs for the mass transfer of large numbers of cells (Mooney et al. 1999). Sterilization of the transplant is also a critical concern. Synthetic polymers allow precise control over strength, processability, molecular weight, degradation, hydrophobicity, microstructures, permeability and other attributes. However, they may not interact with cells in a desired manner. A third choice is to combine the natural and synthetic materials, using critical amino acid sequences from natural polymers that are grafted onto synthetic polymers (Hubbell et al. 1992; Lin et al., 1992; Barrera et al. 1993). Biomaterials do not always need to generate a bioreaction. One more choice is to produce a certain surface topography to get an engineered tissue response (Simon et al. 2003; Dutta Roy et al. 2003).

Bioreactors for the in-vitro fabrication of tissue before implantation need to permit mass transfer of nutrients, gases, metabolites, and regulatory molecules. Regulating the size and structure of the forming tissue, the presence of pulsatile flow, and the types of desired biochemical components are the key issues to produce high quality devices. Most of the early work in tissue engineering relied on the use of standard static cell-culture conditions. However, stirred conditions in bioreactors have been shown to improve the quality of certain tissues such as cartilage (Vunjak-Novakovic et al. 1996).

Alsberg et al. (2002) hypothesized that it would be possible to engineer a growing tissue by presenting appropriate growth stimuli from the cell transplantation scaffold. They tested their hypothesis in the context of engineering growing bony tissues by the cotransplantation of osteoblasts and chondrocytes. Peppas and Langer (1994) believe that it is critical to promote the multiplication of transplanted cells if one is to engineer a growing tissue *in vivo*. A required growth stimulus for most mammalian cell types is needed for an appropriate adhesive substrate. Transplantation of a small number of cells and growing the tissue *in vivo* may bypass current

difficulties in the *in vitro* engineering of large tissue masses for subsequent transplantations that are related to a lack of vascularity and large-scale cell death (Peters et al. 1998). This approach may be ideal for the utilization of small numbers of stem cells in the regeneration of various tissues in the body.

1.5 Joints

1.5.1 Natural joints

A joint is formed by the ends of two or more bones which are held in place relative to each other by thick connective tissues. The functions of joints are first, to permit motion and second, to provide stability. Joints are localized areas of an organism that allow particular types of movement. Joints resist some forces to prevent certain motions and allow other forces to act upon them. The joints can be classified based on structure into three types: fibrous, cartilaginous and synovial joints.

Fibrous joints are those where the bones are fastened together by dense fibrous connective tissue, such as the sutures of the skull and the teeth in their bony sockets. This tough connection between bones prevents much movement at these joints. The dense connective tissue that is used to hold bones together is ligament. There are three major types of fibrous joints: sutures (bones are tightly opposed, and the dense connective tissue seems like a glue holding the bones firmly in place), syndesmosis (the only slightly mobile fibrous joint), and gomphosis (the joint found between teeth and the maxilla or mandible).

Cartilaginous joints are semi-movable. There are two types of cartilaginous joints: synchondrosis and symphysis. Synchondrosis joints are immovable, such as joint between skull and hyoid apparatus. Hyaline cartilage connects the bones in this type of joints. Symphysis joints are somewhat movable (amphiarthrotic) such as pelvic synphysis and mandibular symphysis. Fibrocartilage (coated in hyaline cartilage) connects the bones in this type of joint.

Synovial joints are all freely mobile (diarthrotic) such as knee and hip joints. There is tissue and fluid (synovial fluid) between the bones of the joints. The synovial membrane is

epithelial tissue, and it lines the cavity containing the synovial fluid. The synovial fluid is secreted by the synovium into a space between the bones to create a cushion and a smooth movement. Each bone is covered by the articular cartilage. The synovial membrane attaches to the articular cartilage and forms a bridge between the bones of the joint. The contained space within this bridge is filled with the synovial fluid.

1.5.1.1 Structure of synovial joints

In synovial joints, joints are lubricated by synovial fluid for conjuction with muscles. Synovial joints are sturdy enough to hold the skeleton together and at the same time permit a range of motions. The ends of these joints are coated with cartilage, which reduces friction and cushions against jolts. Each synovial joint has a point in its range of motion where: 1) its surfaces are maximally congruent; 2) its capsule and ligaments are maximally elongated and taut; and 3) its surfaces are maximally compressed (Hertling et al. 1996). The structure of the normal synovial joints can be seen in Figure 1.9.

1.5.1.2 Movement and mechanics of synovial joints

Biomechanics is defined as that area of study wherein the knowledge and methods of mechanics are applied to the structure and function of the living system (Kreighbaum et al. 1985). Knowledge of joint-articulating surface motion is essential for design of prosthetic devices. There are three types of articulating surface motion in human joints: sliding, spinning, and rolling (Kaufman et al. 2003). According to the anatomics, movement, and physiology, synovial joints can also be further classified as plane, ball and socket, ellipsoid, hinge, saddle, condylar and pivot joints (Figure 1.10).

The structure of the joint and the external forces applied to the joint determine the type and the motion of the joint. These forces also influence the nature and the amount of internal forces required of the joint's muscles and ligaments to control the joint. The factors which can affect the motion of a joint are 1) the structure of the joint, such as joint surfaces and ligamentous

support; 2) external forces on the joint; and 3) interactions between joints and the external environment (Oatis 2004).
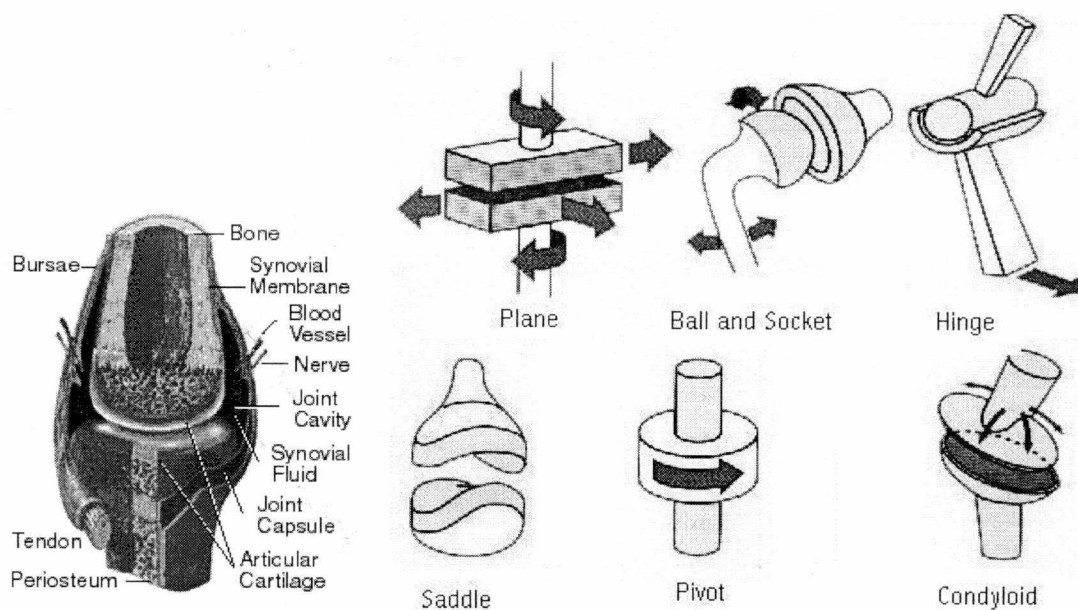
Figure 1.9 Structure of synovial joints

(Vaxa International Inc. 1998)

Figure 1.10 Movements of synovial joints

(Shier et al. 1999)

1.5.1.3 Articular cartilage

Cartilage is defined as: 'Connective tissue dominated by extracellular matrix containing collagen type II and large amounts of proteoglycan, particularly chondroitin sulphate. Cartilage is more flexible and compressible than bone and often serves as an early skeletal framework, becoming mineralized as the animal ages. Cartilage is produced by chondrocytes that come to lie in small lacunae surrounded by the matrix they have secreted' (Association of Cancer Online Resource 2004).

1.5.1.3.1 Structures, compositions, and functions

Cartilage covers the articular surfaces of bone ends in synovial or diarthrodial joints and some cartilage is present in a few organs. There are four types of cartilage: articular (hyaline)

cartilage for joint surfaces; fibrocartilage for tendon and ligament insertion; elastic cartilage for the trachea and ears; and fibroelastic cartilage for meniscus.

Cartilage is a fluid-filled, porous-permeable medium that contains two phases: fluid phase and solid phase. The fluid phase includes about 70% water and other molecules such a glycoproteins and lipids. Water permits diffusion of gases, nutrients and waste products between synovial fluid and chondrocytes. The solid phase contains collagen Type II fibrils, proteoglycans, and some other matrix. Proteoglycans are large protein-polysaccharide molecules, which behave as a strongly hydrophilic gel. Water makes up 60-80% of the tissue. When load is applied to cartilage, most of the water can be squeezed out, which reduces the stress and lubricates the joint. Once the load is removed, water is taken up again. Increasing the content of proteoglycans can increase the rigidity of the cartilage (Tracey 2002; Mow et al. 1980).

Cartilage cells are chondrocytes, which are spheroidal in shape with a single nucleus. They are about 20 microns in diameter. They obtain nutrition by diffusion from synovial fluid in adults and by vascular subchondral loops in immature humans which is eventually closed by calcified layer. Chondrocytes maintain, manufacture, and secrete molecular components.

There are three zones in articular cartilage structure in a joint: the superficial tangential zone (10-20%), middle zone (40-60%), and deep zone (30%). These zones were listed from the surface down to the bone, and there is a graduate transition from one to the next. At the surface the collagen concentration is highest and collagen is tightly packed, and the fibrils are aligned parallel with the surface with a smaller diameter. In the deep zone, the collagen packing is less dense, and the fibrils are oriented perpendicular to bone.

Articular cartilage is load bearing, transfers load (forces) between articulating bones, and distributes joints forces over wide area, so that the stress in the underlying bone is limited. Cartilage acts as a better bearing material than bone because it has a low friction bearing surface and therefore decreases friction and wear during joint movements (Waigh et al. 2004).

1.5.1.3.2 Biomechanical behavior

Cartilage experiences about 100 million cycles of loading in a lifetime. As time goes by, it loses water, and becomes thinner. Permeability of articular cartilage allows fluid flow through the porous matrix, and this is very important for the function of load bearing of the cartilage. The permeability of healthy articular cartilage is relatively low. If the cartilage is damaged, the permeability becomes greater and proteoglycans are washed out from the matrix, resulting in deterioration of the cartilage (Tracey 2002).

In synovial joints the loads are very high, and the compressive load is transferred across a very small surface area at any instant. The loads can come from the weight of human body and the motion of the human body. These forces are induced by the muscles and ligaments of a joint. Cartilage is a viscoelastic material and responds to the action of a constant stress or deformation. It stiffens with increasing strain under tension. The tension varies with structure zone. Cartilage is stronger and stiffer in parallel to the split lines. The superficial tangential zone provides cartilage with a tough, wear resistant, and protective skin.

There are no volumetric changes or pressure gradients produced under pure shear. Friction is caused by the motion of the collagen and proteoglycans. The superficial tangential zone is structured to resist shear stress developed during joint motion.

The natural healthy joint is a very well engineered structure. Frictionless motion is provided by the combination of a smooth articular cartilage surface as well as lubrication of both the articular cartilage and the synovial membrane, which together make up the entire surface area of the inside of the joint. The joints are lubricated by synovial fluid, which contains hyaluronic acid (HA), and have a friction coefficient of 0.002. The friction coefficient of dry cartilage=0.27.

HA serves important biological functions in bacteria and higher animals including humans. It is (poly D-glucuronic acid-n-acetyl-D-glucosamine) sodium salt, tetragonal form. HA is comprised of linear, unbranching, polyanionic disaccharide units consisting of glucuronic acid

(GlcUA) an N-acetyl glucosamine (GlcNAc) joined alternately by beta 1-3 and beta 1-4 glycosidic bonds (Figure 1.11).

D-Glucuronic acid   N-acetyl glucosamine
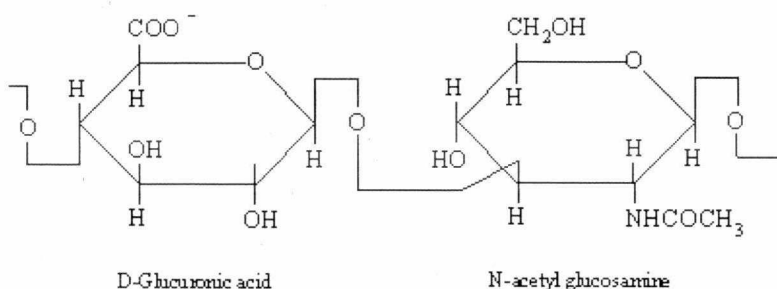
Figure 1.11 Disaccharide repeating unit of HA comprising GlcUA and GlcNAc (University of Queensland, 2004)

HA forms a complex with a protein and forms a HA-protein monolayer (plasma + HA-protein complex called lubricin) between the two surfaces as the lubricated film (McIlwraith 2004). The HA-protein complex increases the viscosity of the synovial fluid. There are three different kinds of lubrication due to different joint motions. They are 1) boundary lubrication, 2) hydrodynamic lubrication, and 3) squeeze film lubrication.

Wear happens in joints when the surfaces are in direct contact without a lubricant film. This causes adhesive or abrasive wear, and when subject to repetitive loading, joints will accumulate microscopic damage to the surface (fatigue wear).

Once surface damage occurs (fibrillation), even in a small area, the whole surface becomes less stiff (Swanson 1980), and more permeable which results in more stress. Once the cartilage is damaged, further deterioration results in osteoarthrosis, a non-inflammatory arthritis. Wear debris can illicit the body's inflammatory response, creating inflammatory arthritis and/or bone resorption.

1.5.1.4 Osteoarthritis (OA)

There are more than 100 different types of arthritis, and the cause of most is unknown. Arthritis causes pain, stiffness, and sometimes swelling in or around joints. Osteoarthritis, or degenerative joint disease, is one of the oldest and most common types of arthritis. It is characterized by the breakdown of the joint's cartilage. Cartilage is the part of the joint that cushions the ends of bones. Cartilage breakdown causes bones to rub against each other, causing pain and loss of movement. As the cartilage breaks down, changes occur in the underlying bone, which becomes thickened with the formation of bony growths from the bone surface called spurs. Fluid-filled cysts may form in the bone near the joint. Bits of bone or cartilage can break off into the joint space and irritate soft tissues, such as muscles, and cause problems with movement. Much of the pain is a result of muscles and the other tissues that help joints move, as a result of damage to the cartilage. Cartilage itself does not have nerve cells, and therefore cannot sense pain (inflammaorory), but the muscles, tendons, ligaments and bones do. The synovium becomes inflamed as a result of the arthritis cartilage. This inflammation leads to the production of cytokines (inflammatory proteins) and enzymes that may damage the cartilage further. There are many factors that can cause osteoarthritis such as genetics, age and environmental stresses. Some common treatments are weight control, pain-control medicine, and hot/cold therapy. When these do not work or the situation is continually getting worse, a surgery is needed to relieve chronic pain (Arthritis Foundation 2004).

1.5.2 Artificial joints

1.5.2.1 Total Replacement of Artificial Joints

One of the main types of replacement is Total Replacement Artificial Joints. It has the goal to relieve the pain in the joint caused by the damage done to the cartilage. The earliest successful implants were bone plates, introduced in the early 1900s to stabilize bone fractures and accelerate their healing. In 1925, a surgeon in Boston, Massachusetts, M.N. Smith-Petersen, M.D., molded a piece of glass into the shape of a hollow hemisphere which could fit over the ball

of the hip joint and provide a new smooth surface for movement. In the 1930's Phillip Wiles from the Middlesex Hospital, London, UK designed and inserted the first total hip replacements. G.K. McKee, who was following Wiles, introduced metal-on-metal hip prostheses. He developed various uncemented prototype total hip replacements in the 1940's and 1950's. McKee's cement fixed McKee-Farrar Total Hip Replacement (THR) from 1960 was the first widely used and successful THR. In the late 1950s, the first total hip replacement was introduced using PTFE as the cup-bearing surface (Blanchard 1995). However, since the PTFE undergoes aseptic loosening, PTFE has not proved to be an appropriate material to use as a load-bearing surface in the body. In late 1960s Sir John Charnley, a British Orthopedic surgeon, developed the fundamental principles of the artificial hip that still sees widespread use today. Frank Gunston developed one of the first artificial knee joints in 1969. Since then, joint replacement surgery has become one of the most successful orthopedic treatments (www.utahhipandknee.com, 2004).

It is now accepted that a Charnley type total hip replacement can give satisfactory results in an elderly inactive population. Several metals are used, including stainless steel, alloys of cobalt and chrome, and titanium and the plastic material is durable and wear resistant UHMWPE. Recent research on hip and knee replacement prostheses covers areas such as tribology of metal-on-metal hip joints, coatings for enhanced tribological performance, soft layer and hard-bearing surfaces in hip replacements, generation and biological activity of wear debris, wear measurement and component geometry, wear of ceramic-on-ceramic joint replacements, validation of knee simulator wear, wear measurement on knee prostheses, lubricating film thickness in hip prostheses, and advances in simulator testing (Hutchings 2002).

Current artificial joints made with UHMWPE and metals undergo degradation after 10-15 years (Spector 1992; Shi et al. 2001). The research on how to improve the design and materials to improve the durability of the artificial joints is the key for the most recent research.

1.5.2.2 Tissue engineered artificial joints

Natural cartilage tissue has a limited self-regenerative capacity; thus, strategies to replenish the lost cartilage would be useful in reconstructive and plastic surgery. Tissue-engineered cartilage using biodegradable polymeric scaffolds is one such approach gaining wide attention (Risbud et al. 2001). During the past decade new strategies have emerged for the treatment of patients. Specifically tailored biomaterials are crucial tools in tissue engineering (Figure 1.12), and need have to provide biocompatibility (which means not eliciting an inflammatory reaction or immunorejection), biodegradibility and a variable design, that depends on the biomechanical profile of the anatomical situation in question. Moreover, they have to ensure an adequate cell distribution, new matrix formation and tissue integration, thus simulating an ideal embryo-like environment (Schultz et al. 2000).

Tissue engineering provides an alternative to transplantation. Cells will grow on and replace lost synthetic extracellular matrices from biocompatible polymers. The strategy of a directed regeneration of musculoskeletal tissue damaged by trauma, chronic inflammation or degeneration will perfectly supplement the treatment with the new biological therapeutics in rheumatology. Joints are composed of various specialized mescenchymal cells which manage individual biomechanical requirements by a finely tuned turnover of their extracellular matrix (Prokop 1997).

For the replacement of joint cartilage, pressure resistance and fixation of the transplant to the bone are even more important. At present, studies are performed using either a heterotopic transplantation or extended cultures *in vitro* with hyaluronic acid. An alternative is the establishment of osteochondral transplants which consist of artificial cartilage tissue cultured directly on porous calcium carbonate (Kreklau et al. 1999) to achieve a permanent, solid connection between cartilage and bone tissue (Shultz et al. 2000).
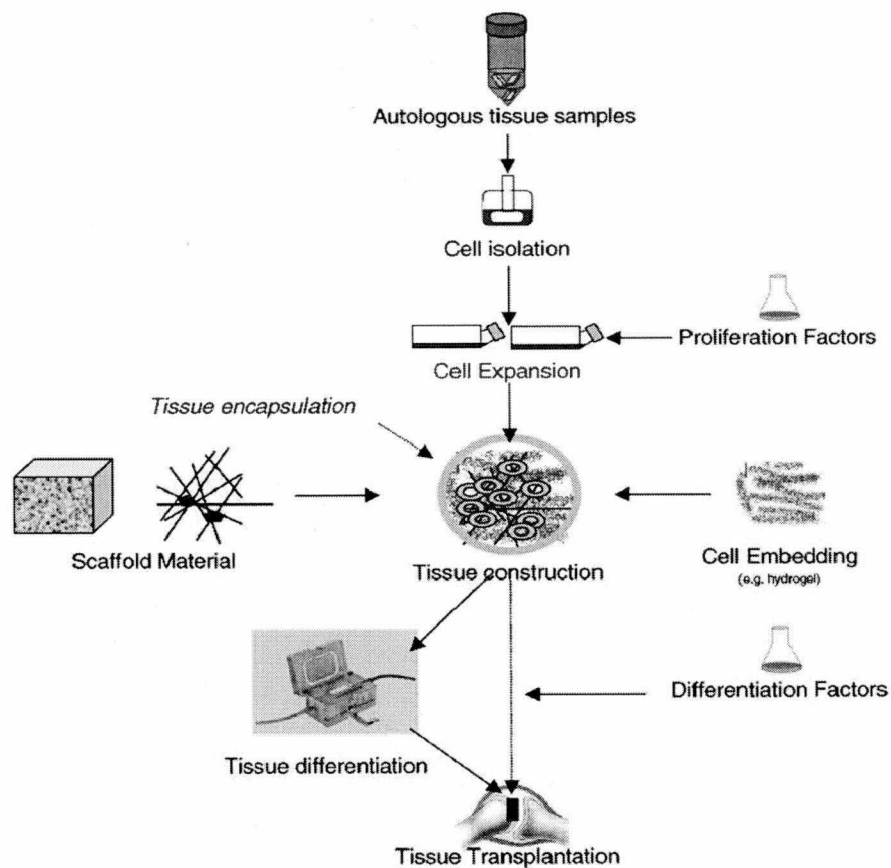
Figure 1.12 General procedure for engineering of bone and cartilage transplants

(Schultz et al. 2000)

1.6 Objective of this thesis

The service time of most the artificial joints now in use is usually 12-15 years or less. Durability is limited by the body's reaction to wear debris of the artificial joints. Wear of the artificial joints should be reduced. The focal areas of this research are (1) study of the tribological performance of bearing materials for Total Replacement Artificial Joints (TRAJ); and (2) study of materials as scaffolds for cell growth from both a tissue engineering and tribological perspective.

The interdisciplinary research conducted in this thesis is a preliminary attempt to design and test novel materials. I hypothesized that metal-on metal with carbon-based coating TRAJ

could be an alternative bearing materials, tissue could be implanted to the matrix materials and the scaffolds with cells could be another alternative for the Total Joint Replacement. As a test of the hypothesis, I report the results of research on alternative load bearing materials in total joint implantation and the results of tissue culture on matrix materials.

Chapter 2

Experimental: materials, equipment, and methods

As indicated in title, this chapter discusses the experimental procedures involved in this thesis research.

2.1 Materials

2.1.1 Cell culture

2.1.1.1 Substrate materials for regular cell culture

A single-use sterile polystyrene plastic substrate, treated with vacuum gas plasma for cell culture, was used as the cell culture substrate. The polystyrene is hydrophobic, so the plastic was treated with γ-irradiation, chemically, or with an electric ion discharge to produce a charged surface that is wettable (Freshney 2000). These substrate materials, including plates and flasks, have good optical qualities, and the growth surface is flat, providing uniform and reproducible cultures. The plates used were 100x20 mm (Becton Dickinson Labware, #353003) dishes and 6 well 2 ml MULTIWELL™ (Becton Dickinson Labware, #353046) plates. Falcon 250 ml flasks (BD Bioscicence, #353136) were also used in tissue culturing. The flasks are treated polystyrene with a canted neck and a 0.2 μm vented plug seal cap. The cap is gas permeable.

2.1.1.2 Substrate materials for special cell culture

Glass-bottom dishes were made for culturing cells on different materials. Single holes, 15 mm in diameter, were drilled through the bottoms of the FALCON 35x10 mm dishes (Becton Dickinson Labware, #351008, not cell culture treated). Microscopic cover glasses (ASSISTANT) sized 22x22 mm were cleaned first by immersion in warm Micro-9 solution (2%) for 30 minutes, then washed 12 times with DI water. They were then dried in a warm oven. Aquarium glue was used to seal the drilled hole with the cover glasses on the bottom of the dishes and to glue the samples to the glass bottom of the self-made dishes before the cell culture experiments. The dishes were then dried overnight and sterilized with UV light for 25 minutes.

2.1.1.3 Artificial ECM materials

Tissues are not made up solely of cells. A substantial part of their volumes is extracellular matrix (ECM). ECM is a complex network of polysaccharides (such as glycosaminoglycans or cellulose) and proteins (such as collagen) secreted by the cells. ECM serves as a structural element in tissues and also influences their development and physiology. ECMs act as a scaffolding to bring cells together in a tissue to control the tissue structure and to regulate the cell

phenotype (e.g. tissue-specific gene expression, Alberts et al. 1994). Protein adsorption always precedes cellular adhesion. Porosity is important to promote anchorage of biomaterials to surrounding tissue (Shi et al. 2004).

Tissue engineering is based on the observation that dissociated cells will reassemble *in vitro* into structures that resemble the original tissue when provided with an appropriate environment (e.g. isolated endothelial cells reform tubular structures *in vitro*; Folkman et al 1980). This approach uses ECMs to engineer materials from isolated cells. ECM are designed to bring the desired cell types into contact in an appropriate three-dimensional environment, and also provide mechanical support until the newly formed tissues are structurally stabilized and specific signals to guide the gene expression of cells forming the tissue are established (Putnam et al. 1996; Kim et al. 1998; Hutmacher 2000). Different kinds of materials were investigated as the scaffolds of cell culture. They were glass and Al_2O_3 (ceramics), nickel (Ni) (metal), Polyvinyl alcohol (PVA), PU (PU-1 and PU-2), and transparency films (TR-1 and TR-2) (polymers).

Glass ceramics are important biomaterial in bone replacement. Bone and dentine are composed of apatite and bioactive glasses. Glass used in this research was in the form of micro slides (VWR). The original size of the slides was 25 x 75 x 1 mm^3. Both a standard microscope and an Atomic Force Microscope (AFM) were used to analyze the surface morphology. The microstructure of the glass slides is shown in Figure 2.1. Under the microscope, the surface of the glass is flat with some small scratches. AFM analysis shows the detailed microstructure of the glass. There are islands sized about 0.5 μm to 3 μm on top of the surface. The glass slide is not porous.

Scan Distance (13.48μm)
Z Distance (2107.59mv)
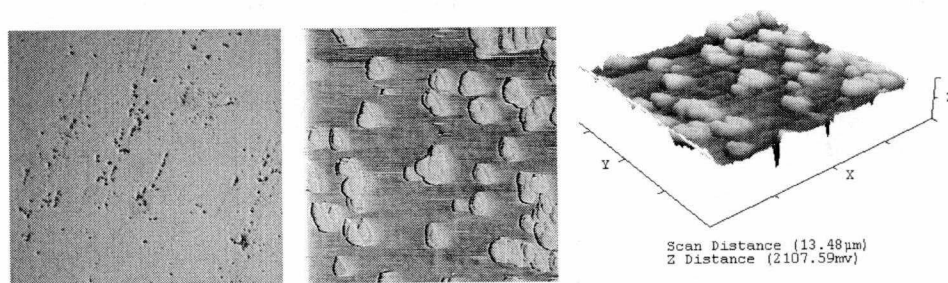
Figure 2.1 Surface and microstructure of glass slide surface
Left: Microscope image, 10x; middle: 1D AFM image; right: 3D AFM image

Al_2O_3 has excellent corrosion resistance, good biocompatibility, high strength, and high wear resistance. It has been used for over 20 years in orthopedic surgery. The Al_2O_3 used in this

research was made as a foam filter. The thickness was 10 mm. The pore size was primarily 0.5-3 mm in diameter (Figure 2.2), with a few larger and smaller sized pores. The Al_2O_3 has an open pore structure, and the variation in pore size can be clearly seen under the microscope.
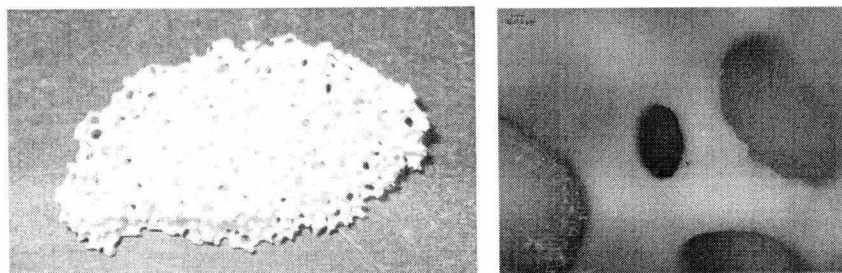
Figure 2.2 Surface and microstructure of Al$_2$O$_3$: left, photo; right, microscope image, 10x.

Metallic biomaterials are classified as nearly inert materials. Because of their mechanical strength and biocompatibility, metals are superior in load-bearing implants. Ni-alloys have been widely used in medicine in cardiovascular (Simon et al. 1977; Wholey et al. 1998), gastroenterologic (Acunas et al. 1996), urologic (Gottfried et al. 1997), and orthopedic (Lu et al. 1986; Castleman et al. 1976) applications, and also some in other tissue applications (Rauber et al. 1990; Hauck et al. 1997; Frank et al. 1995). The Ni sheets used in this research were designed for use as filters. The thickness of the Ni is 4mm. The Ni sheets have macro-pores, mainly from 0.1 mm to 0.5 mm in size, and can clearly be seen with the naked eye (Figure 2.3). Microscopically, Ni has an open pore structure. A pentagonal three-dimensional lattice of Ni wires can be seen under the microscope. These pentagons are the primary micro-shape of the Ni.
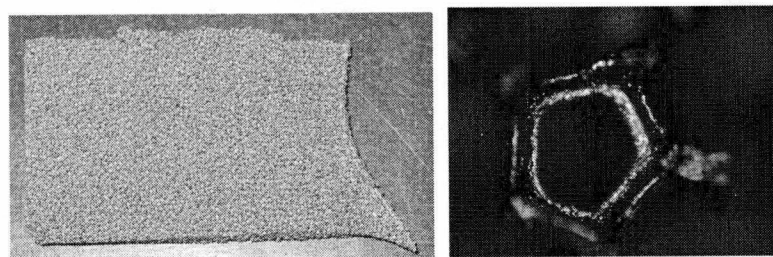
Figure 2.3 Surface and microstructure of Ni: left, photo; right, microscope image, 10x

Polyvinyl Alcohol (PVA) is a synthetic spongy polymer. The formula of PVA is $-CH_2$-$CH(OH)$-CH_2-$CH(OH)$-CH_2-$CH(OH)$-. PVA is white and possesses a three-dimensional open

cell structure. All of its cells are interconnected, not independent (Figure 2.4). PVA is a safe, biodegradable, water-soluble polymer and the material will withstand the action of dilute acids, strong alkalis and solutions of common detergents. Organic solvents do not penetrate the sponge like surface unless they are water-miscible and are applied mixed with 30% - 60% water. PVA sponge polymer behaves in water as a negatively charged colloid and will strongly adsorb metallic cations such as copper or iron. It also has strong affinity for cationically charged organic ions of the quaternary ammonium type. PVA exhibits mechanical strength and abrasion resistance equal to or greater than any other synthetic sponge material (PVA Unlimited 2004). PVA used in this research has a maximum stress of 323.7 kPa and a Young's modulus of 121.2 kPa. The thickness of the PVA sheets is 1mm. PVA has been used in biomaterial research for different purposes, such as soft contact lenses, joint cement, and, as a material that sticks to the skin, it can deliver controlled doses of drugs to wounds, speeding the healing process (Yamamoto et al. 2000; Nuttelman et al. 2001; Geckeler et al. 2003).
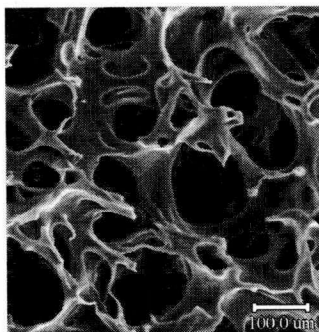
Figure 2.4 SEM image of PVA microstructure

Polyurethane (PU) is another polymer that has high flexural strength and excellent resistance to flex fatigue (Herring et al. 1994; Müller et al. 1994). The formula of PU is
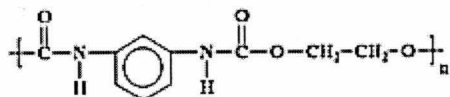
. PU has been used as a biomaterial (e.g., in heart assist devices) since the late 1960s and is the critical biomaterial used in the majority of clinical ventricular assist devices and artificial hearts worldwide (Vance et al. 2003; Petrini 2001; Lambda et al. 1998). PU used in this research is the polishing pad for CMP (Chemical mechanical polishing). Two kinds of PU were used in this research: PU-1 and PU-2. The microstructures of PU-1 and PU-2 were analyzed by ESEM. The analysis shows that PU1 and PU-2 have different

microstructures. PU-1 has an open-pore microstructure (Figure 2.5) and PU-2 has a closed-pore structure (Figure 2.6).
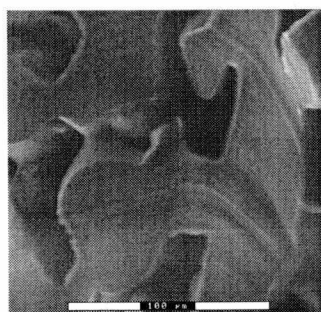
Figure 2.5 ESEM image of PU-1   **Figure 2.6 ESEM image of PU-2**
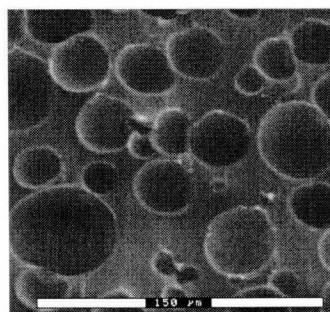
The PU-1 sheets are 1mm thick and have a coating on the top surface. The topography of the top surface and the reverse surface of PU-1 are shown in Figure 2.7. In order to confirm the existence of the coating, a polishing experiment was conducted to remove the coating. The PU-1 sample was polished with a diamond pad for 30 minutes. The polished surface and the raw surface were different after the polishing procedure. The polished surface (Figure 2.7, right) is identical to the reverse surface (Figure 2.7, left). This proved that the PU-1 had a coating on the top surface.
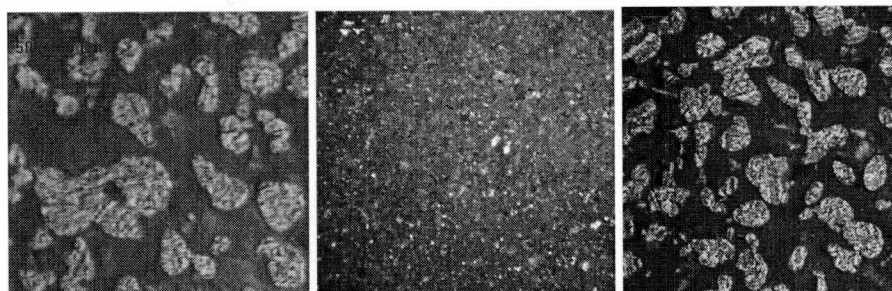
Figure 2.7 Microscope images of the surfaces of PU-1

Left: uncoated surface, 10x; middle: reverse surface, 5x; right, polished surface, 10x.

The PU-2 sheets are 2mm thick. The topography of PU-2 surface can be seen in Figure 2.8. The edge area (little darker) is the original morphology of the PU-2 surface. PU-2 does not have a coating on the surface. The same polishing procedure as above was performed on PU-2. After the polishing procedure, no obvious differences could be seen under the microscope

between the polished area and the unpolished area (Figure 2.8). The center area was polished. No obvious edge could be seen the surface was only a little lighter in the middle. This showed that the PU-2 surface was not coated.
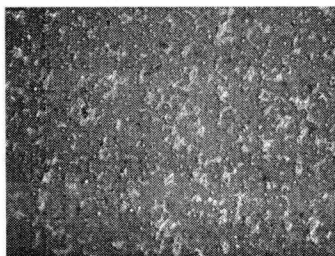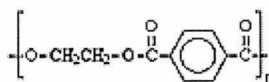
Figure 2.8 Microscope image of polished PU-2

The bright area is the area that has been polished; the dark areas are unpolished, 10x.

The base material of overhead transparency films is polyester. Both sides of the base film are coated with toner receptive coatings, an inkjet receptive coating on one side and an antistatic coating to optimize stream feeding on the other side. The base sheet was made of biaxially oriented polyethylene terephthalate (PET). Polyester does not absorb any of the ink. The ink-receiptive coating on the polyester film functions to absorb the ink. The drying time of the ink depends on the type, density, thickness, and many other charateristics of the coatings.

PET is a linear, aromatic polyester, made from benzene-1,4-dicarboxylic acid and ethane-1,2-diol. The chemical structure of PET is $\left[O-CH_2CH_2-O-\overset{O}{\overset{\|}{C}}-\langle \bigcirc \rangle-\overset{O}{\overset{\|}{C}} \right]_n$. PET is extensively used for soft-drink bottles and can be relatively easily chemically recycled. Current medical applications of PET include implantable sutures, surgical mesh, vascular grafts, sewing cuffs for heart valves, and components for percutaneous access devices (Metzger et al. 2004; Homsy et al. 1968; Vinard et al. 1988; Klinge et al. 1988; llingworth et al. 1998; Recum et al. 1984).
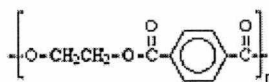
Two kinds of transparency films were used in this research: transparency-1 (TR-1) and transparency (TR-2). TR-1 is a white translucent polyester gloss film with the area of 8.5 x 11 inch^2. The TR-1 sheets are 0.14 mm thick. They have rough surfaces. TR-2 is clear inkjet transparency film with the area of 8.5 x 11 inch^2. The TR-2 sheets are 0.10 mm thick. They are transparent and have smooth surfaces. The morphology of the transparency films' surface and microstructure can be seen in Figures 2.9 and 2.10. The photomicrographs of the two films are

different. TR-1 has a few large dots; TR-2 has many small dots. AFM images show more details. The surface of the TR-1 is coated with separate particles, randomly arranged. The TR-2 surface has a very different coating in which the particles are well organized and densely packed. These make the surface flat and smooth.
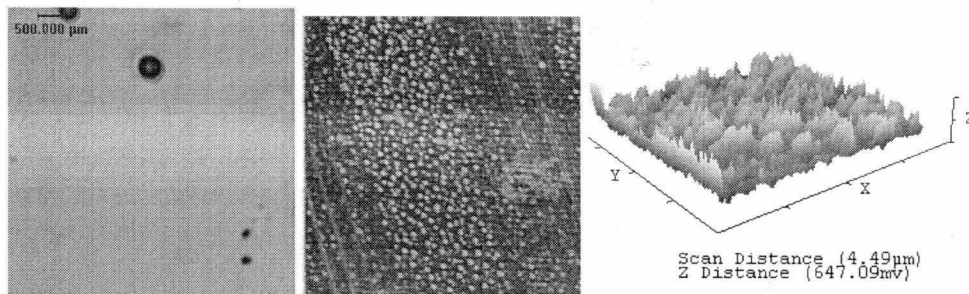
Figure 2.9 TR-1: left, microscope image, 10x; middle, AFM image; right, 3-D AFM image
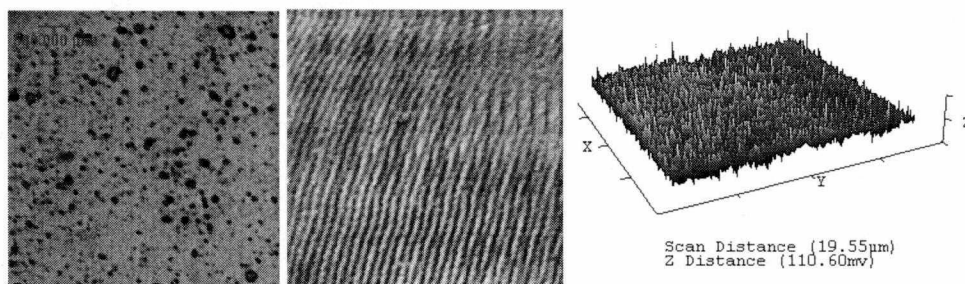
Figure 2.10 TR-2: left, microscope image, 10x; middle, AFM image; right, 3-D AFM image

2.1.1.4 Other cell culture supplies
Media and serum:

Cells were cultured in media selected based on the biochemistry of body fluid and cellular nutrition. The culture media was Dulbecco's Modified Eagle Medium (DMEM, GIBCO), FBS and penicillin-streptomycin (GIBCO) solution. Serum contains minerals, lipids, hormones, growth factors, adhesion factors, and antitrypsin activity. Growth factors in the serum promote cell proliferation. Adhesion factors and antitrypsin activity promote cell attachment.

The balanced salt solution (BSS) was phosphate buffered saline (PBS) without Ca^{2+} and Mg^{2+}. The dissociation solution was trypsin and EDTA solution. The freezing media was a DMEM, FBS, and dimethyl sulfoxide (DMSO) solution. The fixation solution is made with paraformaldehyde (PFA), sodium phosphate buffer (SPB), sucrose, and glutaraldehyde. SPB was

made with $Na_2HPO_4 \cdot H_2O$, $Na_2HPO_4 \cdot 7H_2O$ and DI water. The staining solution was Triton X-100, Bovine serum albumin (BSA, SIGMA), and Rhodamine phalloidin in methanol in PBS buffer.

Cells:

Swiss 3T3 fibroblast cells were used in this research. 3T3 cells are a tissue culture cell line developed from the fibroblasts of an embryonic albino Swiss mouse. First established in the 1960's, for the next twenty years 3T3 cells were principally used in the study of virus oncogenics. The stock of cells is stored frozen in individual ampules of 1×10^6. Cells should not be used for more than 20 passages. The tissue culture use of 3T3 cells has been important in explaining speciation and in placing foreign genetic material into new organisms to attain desired traits (www.olympusmicro.com 2004).

Tubes:

Conical plastic screw cap tubes (VWR) are sterile and disposable polystyrene. The 2 ml microtubes (SARSTEDT) are used for freezing cells and storing solutions.

2.1.1.5 Tribology test supplies

Pin and plates:

Pin-on-disk mode friction tests were conducted in this research. A rectangular aluminum holder was made in order to conduct the lubricated friction tests. The pin was also aluminum from CETR, sized at 6.35 mm in diameter. The test materials were held inside the holder by two aluminum bars that were attached by two bolts to the bottom of the holder.

Lubricant:

1% Bovine Serum Albumin solution (with 0.15M NaCl) was used as the lubricant fluid. In joints there are different kinds of lubrication. These are boundary lubrication, hydrodynamic lubrication, and squeeze film lubrication. As mentioned in Chapter 1, the joints are lubricated by synovial fluid. Normal synovial fluid is a dialysate of blood plasma that is comprised mainly of water (85%), HA and protein (Freemont et al. 1991). Most of the protein in synovial fluid is albumin. Other larger proteins derived from blood, phospholipids and cholesterol are present in small quantities (Berrien 1999). Bovine serum contains bovine serum albumin (BSA) protein. Serum albumin is one of the most widely studied proteins and is the most abundant protein in mammalian plasma. Bovine serum is commonly used in orthopedic testing (Barbour et al. 1995; Ries et al. 1999; Covert 2003).

Serum albumin has a globular structure (Bos et al. 1989) and is chiefly responsible for the maintenance of blood osmotic pressure (Figge et al. 1991). The amino acid composition of BSA is listed in Table 2.1 (Friedli 1996; Brown 1975; Patterson et al. 1977; McGillivray et al. 1979; Reed et al. 1980; Hirayama et al. 1990). The BSA molecule is made up of three domains. Disulphide bonds divide these three domains into nine loops (Figure 2.11). The 17 disulphides in albumin were protected at neutral pH from reducing agents, indicating the presence of disulfide bonds (Friedli 1996).

Table 2.1 Amino Acid Composition of BSA (Friedli 1996)

Ala 48	Cys 35	Asp 41	Glu 58
Phe 30	Gly 17	His 16	Ile 15
Lys 60	Leu 65	Met 5	Asn 14
Pro 28	Gln 21	Arg 26	Ser 32
Thr 34	Val 38	Trp 3	Tyr 21
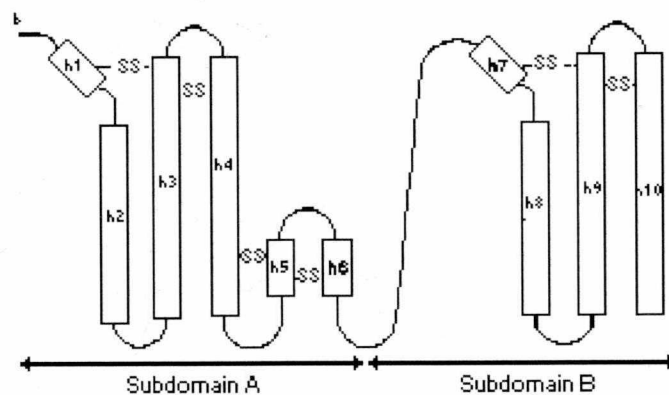
Figure 2.11 Location of disulfide bonds in mature BSA (He et al. 1992)

Serum albumin, when heat-treated, goes through two structural denaturation stages. The first stage is reversible and the second stage is irreversible but does not necessarily result in a complete destruction of the ordered structure (Kuznetsow et al. 1975; Lin et al. 1976; Oakes 1976). In the reversible structural stage, some of the alpha-helices are transformed to random

coils. BSA aggregates are formed through the hydrogen bonding of beta-sheets across monomers. As the temperature is increased past the reversible stage, unfolding of a "pocket" exposing Cys-34 takes place giving easy access for the rearrangement of disulphide bridges. Since disulphide bridges are covalent bonds, this stage is irreversible (Friedli 1996). Albumin with the hydrophobic "pocket" binds reversibly to a variety of ligands.

Standard Fetal Bovine Serum (FBS) (Hyclone) for this part of research was filtered through three sequential 100 nm pore-size rated filters. The fluid was stored in the freezer and before the tribology tests started, the solution was allowed to reach the room temperature.

2.1.2 Total Replacement Artificial Joints

The use of Total Replacement Artificial Joints requires the materials to be biocompatible, resistant to corrosion, wear, fatigue, impact, and high strength. No material has satisfied all of these requirements. Many materials - metals, ceramics, polymers, composites, organics and inorganics- have been used in constructing artificial implants (Kohn et al. 1992). The five materials tested in my research were 440C stainless steel (metal)-balls and plates, alumina (Al_2O_3)-balls, zirconia (ZrO_2)-balls (ceramics), UHMWPE-hemispherically tipped pins and plates (polymer), and diamond-like carbon (DLC) coating deposited on 440C stainless steel balls (composite). The pins are balls and hemispherically tipped pins.

Stainless steel is ductile and easily machined, and recent advancements have significantly enhanced its properties, but because a femoral component fractured with early designs, it is no longer used routinely (McKee 1982; Chan et al. 1996; Long et al. 1998). Stainless steel is considered suitable for use only in temporary implant devices, such as fracture plates, screws and hip nails.

As implanted materials, ceramics are both inert and biocompatible. Ceramics are materials composed of metallic and nonmetallic elements held together by ionic and/or covalent bonds, and are typically used in electrical and thermal insulators. They have high compressive strength, excellent corrosion resistance, low friction, and high wear resistance (Zhou et al. 1997; Begin-Colin et al. 1998; Niihara 1991; Lee et al. 2003). Ceramics are used as components of hip implants, dental implants, middle ear implants, and heart valves.

UHMWPE is a unique polymer with outstanding physical and mechanical properties that has been used in the manufacture of Total Artificial Joint Replacement prostheses since the 1960s. The bearing surfaces of over 90 percent of the artificial joints currently implanted consist of hard metallic alloys or ceramic femoral heads, articulating in UHMWPE acetabular cups. Continuing

research is being done to improve the performance of UHMWPE (Griffith et al. 1978; Sutherland et al. 1982; Eftekhar 1987; Harris 1995; Barrett et al. 1992; Wang et al. 1995; Livermore et al. 1990; Lewis 1997; Campbell et al. 1995; Wang 2001; Turell et al. 2003; Liao et al. 2003). There is considerable concern regarding wear debris from UHMWPE and its effect upon surrounding tissue. Wear and damage of the UHMWPE components are factors limiting implant longevity.

DLC, also known as amorphous hydrogenated carbon, is a class of materials with excellent mechanical and tribological properties (Erdemir et al. 1999). DLC coatings have good haemocompatibility, which is expressed in a decreased thrombus formation. When exposed to blood, an increased ratio of albumin to fibrinogen adsorption as well as decreased platelet activation is observed on coated surfaces. DLC coated cardiovascular implants such as artificial heart valves and stents are already commercially available (Hauert 2003). These properties of DLC suggest the use of this coating for artificial joints.

The 440C stainless steel (SS) was heat hardened and tempered to a hardness of 58-60 R_c. The Al_2O_3 balls were a hot-pressed, single phase (commercially available high purity (99.95%) made by Kyocera Corporation). It has an equaxed grain morphology with a grain size of about 2 μm. The zirconia balls are also manufactured by Kyocera. The yttria (Y_2O_3) is in astabilized tetragonal phase form (YTZP-yttria-stabilized zirconia polycrystals). The ZrO_2 consists primarily of tetragonal phase with an average grain size of about 0.75 μm. All these materials were polished to a surface finish of about 0.08 μm Ra. Table 2.2 has shown some other properties of the materials tested (Shi et al. 2003; Li et al. 1994). The DLC coating was deposited on polished 440C steel balls by a plasma assisted chemical vapor deposition (PACVD) method. Prior to coating deposition, the surfaces were cleaned with Ar^+ bombardment. This was followed by the deposition of a 50 nm thick Si layer to serve as a "bond" coating. These two steps were taken to ensure good adhesion between the DLC coating and the steel substrate. A 2 μm thick DLC layer was then deposited from a methane and hydrogen mixture plasma. Coated balls and plates have different properties by changing conditions when the film is coated. Three kinds of plates (NFC2, NFC6, and NFC7) and one kind of ball (NFC6) samples were tested. Details of the deposition process and the properties of the DLC thin film are discussed in detail by Erdemir et al. (1999; 2000). The hardness and elastic modulus of the DLC coating are included on Table 2.2. Bovine serum was used as the lubricant fluid.

Table 2.2 Some Mechanical Properties of The Balls (Shi et al. 2003; Li et al. 1994)

Material	Elastic Modulus (GPa)	Density (g/cm^3)	Hardness (GPa)
Al$_2$O$_3$	391	3.95	20.6
ZrO$_2$	206	6.0	12.3
SS	200	7.8	6.8
UHMWPE	0.8-1.5	0.926-0.945	60-66 (D)
DLC	94	-	18

2.2. Experimental Apparatus

Tissue culture hood, incubator, and other equipment:

A laminar-flow hood (NUAIR) provided aseptic conditions for cell culture. The horizontal flow provided the best sterile protection for cell cultures. For sterilizing dishes and ECM materials by UV light, a biohazard cabinet was used.

A CO$_2$ incubator was used since petri dishes or multiwell plates require a controlled atmosphere with high humidity and elevated CO$_2$ tension. CO$_2$ in the gas phase appears in the medium as dissolved CO$_2$ in equilibrium with HCO$_3^-$ and lowers the pH. The atmospheric CO$_2$ tension will regulate the concentration of dissolved CO$_2$ directly. Cultures in open vessels need to be incubated in an atmosphere of CO$_2$, the concentration of which is in equilibrium with the sodium bicarbonate in the medium.

Two centrifuges were also used. One was IEC/CENTRA CL2 for 15 ml and 50 ml conical tubes. The other one was Spectrofuge 16M for microtubes. A sterilizer was used to autoclave tissue culture supplies. Other equipment includes a refrigerator and freezers at -20°C and -80°C, cell counter, drying oven, sterilization filters, pH meter, balance, aspiration pump, water bath, ultrasonic cleaner, autoclave, etc.

Scanning Electron Microscope:

A scanning electron microscope (SEM, JEOL 840A) was used to analyze the microstructure of the materials. The unit uses a thermionic emission electron gun. Its capabilities include secondary and backscatter electron imaging, with two backscatter detectors. Images are recorded using Polaroid film. A sputter coater is available for imaging nonconductive samples (Figure 2.12, www.argonne.gov 2004). A Tousimis Samdri-790 critical point dryer, Gold-coating system was used to pretreat the cell culture materials for SEM analysis.

An Environmental SEM (ESEM, ElectroScan Corporation) was also used to analyze the materials. ESEM is a special type of SEM that works under controlled environmental conditions and requires no conductive coating on the specimen. ESEM is able to investigate samples in their natural state or under natural environmental conditions without the need for conventional coating and other techniques that may produce unwanted artfacts in the samples. The ability to image materials without coating and critical point dryer treatment also allows much faster sample throughput and more realistic results, especially in the research on cell adhesion.

Goniometer:

The goniometer is an instrument for measuring angles, especially the angles of crystals, or the inclination of planes. The goniometer used in this research (Figure 2.13, www.rame-hart.com) is for measuring the contact angles of liquids on solids. The contact angle in the liquid phase shows the wettabilty of the surface of the solid material. It is also called wetting angle. This is an important property of biomaterials.
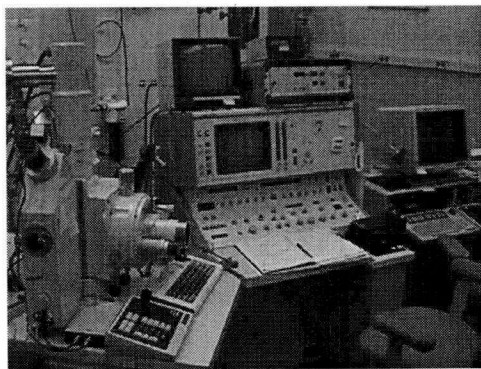
Figure 2.12 JEOL 840A SEM

(www.argonne.gov 2004)
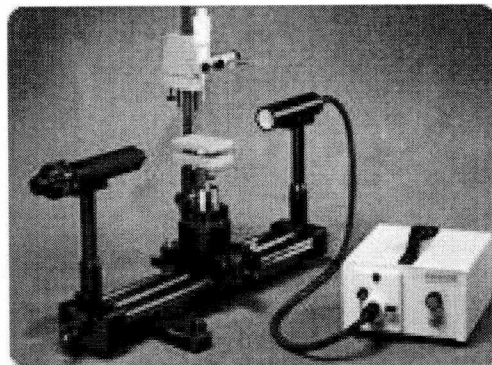
Figure 2.13 Goniometer

(www.rame-hart.com 2004)

Instron 4466 Universal Tensile tester:

A tensile tester (Instron 4466 Universal Tensile tester) can perform tensile, compression, shear, peel, and flexural tests. The load frame capacity is 10kN. The speed ranges from 0.001 to 500mm/min. Data were collected by a computer. Excel was used to process the data.

Optical microscopes:

There are three types of optical microscopes: industrial, biomedical, and stereoscopic microscopes. Industrial and biomedical microscopes were used in this research.

Biomedical microscopes are designed for transparent biological specimens. Biomedical inverted microscopes are used for viewing petri dishes or cells and tissues in culture containers. Microscopes are very important for cell culture because a morphological change is often the first sign of deterioration in a culture. Cells need to be watched every day when cultured. An inverted microscope (Wilovert) was used for watching and counting cells. A phase-contrast, fluorescence microscope (Nikon TE2000U, Figure 2.14) was also used when observing cells, counting cells, and taking pictures. This microscope was also an inverted model, designed for biomedical research.

Industrial microscopes (Olympus BX60, Zeiss Standard 16 microscope) were used in this research. The Olympus BX60 is an optical microscope for reflection and transmission. In both modes polarized light can be employed for sample analysis. Digital images can be acquired directly from the software. The Zeiss Standard 16 microscope is also an optical microscope for reflection and transmission. A regular camera was installed to take pictures.

Profilometers:

A MicroXAM surface profiler (ADE Phase Shift) was used to measure the volume of material worn off flats and balls after the wear tests had been performed. The unit provides three-dimensional maps of surfaces using optical interferometry. A side-to-side resolution is better than 1 micrometer. The vertical resolution is 0.3nm in filtered-light mode (Figure 2.15).

Figure 2.14 Nikon TE2000U Microscope

(www.nikon.com 2004)
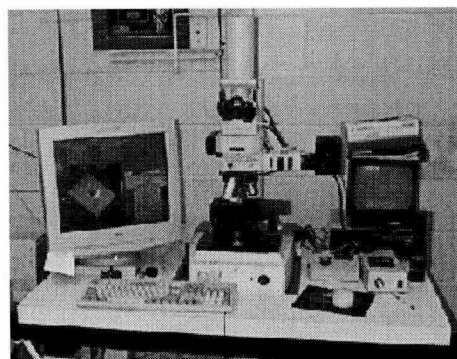
Figure 2.15 XAM Profilometer

(www.argonne.gov 2004)

Atomic Force Microscope (AFM):

AFM (Nano-R from Percific Nanotechnology) was used to investigate the atomic resolution morphology of the raw materials. The tip of the AFM was brought to close contact with the sample surface at the atom level without actually touching the surface. The tip on the cantilever moved back and forth over the sample surface and measured the topography.

Plint Reciprocating Tribology Tester:

This machine was used to perform reciprocating friction tests. A line contact was achieved using cylinder grips. The pin assembly was held stationary and the plate was oscillated back and forth. The load applied to the pin was adjustable by using dead weights applied to the pin assembly or pneumatic force. A Plexiglas enclosure surrounds the pin and disc fixtures permitting testing under nominal laboratory conditions. The friction coefficient was determined from measurements of the friction force obtained from a load cell attached to the pin assembly. Data collection and control of the test variables was via software (Figure 2.16).

Universal Micro-Tribometer:

The Universal Micro-Tribometer from CETR was used for most of the tribology tests. It has been designed for extensive use in tribology and materials research applications from macro- to micro- scale. Pin-on-disc mode was used in this research. Reciprocating friction tests were performed. The load was applied to the pin. The spindle on the bottom rotates to oscillate the plate back and forth while the pin was held stationary. All tribological parameters were recorded simultaneously during the test (Figure 2.17).
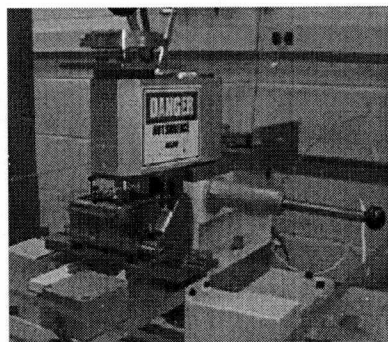
Figure 2.16 Plint Reciprocating Tribotester
(www.argonne.gov 2004)
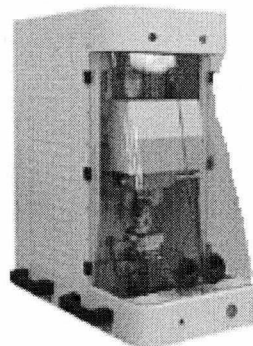
Figure 2.17 Universal Micro-Tribometer
(www.cetr.com 2004)

2.3. Methods and techniques

The methods and the techniques will be introduced in two parts: Total Artificial Joint Replacement and cell culture.

2.3.1 Total Artificial Joint Replacement (TRAJ)

The materials and the techniques for TRAJ will be introduced in detail in the following.

2.3.1.1 Materials preparation

A. Cleaning and sterilizing of stainless and ceramic samples

SS, Al_2O_3, ZrO_2, DLC-coated stainless steel balls and SS, DLC coated plates were prepared by the following protocol.

- Rinse samples in 50 ml fresh hexane solution in the ultrasonic cleaner for 60 seconds.
- Rinse samples in 50 ml fresh hexane solution in the ultrasonic cleaner for 10 seconds.
- Rinse samples with 50ml fresh hexane.
- Rinse samples in 50 ml fresh acetone solution in the ultrasonic cleaner for 60 seconds.
- Rinse samples in 50 ml fresh acetone solution in the ultrasonic cleaner for 10 seconds.
- Rinse samples with 50 ml fresh acetone.
- Rinse samples in 100 ml fresh distilled water in the ultrasonic cleaner for 60 seconds (twice).
- Rinse samples with 100 ml fresh distilled water.
- Dry samples with lint-free tissue.
- Air-dry samples in the dust-free fume hood at room temperature with UV light on for 30 minutes.

B. Cleaning, sterilizing, and pre-soaking of UHMWPE samples

UHMWPE pins and plates were prepared by following protocol.

Rinsing

- Rinse samples with tap water.
- Rinse samples in a 50 ml solution of 1% detergent in the ultrasonic cleaner for 60 seconds.
- Rinse samples with 100 ml distilled water.
- Rinse in fresh 100 ml distilled water in the ultrasonic cleaner for 5 minutes.
- Rinse samples with 100 ml fresh distilled water.
- Dry samples with lint-free tissue.
- Immerse samples in methyl alcohol for 3 minutes.
- Dry samples with lint-free tissue.

- Air-dry samples in a dust-free fume hood at room temperature for 30 minutes.

Pre-soaking

UHMWPE is pre-soaked in the lubricant to minimize fluid sorption during the wear run. Lubricant is FBS. This was done three weeks before the wear tests. Then the samples were weighed once a week.

2.3.1.2 Tribological tests

Tribological tests for this part of research were performed by using the Plint Reciprocating Tribology Tester. Pin-on-flat mode was used in the friction tests. The diameter of the pins is 12.7 mm. The size of the plates is 25.4mm x 50.8mm x 12.7mm. The plates were mounted in a rectangular cup that held liquid bovine serum as the lubricant. The distance the pin traveled was 25 mm. The frequency at which the flat was oscillated is 1 Hz. In this research, the average speed of the pin v (speed) = Frenquency x the distance = 1Hz x (25mm x 2) = 50mm/s. Different axial loads were applied to the pin. A 50N load was applied on all friction pairs. A 150N load was applied on all balls on UHMWPE plates. 50N, 100N, 150N, 200N, and 250N loads were applied on SS balls on UHMWPE plates. The total length was 4,284 cycles, and the total time was 60 minutes. Friction pairs are listed in Table 2.3. Friction force was recorded by software and processed later.

Table 2.3 Friction Pairs

Ball\Plate	SS	NFC2	NFC6	NFC7	UHMWPE
SS	√	√	√	√	√
Al_2O_3	√	√	√	√	√
ZrO_2	√	√	√	√	√
NFC6	√	√	√	√	√
UHMWPE	√	√	√	√	√

2.3.1.3 Wear analysis

The topography and wear of balls and plates were measured using a MicroXAM surface profiler after the friction tests. Images were done for both balls and plates. The wear volumes of the balls were given by the software directly. However, since the wear track of the plates is larger than the size that the profilometry can measure, the wear volumes could not be given directly.

Marks were made to separate the wear track into five equal distances. Then the wear volumes were measured for each of them. The total wear volume is the sum of the five parts.

Electron microscopes were also used to analyze the wear. For the SEM, the non-conductive samples (Al_2O_3, ZrO_2, and UHMWPE) were coated with gold film. These non-conductive samples were also analyzed by the ESEM.

2.3.2 Cell culture

The methods and techniques of cell culture will be introduced in detail in the following.

2.3.2.1 Sterilization

All glass supplies (graduated cylinders, bottles, dishes, beakers, and pipets), filters, and pipet tips were autoclaved for 20 minutes. Self-made glass-bottom dishes were sterilized by UV light for 25 minutes. Test materials were first cleaned by ethanol, and then dried in the hood. 25 minutes of UV light sterilization was applied to both of the surfaces. Then these materials were glued to the bottom of the glass-bottom dishes. The dishes were dried overnight before they were used for tissue culture.

2.3.2.2 Preparing cell culture media and solutions

The culture media for 3T3 cells was made with DMEM, 10% FBS, and 1% 100 unit/ml penicillin-streptomycin and was stored at 4°C. The FBS was heat inactivated in a water bath at 56°C for 30 minutes. The dissociated solution was made in a concentration of 0.5% Trypsin and 5.3 mM EDTA (10X) and was stored at -20°C. The freezing media was made with a concentration of 20% FBS and 10% DMSO in DMEM. The PBS was made with NaCl, KCl, KH_2PO_4, and $Na_2HPO_4.7H_2O$. It was stored at room temperature. The fixation solution was made with 4% paraformaldehyde (PFA), 50mM SPB, 60mM sucrose, and 0.1% glutaraldehyde. The SPB was made with $Na_2HPO_4.H_2O$, $Na_2HPO_4.7H_2O$ and DI water. The staining solution was made with a concentration of 0.5% Triton X-100, 5mg/ml BSA, and 2% Rhodamine-phalloidin in 100% methanol in PBS (1X).

2.3.2.3 Establishing a 3T3 cell bank

A tube of frozen 3T3 cells was used for the cell culture. This tube of cells was amplified and a 3T3 cell bank was established. To establish the bank the cells were thawed and cultured, split, and frozen. The protocols of these steps are listed below.

A. To thaw and culture cells from frozen cells

- Thaw the 3T3 cells in the warm water bath (37°C).
- Pipette 6 ml DMEM/FBS (37°C) culture media into a conical tube.

- Pipette thawed cells into the conical tube and spin in centrifuge at 1000 rpm for 2 minutes.

- Remove the old media from the cells with an aspirator, leaving a cell pellet behind.

- Add 3ml of DMEM/FBS (37°C) to the centrifuge tube, and resuspend the cells with a pipette until all cells are in suspension.

- Pipette 9 ml of DMEM/FBS (37°C) into a 100 mm culture plate.

- Add the cells in the conical tube to the media in the plate.

- Incubate the cells at 37°C in the CO_2 incubator for 24 hours.

- Remove the media in the culture plate with an aspirator.

- Wash the cells by adding 5 ml of DMEM/FBS (37°C) to the plate and gently roll the plate around.

- Remove the media in the culture plate with an aspirator.

- Add 9 ml of DMEM/FBS (37°C) to the plate and incubate at 37°C in the CO_2 incubator until the cells reach confluency (between 24-48 hours).

B. To split cells

- Remove the culture media from the culture plate with an aspirator.

- Wash the cells twice with 5 ml PBS.

- Pipette 900 µl of PBS on the cells and add 100 µl of 10X Trypsin (final concentration 1X).

- Gently roll the plate around so cells are bathed with Trypsin mixture.

- Remove 900 µl of Trypsin mixture from plate.

- Incubate the plate in the CO_2 incubator at 37°C for 4 minutes.

- Remove the plate from the incubator and gently rock it back and forth until the cells become loose.

- Add 5 ml DMEM/FBS (37°C) culture media into the plate and resuspend the cells with a pipette until all cells are in suspension.

- Pipette the cell suspension into a conical tube and spin in centrifuge at 1000 rpm for 2 minutes.

- Remove the old media from cells with an aspirator, leaving cell pellet behind.

- Add 3 ml of DMEM/FBS (37°C) to the centrifuge tube, and resuspend the cells with a pipette until all cells are in suspension.

- Prepare three 100 mm tissue culture plates (or three 250 ml flasks) for splitting by adding 9 ml of culture media to each plate.

- Add 1 ml of cell suspension to the 9 ml of culture media in each plate.

- Incubate the cells at 37°C in the CO_2 incubator until they reach confluence (between 24-48 hours).

C. To freeze cells

- Culture the cells until the cell reach approximately 80% confluency.

- Loosen the cells from the plates using the above protocol.

- Pipette the cell suspension into a conical tube and spin it in centrifuge at 1000 rpm for 2 minutes.

- Remove the old media from cells with an aspirator, leaving a cell pellet behind.

- Add 1 ml freezing media DMEM/FBS/DMSO to the cell pellet and pipette 15-20 times until all cells are in suspension.

- Pipette the cell suspension into a 2 ml microtube and put the tube in ice for 30 minutes before storing the tube in the freezer at -80°C.

By repeating the above protocols, cells can be amplified and a cell bank established for research on tested materials and is stored in the freezer at -80°C.

2.3.2.4 Tissue culture on test materials

A. Sterilization

Glass, PVA, Al_2O_3, Ni, PU-1, PU-2, TR-1, and TR-2 were immersed in 70% ethanol for 5 minutes and then were dried in the hood. These materials were exposed to UV light for 25 minutes on both sides.

B. Preparation of the culture plates with the materials to be tested

Self-made 2 ml sterilized glass-bottom culture dishes were used for this part of the cultures. The materials listed above were cut into small pieces and glued onto the bottom glass. Then the plates and the materials were sterilized by UV light for 15 minutes before cell culturing.

C. Concentrations

Two concentrations were used in the cell culture on the test materials: 200,000 cell/ml and 100,000 cell/ml. Cells were first counted by using a cell counting chamber, then the two different concentration solutions were made.

D. Cell culture on test materials

Dishes containing the test materials and a control dish were filled with 2 ml 200,000 cell/ml cell solution. A duplicate set of dishes was filled with 100,000 cell/ml cell solution. Then these 18 dishes were incubated in the CO_2 incubator for 2 days.

2.3.2.5 Fixation and staining

A. Fixation

In chemical terms, fixation makes cells permeable to staining reagents and cross-links their macromolecules so that they are stabilized and locked in position. Cells were fixed with formaldehyde or glutaraldehyde solution. Covalent bonds were formed among the free amino groups of proteins and thereby cross-link adjacent proteins with the treatment of formaldehyde or glutaraldehyde. Cultured cells were fixed with fixation solution at room temperature for 20 minutes. The dishes were then rinsed twice with warm PBS (1X).

B. Staining

The dishes with fixed cells were then filled with staining solution and incubated in a CO_2 incubator for 30 minutes. The cells were washed three times with a solution of 0.5% Triton X-100 and 5 mg/ml BSA in PBS (1X) after staining and then washed with PBS (1X). The dishes of cells were filled with DI water and then stored in the refrigerator for further analysis.

2.3.2.6 Viewing cultured cells

Different instruments were used to study the cells: an inverted optical microscope, a Confocal Microscope, an SEM, and an ESEM.

Under the inverted microscope, the cell cultures on transparent materials were clearly viewed. Since the biomedical inverted microscope is designed for transparent samples, analysis for the non-transparent samples was more difficult.

A Confocal Microscope can trace a fluorescence probe, but because the non-transparent materials in this research (PU-1, PU-2, and PVA) are all originally fluorescent, results cannot be conclusive even though analysis showed fluorescence.

For SEM analysis, the cell culture samples first dehydrated and then dried in a Critical Point Dryer. Samples were immersed in a series of ethanol solutions of the following concentrations: 30%, 60%, 70%, 80%, 90%, and 100% (twice) for dehydration. Each immersion was for 10 minutes. Then the samples were transferred to the pressure chamber of the critical point dryer. 100% ethanol was added until the chamber was full. CO_2 was then used to purge the samples until all ethanol was exhausted and the chamber was full of CO_2. The samples in the

dryer were dried at the critical point of CO_2 which is 1072 psi and 31.1°C. Then a high resolution super coater was used to coat a gold film on top of the samples.

The ESEM does not require a conductive sample. The samples can be wet and therefore the cells keep their original shape.

2.3.2.7 Characterization of the cell culture materials

2.3.2.7.1 Structure of the materials

The structures of the raw materials were investigated by using an Olympus BX60 microscope, an SEM, and an AFM. These structures have been explained in the beginning of this chapter.

2.3.2.7.2 Wettability

Wettability of these materials was investigated by Goniometer. The contact angles of DI water on the surface of these materials were measured and images of the drops on the surface of these materials were also taken.

2.3.2.7.3 Tribological tests

Tribology tests were conducted by using the UMT. Dry friction, lubricated friction, tissue culture lubrication tests were done. The friction mode was pin-on-disk. The applied force on the carriage was 5mN and constant. The test time was 10 minutes. The velocity was 1mm/sec. The lubricant was BSA solution with 0.15M NaCl. Wear analysis was done using Olympus BX60 microscope. The wear track images were taken.

2.4 Experimental phases

Two experimental phases were completed with this research: study on alternative bearing materials for Total Replacement Artificial Joints and study on tissue culture materials used for used in artificial joints. The following chapters discuss each experimental phase, their results and conclusions.

Chapter 3

Tribological performance of alternative bearing materials for TRAJ: results and discussion

In this chapter, the tribological performance of several candidate implant materials, including the DLC thin film coating on different plates, was investigated. A pin-on-flat contact configuration in reciprocating sliding was used for friction and wear testing. In current artificial joints consisting of metals, ceramics, and polymers, the wear debris causes the shortening of the implant's life. The objective of this research is to investigate the possibility of using carbon-coated materials as alternative bearing materials in artificial joints.

3.1. Presoaking measurements

UHMWPE has been used in artificial joints implants. The change of the creep property is important for implant materials. The UHMWPE samples were presoaked in bovine serum for different time period before the friction tests. The presoaking procedure of UHMWPE in lubricant can minimize the fluid sorption during the friction test runs. It can also reduce creep of UHMWPE (Figure 3.1, Armini et al. 1998). The relative creep decreased dramatically for the first few hours when the samples were presoaked showed in Figure 3.1. Presoaked for 5 hours could decrease relative creep to about 40%. The decreasing trend became slow afterwards. According to this result, the samples should be soaked more than 5 hours.
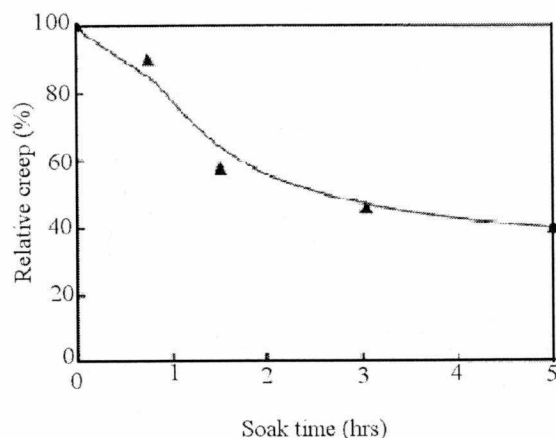
Figure 3.1 Static creep test measurements vs. soak time of UHMWPE (Armini et al. 1998)

Normally when a load is applied, a material will develop a full strain. This is not the same when the creep happens. The material continues to deform at a slow rate when a load is

applied. This behavior is called creep. Creep is the time-dependent part of strain resulting from stress. It occurs when a plastic part is subjected to a load for a longer period of time. At a constant stress and temperature, the creep rate is approximately constant for a long period of time. After a certain amount of deformation, the creep rate increases and fracture soon follows. High temperature can be an accentuating factor. Decrease of the creep rate will increase the service time of the material.

Eight UHMWPE samples were measured for presoaking investigation. The samples were weighted before, in between, and after soaking. Each sample was weighed 3 times and the weight is the average of the three. Weight measurements of the samples before soaking were listed in Table 3.1 and after soaking were listed in Table 3.2. The net weight gain and gain percentage were listed in Table 3.3. The total soaking time was three weeks. The weight increased in the first week. There were no weight changes after the first week. The average weight gain percentage of the 8 samples is 3.83% and the standard deviation is 0.0033. The result showed that the measurements dispersed narrow from the average value.

UHMWPE samples rapidly absorbed the bovine serum fluid and reached a steady state of saturation. This result is similar to those reported by Blanchet et al. (2002). They stated that 'the time-response of serum absorption is biphasic, with an initial *soak-in* phase (<1 week) of rapidly increasing mass before settling to a steady-state phase of mass increasing more gradually and linearly with time'.

Table 3.1 Measurements of Weight of UHMWPE Samples before Soaking

UHMWPE	1	2	3	Average
1	2.152510g	2.152510g	2.152520g	2.152513g
2	2.149765g	2.149770g	2.149785g	2.149773g
3	2.145740g	2.145740g	2.145740g	2.14574g
4	2.147875g	2.147865g	2.147885g	2.147875g
5	2.148780g	2.148770g	2.148770g	2.148773g
6	2.148435g	2.148430g	2.148440g	2.148435g
7	2.148640g	2.148640g	2.148655g	2.148645g
8	2.148080g	2.148080g	2.148075g	2.148078g

Table 3.2 Measurements of Weight of UHMWPE Samples after Soaking for 3 Weeks

UHMWPE	1	2	3	Average
1	2.153380g	2.153370g	2.153370g	2.153373g
2	2.150540g	2.150540g	2.150540g	2.150540g
3	2.146510g	2.146460g	2.146510g	2.146493g
4	2.148620g	2.148600g	2.148600g	2.148607g
5	2.149580g	2.149580g	2.149580g	2.149580g
6	2.149280g	2.149260g	2.149250g	2.149263g
7	2.149540g	2.149550g	2.149540g	2.149543g
8	2.149010g	2.149010g	2.149010g	2.149010g

Table 3.3 UHMWPE Weight Gain after Soaking in Bovine Serum for 3 Weeks

UHMWPE	Weight Gain	Gain Percentage
1	0.000860g	4.00%
2	0.000767g	3.57%
3	0.000753g	3.51%
4	0.000732g	3.41%
5	0.000807g	3.76%
6	0.000828g	3.86%
7	0.000898g	4.18%
8	0.000932g	4.34%
Average		3.83%
Standard Deviation		0.0033

3.2. Friction tests

3.2.1 Surface roughness measurements

When two solids are brought together, they touch first where high hill on one contact the surface of the other. So the true contact surface is different from the bulk surface area. The smoother the surface, the larger the contact area. Therefore surface roughness is a very important

factor in friction. A lower surface roughness often yield a lower friction coefficient.

Before the friction tests were performed the surface roughness, Ra, of the SS, NFC2, NFC6, NFC7, and UHMWPE plates was measured using a profilometer (Table 2.4). The average roughness is the total area of the peaks and valleys divided by the evaluation length. It is expressed in μm (thousandths of a millimeter). Ra is the most commonly used parameter to describe the average surface roughness and is defined as an integral of the absolute value of the roughness profile measured over an evaluation length:

$$Ra = \frac{1}{l} \int_0^l |z(x)| dx$$

The average surface roughness of the plate materials is listed in Table 2.4.

Table 3.4 Average Surface Roughness of Plate Materials

	SS	NFC2	NFC6	NFC7	UHMWPE
Ra (μm)	0.028	0.018	0.0197	0.020	0.160

Among all the samples, UHMWPE has the greatest surface roughness. SS plates have an average surface roughness Ra of 0.028 μm. NFC2, NFC6, and NFC7 are all the same kind of SS that have coated with DLC films. The coatings change the surface roughness. All of the coated plates have lower average surface roughness. For tribology tests, the change of surface roughness will also cause the change of the plates' tribological performance.

3.2.2 Friction tests

The vast majority of wear testing for joint material involves UHMWPE as a bearing surface. Over the years wear testing method of implant materials has evolved by trying to match the laboratory test results with clinical performance and experience. The wear rate for UHMWPE is known to be motion-dependent due to the molecular structure of the material. Indeed the test method that has shown the best correlation with clinical performance for UHMWPE in hip joint implant is the multi-directional motion hip joint simulator. Such tests are too involved and expensive for alternative material screening purposes, although multi-directional motion may still be needed in even screening tests involving polyethylene. Since all the materials being evaluated in the present study are isotropic and their wear is unlikely to be direction dependent, the contact configuration of pin-on-disk (pin-on-disk is also called as pin-on-flat, pin-on-plate, ball-on-flat, ball-on-disk, ball-on-plate etc.) in reciprocating motion of ASTM Standard F732 for evaluating

material for joint prostheses was used for testing (Figure 3.2). Of course, it is recognized that hip-simulator testing will be necessary before any of material tested can be a candidate for joint implant.

All the experiment specimens and holders were cleaned and sterilized before the friction tests. The plates were secured in the rectangular cup specimen holder by four screws (Figure 3.3). Lubricant fluid was added until the whole plate was totally immersed in the bovine serum. The friction tests were performed with the contact area of the friction pair submerged in the lubricant fluid. A repeat test was done for all the friction pairs.
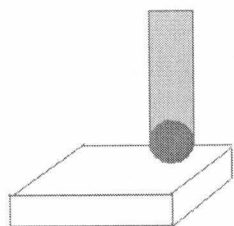
**Figure 3.2 Schematic picture
of the pin-on-disk test**
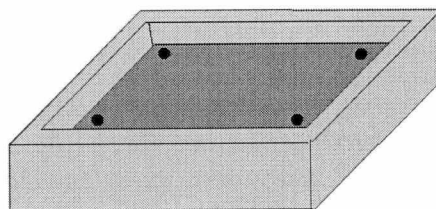
**Figure 3.3 Schematic picture
of the holder with plate**

The software automatically recorded the experiment data. One example data file is listed in Appendix A. This is the friction test data of SS ball on SS plate recorded by the software of the Plint Reciprocating Tribology Tester. The data were then processed using Excel. The curves of friction coefficient vs. time were plotted.

The distance the pin traveled was a 25 mm stroke length. The frequency at which the flat was oscillated is 1 Hz. In the part of the research, the average speed of the pin v (speed) = Frenquency x the distance = 1Hz x (25mm x 2) = 50mm/s. A 50N load was first applied on all friction pairs. To evaluate pin materials, the friction tests of SS, Al_2O_3, ZrO_2, NFC6, and UHMWPE balls were all conducted on the same plate. The wear tracks were marked right after the tests. The results of the friction tests were plotted as curves of friction coefficient vs. time as shown below. The friction coefficient curves show the trend of gradual increase in friction coefficient to a maximum value during the early stage, just 500 seconds. Thereafter, the friction decreased to a near-steady value, as in the tests of SS ball on SS plate (Figure 3.4), Al_2O_3 ball on SS plate (Figure 3.5), and ZrO_2 ball on SS plate (Figure 3.6).
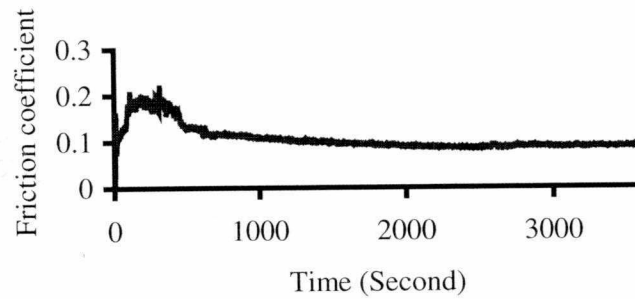
Figure 3.4 Friction coefficient vs. time of pin-on-disk test (SS ball on SS plate)
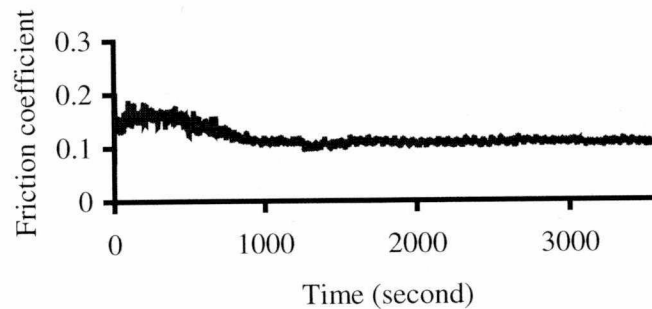
Figure 3.5 Friction coefficient vs. time of pin-on-disk test (Al$_2$O$_3$ ball on SS plate)
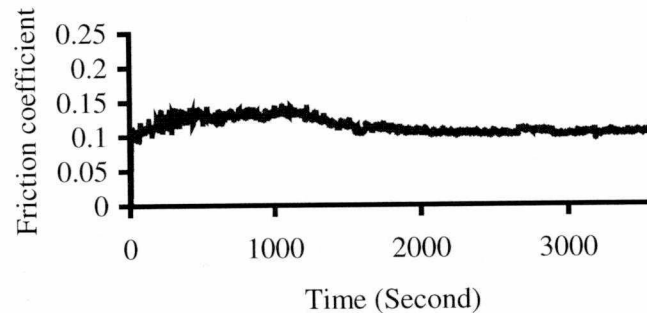
Figure 3.6 Friction coefficient vs. time of pin-on-disk test (ZrO$_2$ ball on SS plate)

This friction trend and the magnitude of the friction coefficients are typical for boundary lubrication regimes. The increase in the friction in the early stage is the result of run-in phenomenon. The average friction coefficients are 0.087 for SS ball on SS plate, 0.110 for Al$_2$O$_3$ ball on SS plate, and 0.115 for ZrO$_2$ ball on SS plate.

The friction characteristics of the tests with the DLC coated NFC6 ball and UHMWPE

pin were different from SS, Al_2O_3 and ZrO_2. They do not show the increasing period; they have steady friction coefficients over time.

During the test with the NFC6 ball, the friction coefficient remained steady at a value of about 0.052 for the entire duration of the test (Figure 3.7). This frictional behavior can be attributed to the very low friction of the DLC coating used. Under a boundary lubrication regime of the current test conditions the measured friction coefficients consist of contributions from shearing of the fluid film, the boundary film and asperity contact interface. The DLC coating has been shown to exhibit very low friction coefficients under dry sliding contact in which friction is due primarily to the shearing of asperity contact interface (Erdemir et al. 1999, Erdemir et al. 2000). Consequently, the contribution of asperity friction to the measured friction value in the tests with the DLC coating is expected to be minimal.
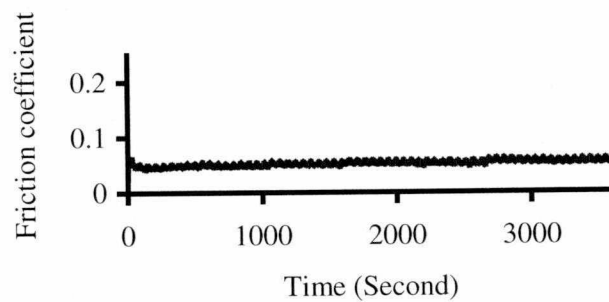
Figure 3.7 Friction coefficient vs. time of pin-on-disk test (NFC6 ball on SS plate)

During the test with the UHMWPE pin, the friction coefficient remained steady at a much lower value, a value of about 0.033, for the entire duration of the test (Figure 3.8). These friction properties of UHMWPE explain the continued usage of this material in joint implant replacement even with the disadvantage of wear debris causing a shortened life of the implant.
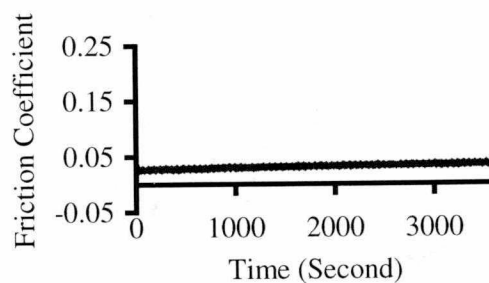
Figure 3.8 Friction coefficient vs. time of pin-on-disk test (UHMWPE pin on SS plate)

A summary of the friction tests of the various balls on SS plate is given in Figure 3.9. On the SS plate, the friction coefficient of the UHMWPE pin's test is the lowest. The ZrO_2 ball has the highest friction coefficient. The DLC coated NFC6 ball has a friction coefficient of 0.052, which is higher than the UHMWPE pin's test, but much lower than ceramics Al_2O_3 and ZrO_2's friction coefficients. It is half of the value for the two ceramic balls (Al_2O_3 and ZrO_2) when sliding against the SS plate. The SS ball has a friction coefficient of 0.087. After coating the SS ball with a DLC film the friction coefficient dropped to 0.052. The standard deviations for the tests of SS, Al_2O_3, ZrO_2, NFC6, and UHMWPE balls on SS plate are 0.0192, 0.019, 0.010, 0.004, and 0.002.
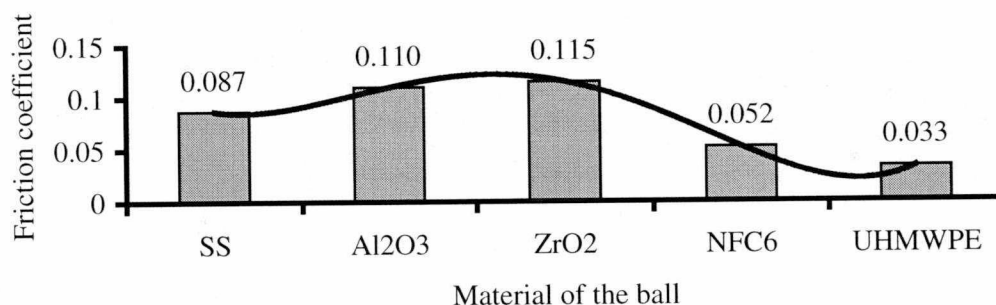
Figure 3.9 Comparison of friction coefficients of different balls on a SS plate

These friction results indicate that if ceramic bearing surfaces are matched against metal bearing surfaces in artificial joints, the friction coefficient will be relatively high. A requirement for materials used in artificial joints is low friction. The friction in the natural joint is very low. A feature of the current commonly used configuration of ceramic or metal against UHMWPE bearing surfaces is the low friction coefficient. The tests with DLC coatings in the present study show relatively low and steady friction coefficients. Thus, from a friction standpoint, replacement of an UHMWPE bearing surface with a DLC coated metal surface (NFC2, NFC6, and NFC7) in artificial joint is a viable option.

Other combinations were tested on NFC2, NFC6, NFC7, and UHMWPE plates. Friction coefficients of balls on NFC2, NFC6, NFC7, and UHMWPE plates are shown in Figure 3.10, Figure 3.11, Figure 3.12, and Figure 3.13.
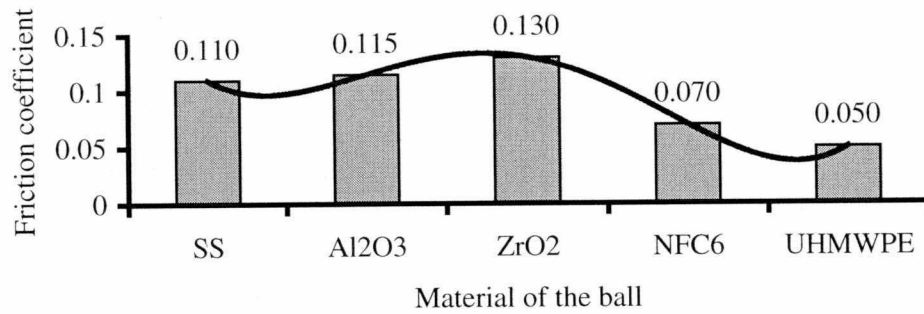
Figure 3.10 Comparison of friction coefficients of different balls on a NFC2 plate
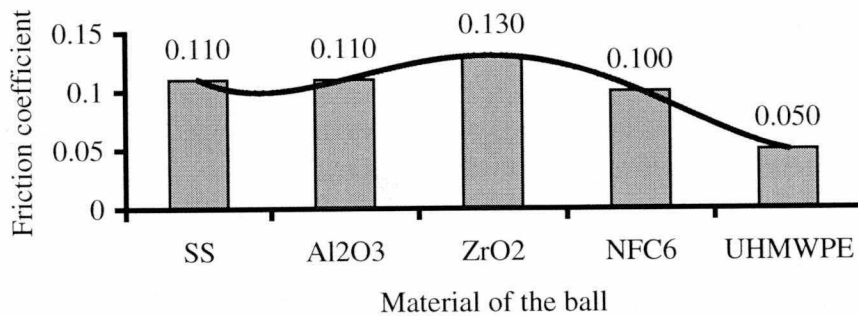
Figure 3.11 Comparison of friction coefficients of different balls on a NFC6 plate
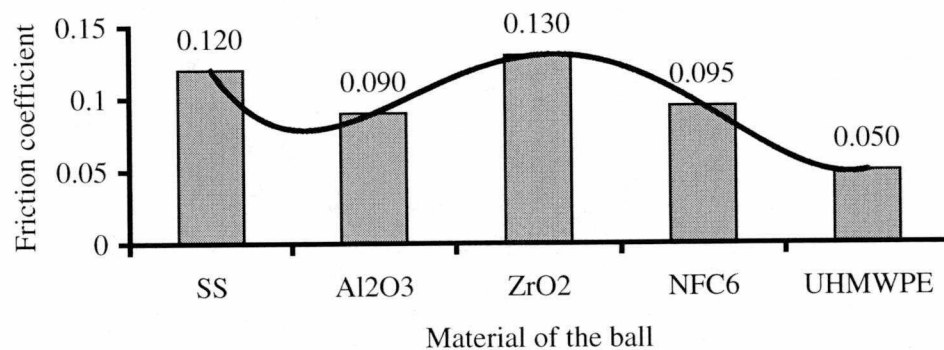
Figure 3.12 Comparison of friction coefficients of different balls on a NFC7 plate
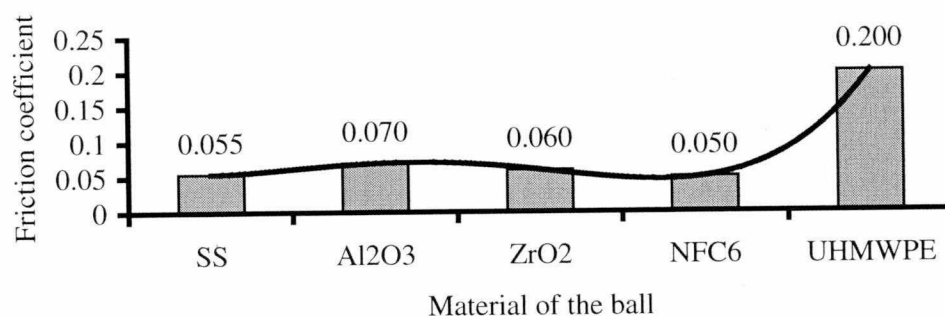
Figure 3.13 Comparison of friction coefficients of different balls on an UHMWPE plate

The measured friction coefficients of the balls varied with the type of the plates. The ceramic ZrO_2 balls have the highest friction coefficients on all plates except on the UHMWPE plate. The UHMWPE pins have the lowest friction coefficients on all plates except on the UHMWPE plate. UHMWPE has the highest friction coefficient on the UHMWPE plate. After coated with DLC thin film, NFC6 balls have lower friction coefficients than SS balls on all plates. This experiment showed that the coating improved the tribological performance of the balls. UHMWPE has the best friction performance among the balls tested. NFC6 has the second best friction performance. In summary, the friction coefficients of experiments on SS, NFC2, NFC6, NFC7, and UHMWPE plates are listed in Table 3.5.

Table 3.5 Friction Coefficients for All Tests

Ball\Plate	SS	NFC2	NFC6	NFC7	UHMWPE
SS	0.087	0.110	0.110	0.120	0.055
Al_2O_3	0.110	0.115	0.110	0.090	0.070
ZrO_2	0.115	0.130	0.130	0.130	0.060
NFC6	0.052	0.070	0.100	0.095	0.050
UHMWPE	0.033	0.050	0.050	0.050	0.200

Student t-test is designed for the comparison of two samples. Since there are more than two samples in the tests, the variances of the friction test results were analyzed using analysis of variance – an extension method of student t-test. The calculation procedures were shown with the example of balls on SS plate.

There are five ball samples and each sample was conducted three friction tests. The degrees of freedom of total, between groups, and within groups are 14, 4, and 10.

The sum of squares of total is

$$\sum y^2 - (\sum y)^2 / N = 0.0171$$

where y is the friction coefficient and N is the total number of experiments.

The sum of square between groups is

$$\sum T^2 / 3 - (\sum y)^2 N = 0.0155$$

where $T_i = \sum y_i$.

The sum of squares within groups is

The sum of squares of total - The sum of square of between groups = 0.0016

The variance between groups is

The sum of squares between groups/degrees of freedom between groups = 0.0039

The variance within groups is

The sum of squares within groups/ degrees of freedom within groups = 0.0002

The Variance ratio F is

The variance between groups/ The variance within groups = 19.5000

The p value was then checked from the F table and p value was determined.

The p values were calculated using an online software (Pezzullo 2004). An example calculation including input and output of the balls on SS plate is shown in Appendix B. The p-values of balls on SS, NFC2, NFC6, NFC7, and UHMWPE are 0.0000, 0.0000, 0.0001, 0.0001, and 0.0000. A p-value less than 0.05 indicate that there is a significant difference somewhere among the various groups (Pezzullo 2004). The p values in these experiments indicated that there is a highly significant difference among these samples (p<0.01).

Previously, friction research has been focused on two aspects: adhesion and the interlocking of asperities. The adhesion theory assumes that two contacting surfaces will bond or weld together and the resulting bonds must be broken for sliding to occur. The interlocking theory views surfaces as being composed of relatively rigid asperities which must follow complex paths to move around or over each other. The modern view is that friction is primarily due to adhesion that is limited by the oxides and adsorbed gases found on all surfaces during sliding and destroyed by peeling when a load is removed. In some instances of very rough surfaces, where some of the roughness may be due to carbide particles, there may be a second component of

friction due to asperity collision (Booser 1984). In my study, results showed that another aspect, the plastic deformation should be focused as well for the hard-soft friction pairs.

A SS ball showed different friction coefficients on different plates (Table 2.5), because the adhesion forces are different and surface roughness has little effect. For DLC-coated balls the slight change in the coatings did not bring a large change in the friction coefficient. However, for the NFC6 balls on DLC-coated plates (NFC2, NFC6, and NFC7), The friction coefficients varied more because of the chemical composition of the ball and plates.

UHMWPE is a soft material compared to the other balls and the surface roughness of UHMWPE is larger. The difference of the friction coefficient is due to both the surface adhesion between the different friction pairs, and to the surface roughness.

When large loads were applied to select materials pairs the friction coefficient decreased as the applied load increased. The effect of increasing the contact pressure between clean surfaces causes the plastic deformation and is to increase adhesive bonding over the entire macroscopic area when causes plastic shear flow at the original surface. When 150N load was applied for balls on the UHMWPE plate, unexpectantly the friction coefficient did not increase for some balls (Figure 3.14). Figure 3.14 shows no change in friction coefficient of an UHMWPE pin on an UHMWPE plate was observed. ZrO_2, and NFC6 balls' tests showed a decrease in friction coefficients. SS and Al_2O_3 balls' tests showed an increase in friction coefficients.
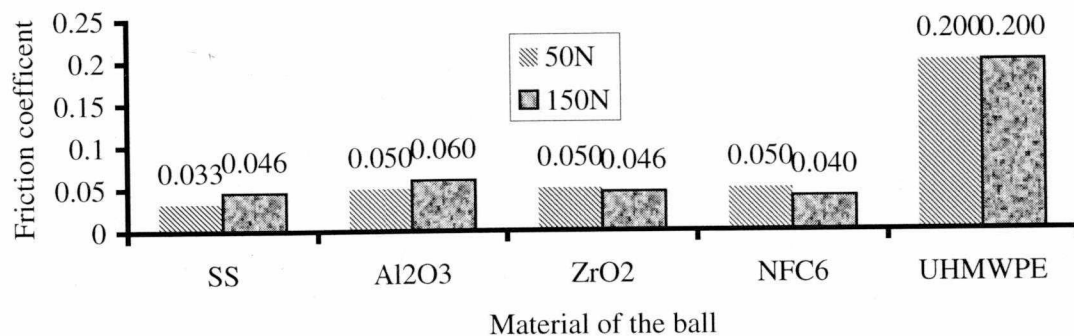
Figure 3.14 Friction coefficients of different balls on an UHMWPE plate under 150N

The student t-test method was used to analyze the difference between the two loads. The p values were calculated using an online software (Pezzullo 2004). The p values of SS, Al_2O_3, ZrO_2, NFC6, and UHMWPE are 0.011, 0.038, 0.288, 0.023, and 1.000. The results showed that experiments of UHMWPE under two loads are the same. The others showed differences at

different levels. The difference of ZrO_2 is not significant (p>5%). The differences of SS, Al_2O_3, and NFC6 are significant (p>1%).

When 50N, 100N, 150N, 200N, and 250N were applied on SS balls on UHMWPE plates (Figure 3.15), a similar result was observed. For the tests of a SS ball on UHMWPE under different loads, the friction coefficient decreased when the load changed from 100N to 150N. At 50N and 100N, the friction coefficient is 0.055. At 150N, 200N, and 250N, the friction coefficient is 0.050. The increase of the load caused deformation of the UHMWPE and the change of the thickness of the lubricant film. A combination of these factors caused the decrease of the friction coefficient when applied loads were changed.
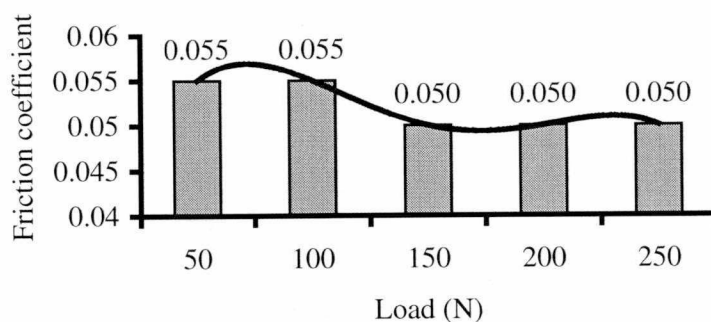
Figure 3.15 Friction coefficients of SS ball on UHMWPE plate under different loads

The variance of this set of tests was analyzed with the online software and the p is 0.155, which shows that the variance of the tests under different loads tested is not significant.

3.3 Wear

The Micro-XAM optical surface profilometer was used to measure the wear volume on the balls and flat samples after the friction tests. A Scanning Electronic Microscope (SEM) was used to investigate the worn surfaces. The non-conducting ceramic samples were sputter coated with a thin layer of Au prior to examination in the SEM to prevent charges. An Environmental Scanning Electronic Microscope (ESEM) was used to investigate the worn surfaces of UHMWPE.

The topographies from the micro-XAM surface profilometer of wear scars of each of the various ball materials on a SS plate are shown in Figure 3.16, Figure 3.17, Figure 3.18, Figure 3.19, and Figure 3.20.
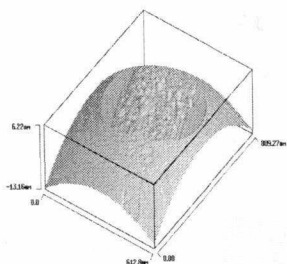
Figure 3.16 Morphology- SS

809.27 μm x 612.82 μm
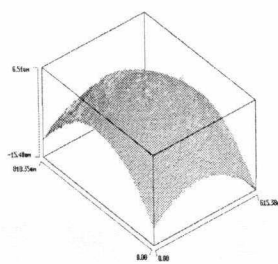
Figure 3.17 Morphology- Al₂O₃

810.35 μm x 615.38 μm
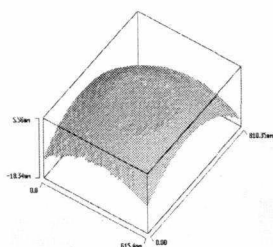
Figure 3.18 Morphology- ZrO₂

810.35 μm x 615.38 μm
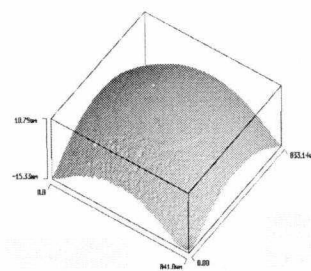
Figure 3.19 Morphology- NFC6

833.14 μm x 841.03 μm
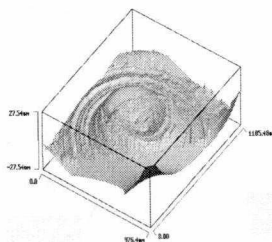
Figure 3.20 Morphology- UHMWPE

1185.48 μm x 976.41 μm

Comparing the topography of the balls on the SS plate, the NFC6 ball shows the lightest wear track (Figure 3.16). The wear track can be clearly seen on the flat specimen. In tests with DLC coated balls only a slight dislocation was observed (Figure 3.19). Quantitative measurement of wear on the plate was difficult because of the roughening of the wear track and, perhaps, deposition of some material from the bovine serum lubricant.

UHMWPE is a soft material compared to the other candidate materials used in this study. The UHMWPE pin shows the greatest wear against the SS plate even though it has the lowest friction coefficient on the SS plate (Figure 3.20). The wear scar is rough and large. The wear

volumes from the balls of the two ceramics (Al_2O_3 and ZrO_2) and the SS are in between and the wear scars are smoother compared with other balls and pins (Figure 3.17, Figure 3.18). The wear volume of the DLC thin film coated ball on a SS plate is much lower than for both ceramics and SS balls. In some of the repeat test over DLC coatings, no measurable wear was detected.

Different balls on other plates, NFC2, NFC6, NFC7, and UHMWPE, were also measured with a micro-XAM surface profilometer and part of the topography are shown in Figure 3.21 (SS ball on NFC2 plate) and Figure 3.22 (Al_2O_3 ball on NFC6 plate). Unlike the experiments on the uncoated SS plate, a few tiny debris particles were found on the worn area of all of the other balls.
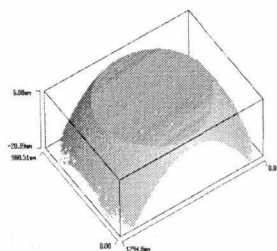
Figure 3.21 Morphology- SS
1294.83 μm x 980.51 μm (on NFC2)
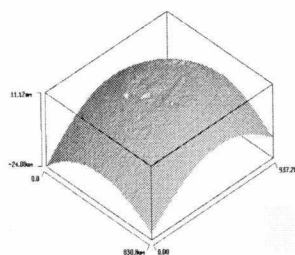
Figure 3.22 Morphology- Al_2O_3
937.28 μm x 830.77 μm (on NFC6)

The wear results from the present study are even more significant that the friction results in terms of consideration for joint application. A combination of ceramic and metallic bearing surfaces produced the most wear and the highest friction coefficient. The DLC coating sliding against uncoated SS showed little or no wear on either the coating or the uncoated steel counterface, thereby eliminating the generation of wear debris. Since osteolysis with artificial joint use is due to wear debris, elimination of wear debris with the DLC coating would be beneficial.

Wear on the plates was also observed with a micro-XAM surface profilometer. Since the tracks are long, the end and the middle parts of the track of a SS ball on a SS plate were recorded separately (Figure 3.23). The other balls (Al_2O_3 ball, ZrO_2 ball, DLC thin film coated ball, and UHMWPE pin) on SS plates were recorded in a similar manner (Figure 3.24, Figure 3.25, Figure 3.26, Figure 3.27).
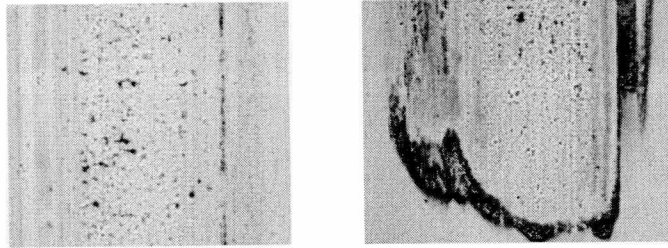
Figure 3.23 Wear track on the plate (SS ball on SS plate)

a. left: the middle of the track; b. right: the end of the track
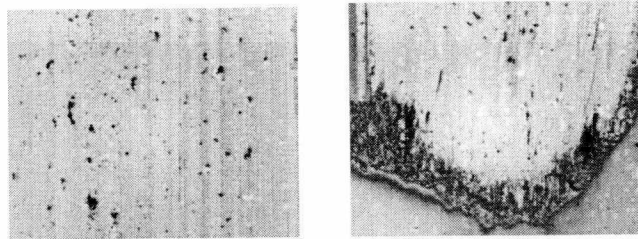
Figure 3.24 Wear track on the plate (Al_2O_3 ball on SS plate)

a. left: the middle of the track; b. right: the end of the track
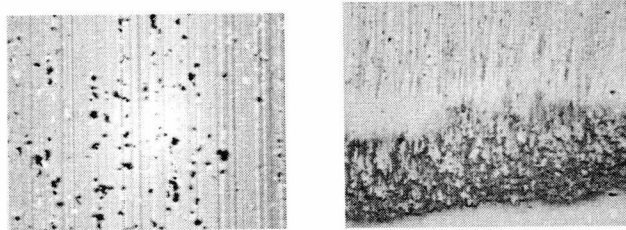
Figure 3.25 Wear track on the plate (ZrO_2 ball on SS plate)

a. left: the middle of the track; b. right: the end of the track
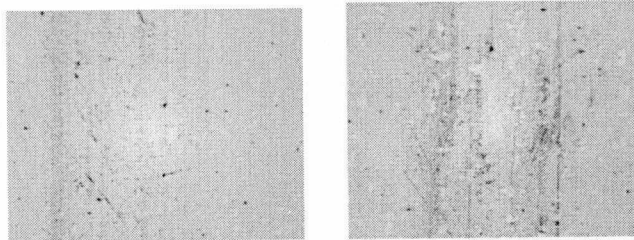
Figure 3.26 Wear track on the plate (NFC6 ball on SS plate)

a. left: the middle of the track; b. right: the end of the track
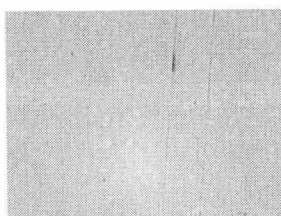
Figure 3.27 Wear track on the plate (UHMWPE pin on SS plate)

SS, Al_2O_3, and ZrO_2 balls had larger and deeper wear tracks compared to the NFC6 ball and UHMWPE pin. The NFC6 ball and UHMWPE pin produced only tiny wear on the surface of the SS plate. This can be also seen from the wear rate of the experiments (Figure 3.28). In this figure the wear rate of the SS plate was calculated using the equation of calculating the wear rate is $k = V / F * s$, where F is the normal load, s the sliding distance, V the wear volume and k the specific wear rate. The UHMWPE pin had no wear track, but the wear of the pin itself was greater. Based on the wear of the balls, NFC6 has the least wear and also the smaller friction coefficient. The DLC thin film coated NFC6 ball is a good candidate for implant material.
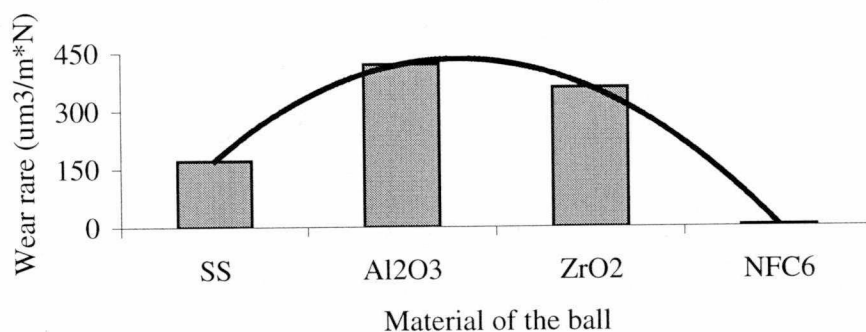
Figure 3.28 Wear rate of balls on SS plate

The statistic calculation of this set of experiments showed that p = 0.000, which showed that the differences among the groups are highly significant.

The topography analysis showed that the tracks from the SS, Al_2O_3, and ZrO_2 balls had the micro cracks. These could be critically important because of the potential for subcritical cracks to propagate under cyclic loading of the joint in function. This phenomenon, however, was beyond the scope of this thesis. Plowing and delamination showed on the surface of the plate (Figuer 3.28, Figure 3.29). More deformation showed in the middle of the wear track. Surface

characterization by SEM was used to assess the predominant mechanisms of wear in tests with the various friction pairs. Figure 3.28 shows the SEM images of wear track on the steel plate that was tested against the SS ball. There is clear evidence of abrasive wear mechanism as scratches running in the direction of sliding are seen. At higher magnification, there is also evidence of polishing wear and corrosive wear as well. Similar groove features as observed for steel plate (Figure 3.28) were also observed on the mating SS ball surface (Figure 3.29).

In the tests with the ceramic balls Al_2O_3 and ZrO_2, the wear on the steel plates occurred primarily by an abrasive mechanism. Figure 3.30 shows a typical wear track on the plate with relatively deep scratches and grooves. With the hardness of the two ceramics significantly higher than the hardness of the SS plate, it is not surprising that abrasive wear is the predominant wear mechanism. For joint applications, abrasive wear that can produce relatively hard wear debris is undesirable. Wear rate may increase as a result of third body wear and is faster for hard than soft third bodies. Figure 3.31 shows the SS plate surface tested against a DLC coated ball. There was slight coloration but no evidence of wear or surface damage was observed.
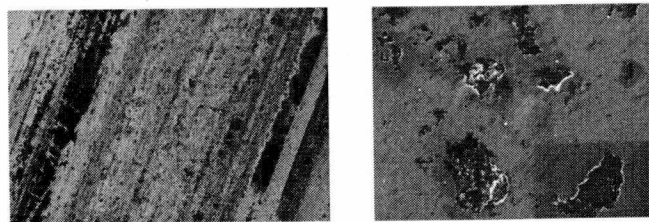
Figure 3.29 SEM images of the wear track of SS ball on SS plate
(left: plate, 140x; right: ball, 600x)
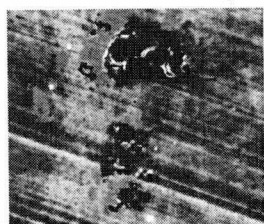
Figure 3.30 SEM micrograph of SS plate tested against ZrO$_2$ ball: showing abrasive wear scratches and grooves (1000x)

Figure 3.31 SEM micrograph of SS plate tested against DLC-coated balls: showing no evidence of wear

The ESEM research showed that the surface of the UHMWPE plate had abrasive

scratches and plowing (Figure 3.32). Wear debris stayed on top of the surface when the UHMWPE plate was tested with the ZrO_2 ball.
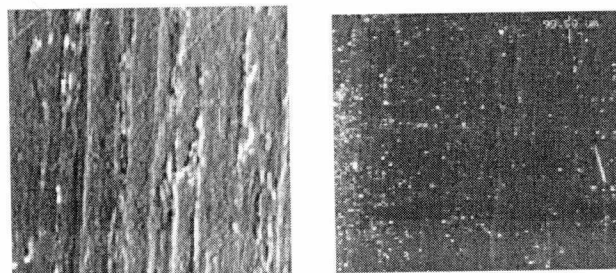
Figure 3.32 ESEM micrograph of UHMWPE (left: SS ball; right: ZrO_2 ball)

The results of these tests clearly show that DLC coated bearing against uncoated SS materials is a viable bearing surface combination for an artificial joint. The lower friction coefficient and wear resistance of this combination are desirable tribological properties for artificial joint material. Joint simulator testing of the combination will be used to confirm the viability of the combination.

Chapter 4

Tribological performance of materials as scaffolds for cell growth:
Results and discussion of cell culture – a tissue engineering approach

To construct biocompatible artificial implants, there are two main strategies for modulating the cell-material interactions. One is to create inert surfaces. These surfaces prevent cell adhesion, protein adsorption, and ECM's deposition. The other is to create a surface to which cells can attach, proliferate, and function. The tissues being explored by biological engineers include skin, cartilage, bone, tendon, intestine, heart valves, bone marrow, and trachea. This research was targeted towards joint cartilage.

Joint cartilage normally does not regenerate in the body; hence, damage from injury or illness tends to increase over time. Current clinical practices treat damaged cartilage by the use of tissue transplants or prosthetic implants. While these surgical procedures restore joint function, they can also present long-term complications. Tissue engineering focuses on the creation or regeneration of tissues as an alternative to cartilage replacements. Over the last decade the research has focused on cell-based repair approaches for articular cartilage lesions. Utilizing engineering principals, tissues can be generated using scaffolds that support encapsulated cells and their production of tissue matrix materials (Service 1995; Caplan et al. 1997; Grande et al. 1999; Temenoff at al. 2000; Raimondi et al. 2002; Ashammakhi et al. 2003).

In this research, different materials were compared as cell-culture scaffolds. Materials are Glass (SiO_2), PVA, Al_2O_3, Ni, PU-1, PU-2, TR-1, and TR-2. The basic properties of these materials have been reviewed in chapter 2.

4.1 Sterilization of matrix materials

Biomaterials must be non-toxic, biocompatible, effective and sterilizable. Sterilization methods for biomaterials include autoclaving, γ-irradiation, exposed to ethylene oxide gas, dry heating, and various chemical treatments. All of my matrix samples were sterilized by ethanol treatment followed by UV light as described in chapter 2.

The 70% ethanol solutions affected the TR-1 and TR-2 samples which became sticky and cloudy. After 5 minutes of treatment, it could be observed that the coating on the surface of the TR-1 and TR-2 was peeling off slowly. After the sterilization using ethanol, the surfaces of the TR-1 and TR-2 were different from their original surface. Part of the coating was dissolved in the ethanol solution, and the majority of the coating had settled on the transparency still. The surfaces

of the TR-1 and TR-2 showed both base material PET and coating clumps. Under the fluorescence microscope the coating fluoresced, but the base material PET did not.

For metal and ceramic materials, both of the sterilization methods have no visible effect on the materials. However, UV can have non-visible effects on the polymers since radiation can cause bonds in the molecular chains in the polymer to break and, in some cases, form cross-links (Gupta et al. 1983; Gidling et al. 1979; Chu et al. 1983; Puolakkainen et al. 1993; Ijiri et al 1994). This UV radiation process is called photodegradation and ultimately causes cracking, chalking, color changes and the loss of physical properties (Figure 4.1).
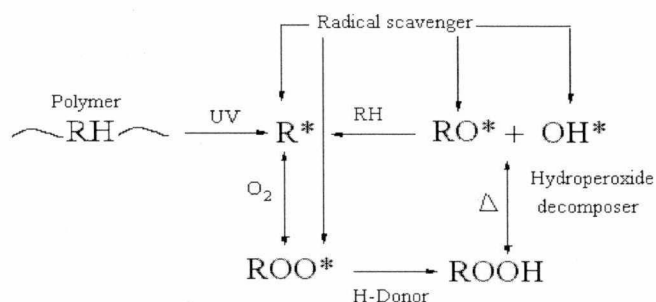
Figure 4.1 Schematic picture of UV light initiated photodegradation on polymers

In order to investigate the effects of UV light on the test materials, tensile tests were conducted using an Instron 4466 Universal Tensile Tester. Tensile tests were designed to measure the ultimate strength (static testing) and cycles to failure (dynamic testing). The ultimate strength is used by designers to avoid structural failure by keeping well below the ultimate strength limit. The dynamic tests are used to predict material life. Tensile stress (σ) is the applied force per unit of original cross-sectional area of the specimen $\sigma=F/A$, where σ is the stress, F is the force applied, and A is the cross-sectional area. Strain is defined as the ratio of increase in length to original length. $\varepsilon=\Delta L/L$, where ε is the strain, ΔL is the length increase, and L is the length of the original length (Figure 4.2). Young's modulus (E) is key to understanding the mechanical properties of a material. Unlike metals and ceramics, E for polymers is often a time dependent viscoelastic modulus. When load is applied to polymers they stretch instantaneously and elongate viscously as the macromolecules find new avenues for relaxing and uncoiling.

The polymer materials PU-1, PU-2, PVA, TR-1, and TR-2 were exposed to UV-light for different periods: 20 minutes, 40 minutes, and 60 minutes. The sterilization time used in this study was 40 minutes. Then these samples were cut into standard size and then tested. Each

sample was tested four times. The results were plotted as stress vs. strain. The results for TR-1 are shown in Figure 4.3, Figure 4.4, Figure 4.5, and Figure 4.6 as representative of all tested samples.
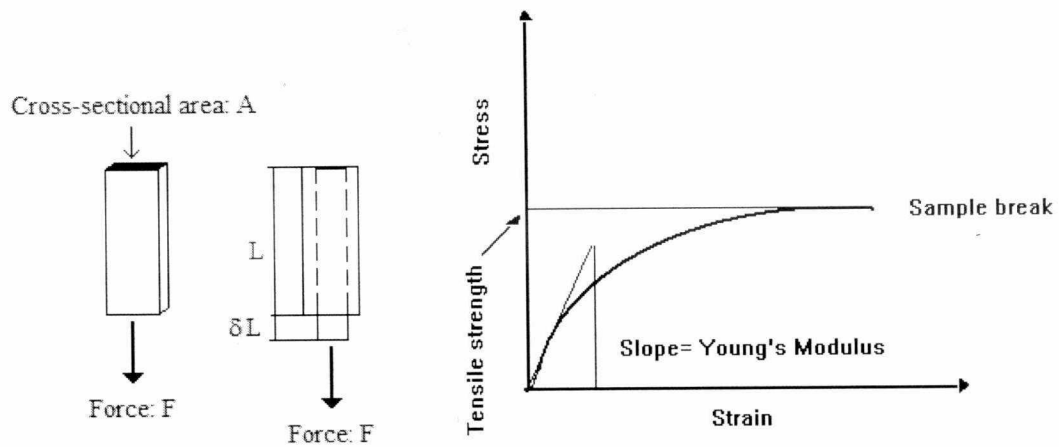
Figure 4.2 Schematic pictures of stress-strain tensile behavior

The TR-1 samples that have been sterilized by UV light showed a similar tensile strength to those samples that were not exposed to UV-light. Also, UV light had no effect on the TR-1 samples that had been sterilized for 20 to 60 minutes.
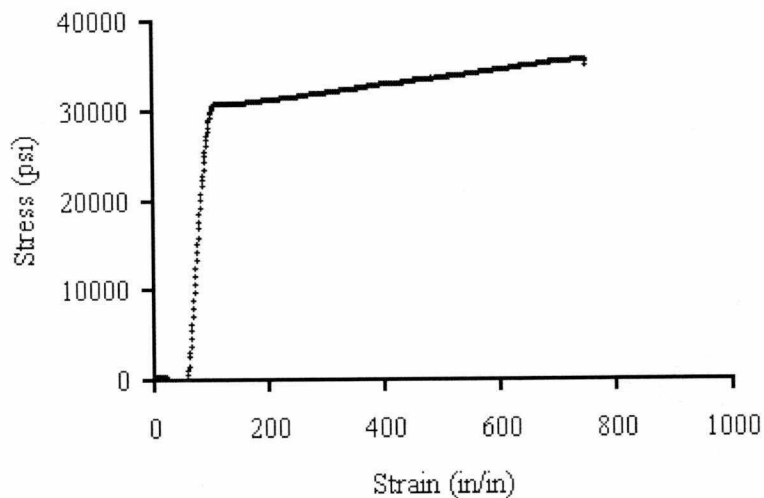
Figure 4.3 Stress-strain tensile behavior of TR-1 (not exposed to UV light)
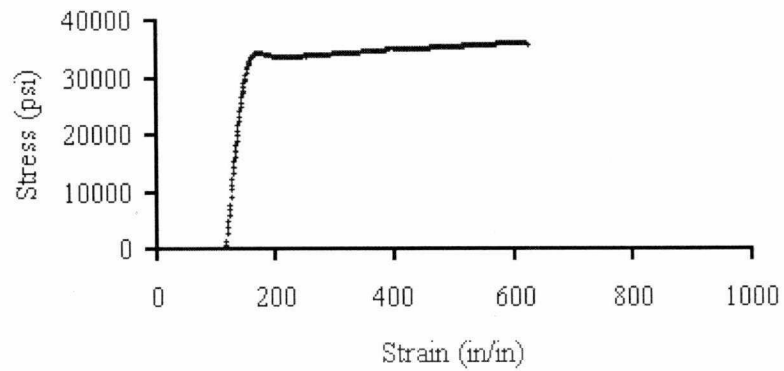
Figure 4.4 Stress-strain tensile behavior of TR-1 (exposed to UV light for 20 minutes)
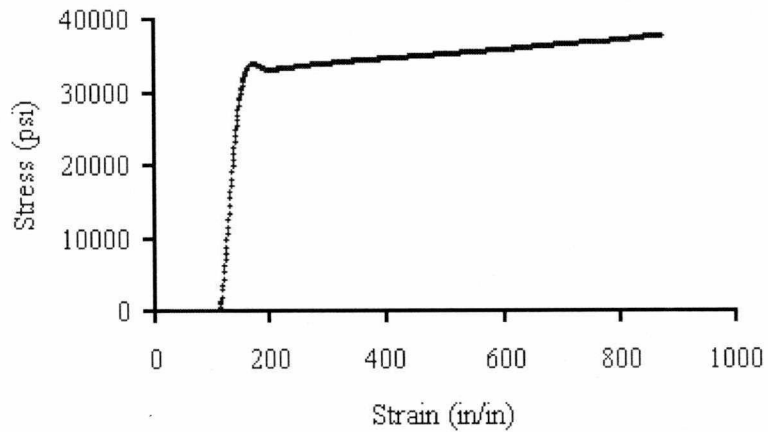
Figure 4.5 Stress-strain tensile behavior of TR-1 (exposed to UV light for 40 minutes)
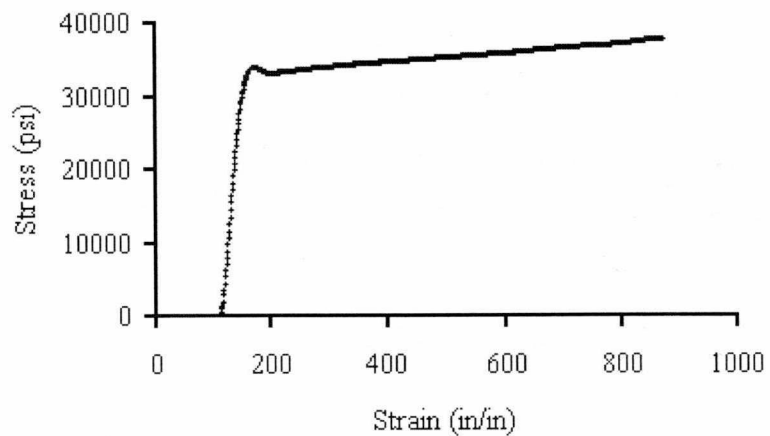
Figure 4.6 Stress-strain tensile behavior of TR-1 (exposed to UV light for 60 minutes)

For TR-2, PU-1, PU-2, and PVA the results showed that UV light did not affect the tensile strength of the polymer samples. The samples prepared for tensile tests were exposed to UV light for 20 minutes, 40 minutes, and 60 minutes. Since the time used in the sterilization procedure was 40 minutes, the sterilization procedure using UV light did not affect the material's tensile strength. Two explanations for the of lack effect are:

First, photodegradation is initiated by absorption of UV light. Double bonds are more sensitive to UV light and absorb it more easily than single bonds. PVA ($[-CH_2-CH(OH)-]_n$) does not have double bonds. Therefore PVA does not photodegradate. The two polyurethane
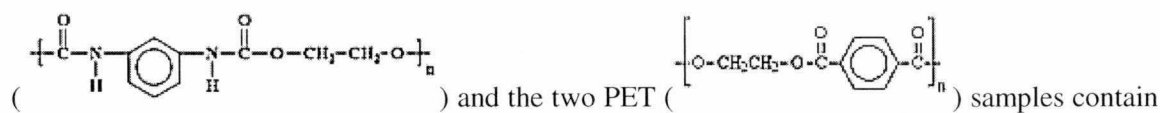
 ( ) and the two PET ( ) samples contain carbon-oxygen double bonds that are probably less sensitive than carbon-carbon double bonds.

Second, the sterilization time periods are not long enough to break the bonds in these polymers. The literature shows that a longer exposure (several days or weeks) to UV light is necessary to cause the degradation of these materials. Even the results of the 60-minute exposure to UV light showed no effect on the materials' tensile strength.

Photodegradation begins with the absorption of UV light. Many polymers are incapable of absorbing UV light directly. However, trace amounts of other compounds within the polymer, such as degradation products or catalyst residues, can absorb UV. Effective thermal and processing stabilization is a prerequisite for effective long-term UV stabilization. A UV stabilizer called a "competitive absorber" is used. The polymers used in the study were all commercial products and UV stabilized when they were synthesized.

UV light sterilization of the materials in this study had no effect on the mechanical property tested. Since UV light modification is a method that can place oxygenated functional groups (CO, COOH, and OH) on the surface, this step may enhance cell adhesion (Liu et al. 1998).

4.2 Counting the cells

After the materials were sterilized, special culture dishes were prepared as described in Chapter 2. 3T3 cells were cultured until the cells reached desired number ($\sim 10^6$).

A counting chamber (also called Hemacytometer) was used for cell counting (Figure 4.7, Caprette 2000). The depth of the sample chamber is 0.1mm. The entire grid on a standard counting chamber with Neubauer rulings can be seen under the microscope (Figure 4.8, Caprette 2000). The main divisions separate the grid into 9 large squares. Each square has a surface area of

1 mm^2 and has a volume of 0.1 mm^3. Thus the entire counting grid lies under a volume of 0.9 mm^3.
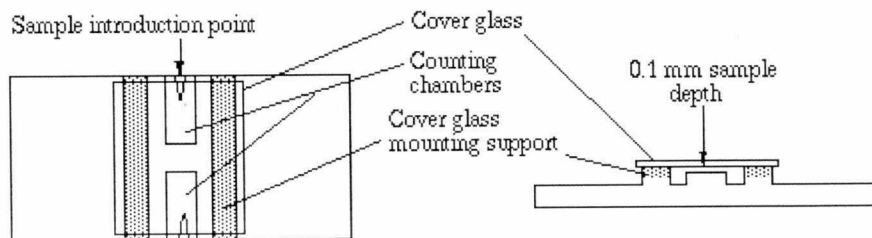
Figure 4.7 Schematic picture of the cell counting chamber (Caprette 2000)
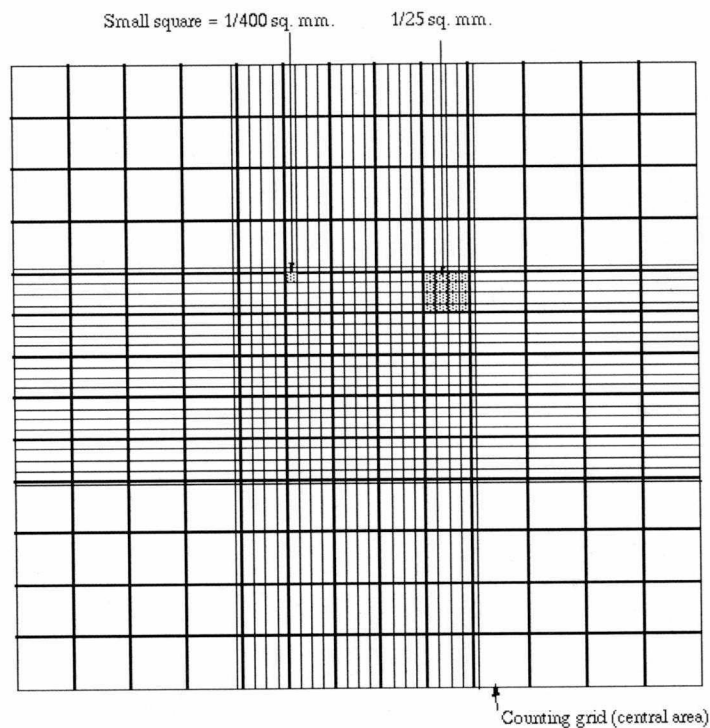
Figure 4.8 Diagram for cell Counting Chamber (Caprette 2000)

The concentration (c) of the cells can be determined from the numbers of the cells that has been counted (n) in a grid area.

$$c = n/v \qquad \text{(Eq. 4.1)}$$

c = cell concentration (cells/ml)

n = number of cells counted

v = volume counted (ml)

The volume counted is defined by the number of the large squares that have been counted (N). Since the concentration of the cells is in cells/ml, the unit of volume needs to be converted from mm^3 to ml. Therefore:

$$v = N*0.1 \text{ mm}^3 / 1000 \text{mm}^3/\text{ml} = N/10000 \text{ (ml)} \qquad \text{(Eq. 4.2)}$$

N = number of the large squares counted

The concentration of the cells can be calculated by:

$$c = n/v = n*10000/N \text{ (cells/ml)} \qquad \text{(Eq. 4.3)}$$

A 1ml tube of 3T3 cells from the cell bank established previously (reviewed in Chapter 2) was used to start the cell culture. The cells were cultured in the 100 mm flask. After 48 hours in the 37°C incubator the cells in the culture plate reached confluency. A small aliquot the suspended cells was introduced into the V-shaped well of the counting chamber with a pipet. Because of the capillary effect, the suspension solution filled the area under the cover glass. The hemacytometer was placed under the microscope and the concentrations of the cells were calculated using Equation 4.3.

4.3 Cell culture on the matrix materials

After the concentration of the cells was calculated, the cells were diluted to 200,000 cell/ml by using

$$C_1V_1 = C_2V_2 \qquad \text{(Eq. 4.4).}$$

C_1 = concentration of the cells in the culture plate

V_1 = volume of the cell solution in the culture plate

C_2 = 200,000 cell/ml

V_2 = 20 ml

The volume of the diluted solution was 20 ml, because each set of the experiment had 9 cultures plates (glass, PVA, Al_2O_3, Ni, PU-1, PU-2, TR-1, TR-2, and a control dish). The same procedures were repeated for making the 20 ml 100,000 cell/ml cell solution.

The sterilized materials were cut to small thin pieces and glued to the bottom of the self-made glass bottom slide (Figure 4.9). The 100,000 cell/ml and 200,000cell/ml of cell solution were distributed across the cell culture slides with different matrix materials. The 18 plates were then put into the incubator for 48 hours. After that the plates were fixed and stained. An optical-fluorescence microscope, SEM, and ESEM were used to analyze the cell culture.
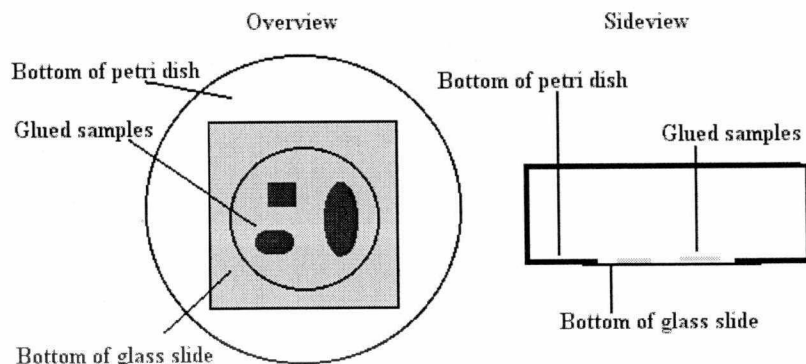
Figure 4.9 Schematic picture of the self-made glass-bottom culture plate

4.4 Visualizing cells

Cells adhere to each other and to the materials through the points of contact with cell adhesive proteins. The cells secret extracellular matrix (ECM), various biopolymers, small molecules, and ions. The ECM is composed of mainly collagen proteins, which are connected to each other by four kinds of bonding: ionic bond; hydrogen bond; van de Waals attraction; and hydrophobic force. Biomaterials could provide the matrix sites that the proteins could combine and allow the cells would grow on. Cellular adhesion is a complex process involving cells and material interactions. The process has four stages: protein adsorption on the surface, contact of the rounded cells, attachment of cells to the substrates, and finally spreading of cells.

After 48 hours culture, cells were observed attached to the substrates. Because of the different surface chemistry of the different materials, cell attachment varied. The adhesion and proliferation of each sample are described below.

Control:

Control plates were used for each set of experiments. At both concentrations (100,000 cell/ml and 200,000 cell/ml) the morphology of the cells in the plates showed similar results. 3T3 cells grew on the bottom of the control plates, although not totally uniformly. Under the phase contrast microscope, at the time of observation, some places reached confluency quicker than the other (Figure 4.10). Similar results were observed under the fluorescence microscope (Figure 4.11). Cells were well spread into a monolayer on the bottom of the plates. There was no clumping of cells. Cells were attached to each other, and 80% confluent. Repeat experiments showed the same results.
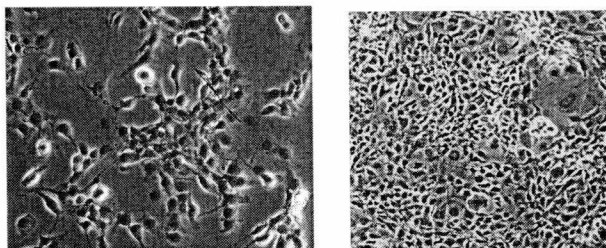
Figure 4.10 Control plates, phase contrast microscope

Left: cells did not reach confluency, 20x; right: cells reached confluency, 10x
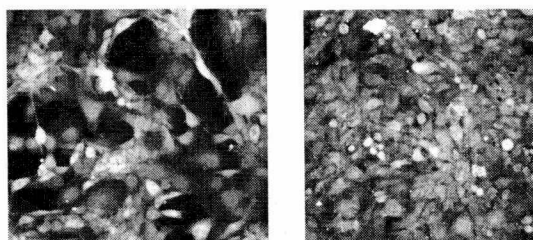
Figure 4.11 Control plates, fluorescence microscope

Left: cells did not reach confluency, 20x; right: cells reached confluency, 20x

Glass:

Tissue cultures on the transparent glass slides could easily be observed using the phase contrast and fluorescence microscope (Figure 4.12, Figure 4.13). Unlike the Al_2O_3 and Ni, glass samples are thinner. It is easier for cells to immigrate up to the glass samples than to the Al_2O_3 and Ni samples. Cells were observed to grow on both sides of the material samples. The confluency of the cells is less than that of the control plates. Cells remained around the corner and edge areas. Around these edge areas cells were attached to each other and there was no clumping. The cells were well spread and randomly oriented as in the control plates. The confluency was less in the middle area of the glass slides than that in the edge areas. Cells migrated vertically along the edge of the glass slide up; they crowded into the space between the glass samples and the bottom of the dish, and attached to the bottom of the slide. Cells are randomly spaced on both surfaces of the glass slides. Clumps of cells and isolated cells could be seen in the middle of the glass slides. Repeat experiments showed the same results. Although the bottom of the sample well was also made by the same glass as the samples (see Figure 4.9), the confluency of the sample well's bottom was higher because cells could more easily grow on it than migrating up onto the samples though the samples were much thinner than Al_2O_3 and Ni samples (Figure 4.14).

Figure 4.12 Cell culture on glass slides, phase contrast microscope (20x)

Left: edge; middle: middle; right middle
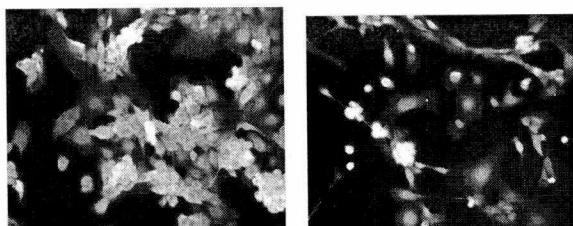
Figure 4.13 Cell culture on glass slides, fluorescence microscope (20x)

Left: edge; right: middle
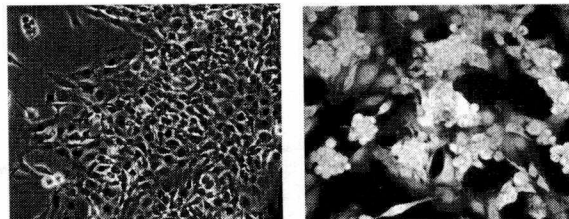
Figure 4.14 Cell culture on glass slides – image of the bottom of the culture plate (20x)

Left: phase contrast microscope; right: fluorescence microscope

Al_2O_3:

The pure cell growth on Al_2O_3 showed that Al_2O_3 is not a good substrate material for a culture matrix. After 48 hours of growth, cells were located on the bottom of the petri dishes but not on Al_2O_3. Since Al_2O_3 is not transparent, a phase contrast microscope showed only the edge area of the Al_2O_3 (Figure 4.15). When a fluorescence microscope was used, the background fluorescence interfered (Figure 4.16). Only the areas, where the background fluorescence is weak, could the cells be observed. These areas are the smooth areas in Figure 4.17. Al_2O_3 samples have macropore structure and are thicker than glass samples. Cells had to immigrate up onto the surface along the filament of the pores to reach the surface. Cells could grow on the surface only

if the cells reached that area. Isolated cells were on the Al_2O_3 surface and were in distress because these 3T3 cells balled up to present minimal surface contact. Repeat experiments showed the identical results.

Figure 4.15 Cell culture on Al_2O_3, phase contrast microscope (20x)

Left: Cells were clumping together in the right center area; middle and right: Cells were migrating vertically up the edge of the Al_2O_3 and cells isolated after vertical migration.

Figure 4.16 Cell culture on Al_2O_3, fluorescence microscope (20x)

Left and middle: Cells were clumping together;

Right: Cells were migrating up and the cells that had migrated up were isolated.
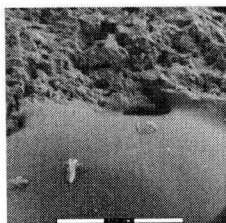
Figure 4.17 ESEM image of Al_2O_3

Rough area showed fluorescence background under fluorescence microscope.

Ni:

After 48 hours of growth on Ni, it showed that seldom did cells attach to the matrix. A phase contrast microscope was used to observe the cells, but since Ni is not transparent, only the edge area could be observed (Figure 4.18). Using the fluorescence microscope Ni had weak

fluorescence signals (Figure 4.19). The fluorescence from the cells could easily be confused with fluorescence from the Ni. Ni samples are thicker than the glass samples and have the same large porous structure as Al_2O_3 making it difficult for the cells to climb. Since few cells could migrate up and Ni is poisonous to cells (Monteilh-Zoller ea al. 2003), almost no cells were observed to attach to the Ni matrix. For the cells that did migrate, they clumped together instead of attaching to the surface of the Ni.
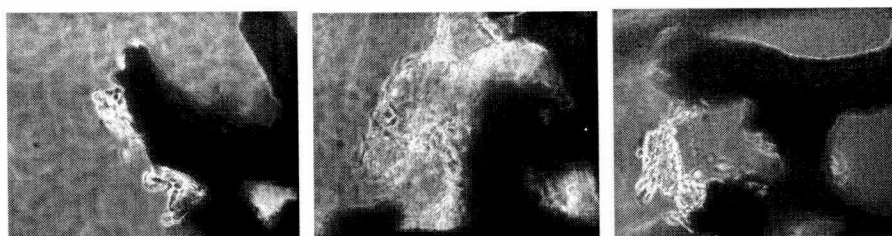
Figure 4.18 Cell culture on Ni, phase contrast microscope (20x)

Cells were forming clumps with minimal anchoring.
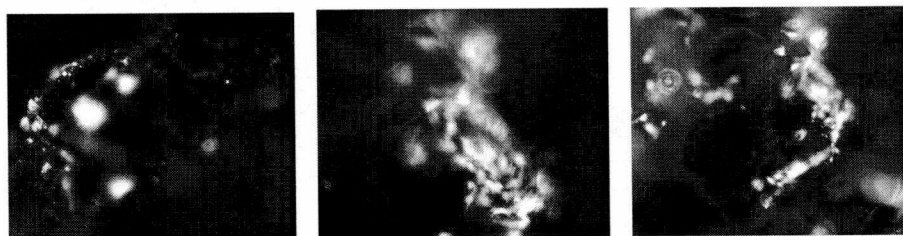
Figure 4.19 Cell culture on Ni, fluorescence microscope (20x)

Left: Ni is fluorescence sensitive;

Middle and right: Cells were forming clumps with minimal anchoring.

PVA:

Since PVA is not transparent, only the edge and thin areas could be observed under the phase contrast microscope (Figure 4.20). PVA gave a fluorescence background, so only the edge and thin areas, where the fluorescence signals were not too strong, could be observed using the fluorescence microscope (Figure 4.21). Cells were observed migrating up along the edge of the PVA and staying on the PVA porous structure. ESEM analysis showed that cells could attach to the PVA (Figure 4.22), but the cells were isolated and not well extended. 3T3 cells should be able to attach to PVA ($[-CH_2-CH(OH)-]_n$), since it has the alcohol groups that provide attachment sites.

The PVA has large pores with very thin pore walls and some filaments. The pores are very large and may inhibit stretching over them and form a monolayer. Since the cells did not spread out, they were balled and clumped together. When the cells migrated, they could only move along the walls and filaments. This is a disadvantage for 3T3 cells to grow on a large pore structured matrix. If the pore walls were thicker there would be more surface area for the cell surface protein-polymer interactions, and more cells would have attached to the surface.

Figure 4.20 Cell culture on PVA, phase contrast microscope (20x)

Left: Cells were forming clumps; right: Cells were migrating up.

Figure 4.21 Cell culture on PVA, fluorescence microscope (20x)

Left: Raw PVA without cell culture; right: Cells were migrating up.
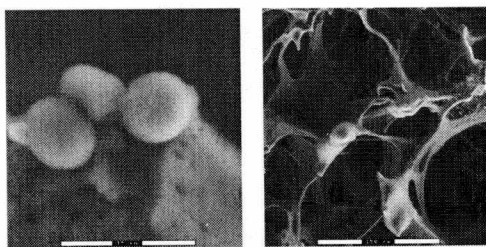
Figure 4.22 Cell culture on PVA, ESEM

PU-1 and PU-2:

Based on the chemical composition, the surface of the polyurethane samples should offer a good chemical surface for cells to attach to. Two kinds of polyurethane, with differing

microstructures, were used. As introduced in chapter 2, PU-1 has an open pore structure and PU-2 has a closed pore structure.

Like the other nontransparent samples, only the edge and thin areas could be observed by the phase contrast microscope (Figure 4.23, Figure 4.27). Both PU-1 and PU-2 show background fluorescence and only the thin and edge areas could be observed by fluorescence microscope (Figure 4.24, Figure 4.25, Figure 4.28). ESEM analysis showed that cells attached to the PU-1 and PU-2 in big clumps. Some isolated cells were observed to attach to PU-2 as well (Figure 4.26, Figure 4.29).

3T3 cell was observed migrating up along the edge of the samples and growing on the PU-1 porous structure (Figure 4.23). The structure of PU-1 is similar to PVA, but the connections between the pores are much thicker as shown in the SEM analysis of the matrix materials in Chapter 2. The PU-1 pores are still too large for cells to stretch out over them to form a flat monolayer. 3T3 cells were balled and clumped together. Since PU-1 has lower porosity compared to PVA, it provides more surface area for the cells to attach to, and therefore it has more cells adhered.
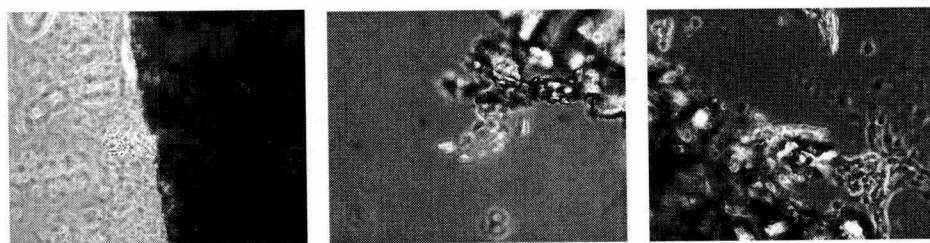
Figure 4.23 Cell culture on PU-1, phase contrast microscope (20x)
Left and middle: Cells were forming clumps; right: Cells were migrating up.

Figure 4.24 Cell culture on PU-1, fluorescence microscope (20x)
Left: PU-1 showed background fluorescence without cells;
Middle and right: Cells attached to PVA as separate cells and clumps.
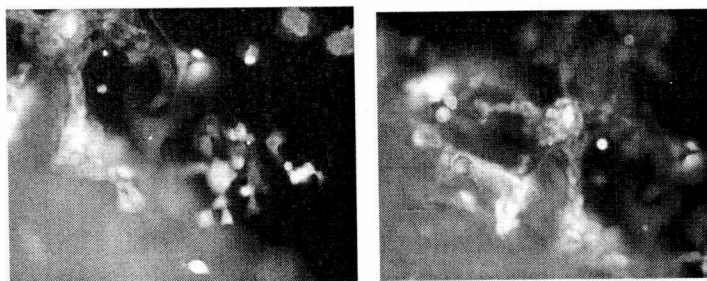
Figure 4.25 Cell culture on PU-1, fluorescence microscope (20x)

Left: Cells from the bottom of the dish starting to migrate up (focused on the bottom of the plate)

Right: Cells attached to PU-1 after migrating up and forming a clump (focused on the clump)
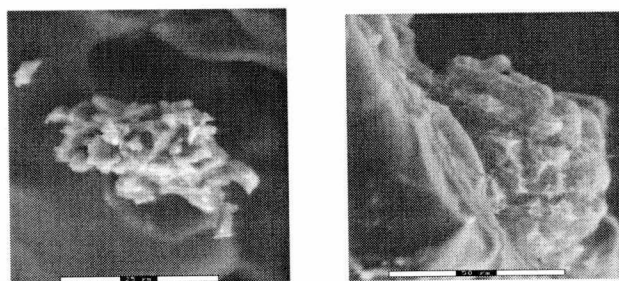
Figure 4.26 Cell culture on PU-1 under ESEM

Cells forming big clumps clump

Under the phase contrast and fluorescence microscope, similar results were observed for PU-2. Cells were observed migrating up along the edge of the samples and forming clumps. Besides the clumps, isolated single cells were also observed. Even though they have the same surface chemistry, cells were more confluent on PU-1 than PU-2. Cells selected open pores structures more than closed pore structures.

Figure 4.27 Cell culture on PU-2, phase contrast microscope (20x)

Left: Cells were forming clumps; middle and right: Cells were migrating up.
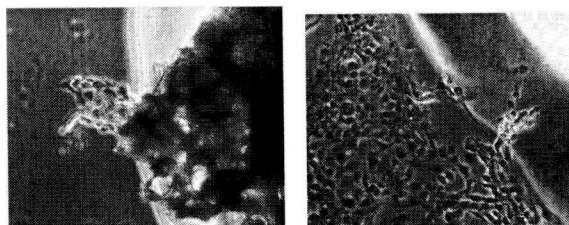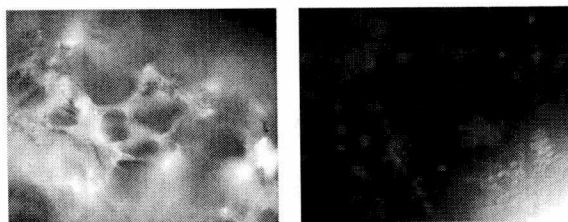
Figure 4.28 Cell culture on PU-2, fluorescence microscope (20x)

Left and middle: Cells from the bottom of the dish starting to migrate up.

Right: Cells migrated up and formed clumps or remained isolated single cells.
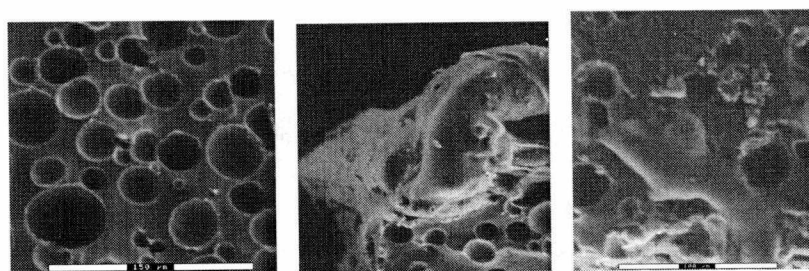
Figure 4.29 Cell culture on PU-2, ESEM

Left: PU-2 surface without cells; middle: a big clump of cells;

Right: a big clump and some single cells

TR-1 and TR-2:

The base sheet of TR-1 and TR-2 was made of polyethylene terephthalate. The film has two coatings with each side of the base film, coated with a different coating. TR-1 is thicker and rougher. TR-2 is thinner and smoother. During the process of sterilization with ethanol, part of the coatings peeled off. The 3T3 cells grew on both the surface of the coatings and the exposed PET. Since both TR-1 and TR-2 are transparent, they can be observed under the phase contrast microscope (Figure 4.30, Figure 4.32). A fluorescence microscope was also used (Figure 4.31, Figure 4.33). Under the fluorescence microscope, both of the samples had weak fluorescence signals. The areas where the coatings were totally peeled off had little background fluorescence.

3T3 cells were growing on both sides of TR-1. Cells grew less in the middle of TR-1 than the edge area. Areas without coatings showed more attached cells than areas with coatings. Cells attached to the monolayer-coated areas, but not to those areas where the peeled coatings folded over. Cells attached to the edges were well spread and formed monolayers. Some of the cells

attached to the middle area were well spread and the rest were either isolated single cells or formed clumps.
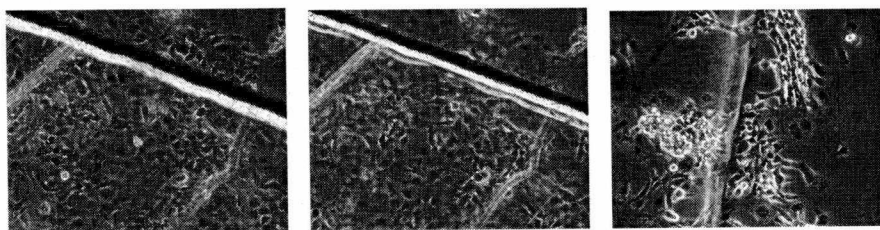
Figure 4.30 Cell culture on TR-1, phase contrast microscope (20x)
Left: edge area - focused on the bottom; middle: same edge area - focused on the top
Right: edge area - focused on the edge.

Figure 4.31 Cell culture on TR-1, fluorescence microscope (20x)

TR-2 also showed more cells attached to the edge area than in the middle of TR-2, but the cell number was higher than for TR-1. The cells in the middle of the TR-2 were well spread and formed monolayers. Cells were growing on both sides of the TR-2. Cells did not grow on the areas where peeled coatings were folded over. TR-2 coatings had weaker background fluorescence than TR-1.
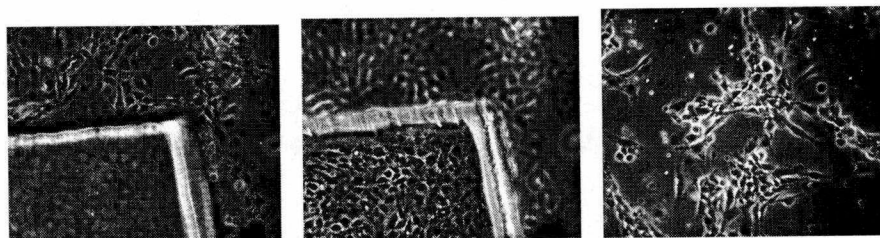
Figure 4.32 Cell culture on TR-2, phase contrast microscope (20x)
Left: corner area - focused on the bottom; middle: same corner area -focused on the top
Right: center area of the sample
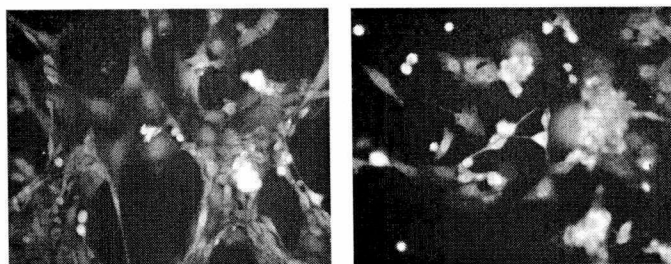
Figure 4.33 Cell culture on TR-2, fluorescence microscope (20x)

4.5 Visual Techniques

A phase contrast microscope requires the samples to be transparent. Some of the samples were not transparent. A fluorescence microscope requires the samples do not have background fluorescence signals. Cells are usually labeled with a fluorescence probe so that, under the fluorescence microscope, the cells will be the only bright spots. However, some samples that are not transparent have a high background fluorescence, such as PVA, PU-1, and PU-2, which interfered with the fluorescence method.

A confocal microscope requires the samples to be flat enough to get clear focused images. The samples that needed to be analyzed with the confocal microscope (PVA, PU-1, and PU-2) are all porous and all have strong background fluorescence, so a confocal microscope did not work well.

For the SEM, the samples must be dehydrated, critical point dried, and coated with a conductive material. Dehydration will definitely change the state of the cells even fixed cells. The critical point dryer blow the cells away. The observed samples consisted of only some of the secreted materials from the cells. The visual techniques used to observe the various materials in this study are summarized rated in Table 4.1.

4.6 Wettability of the matrix materials

Wettablity is a surface property of a material. The surface tension value can be utilized to determine the wettability by measuring the contact angle between a solid surface and a droplet of liquid on the surface. The measurements of the wettabilties of the matrix materials with water were conducted using a goniometer. Matrix materials have an attractive (hydrophilic) or repulsive response (hydrophobic) to the water. The wettability of a material is determined by the surface polarity of the materials. The goniometer results of the measurements are in Table 4.2.

Table 4.1 Summary of Usefulness of Visual Techniques for Test Samples

Test Sample	Phase Contrast Microscope	Fluorescence Microscope	ESEM
Al_2O_3	Fair	Fair	Good
Glass	Good	Good	-
Ni	Fair	Fair	Good
PU1	Fair	Fair	Good
PU2	Fair	Fair	Good
PVA	Fair	Fair	Good
TR1	Good	Good	-
TR2	Good	Good	-

Table 4.2 Measurements of Goniometer Contact Angles

Test Sample	Contact angle	Standard deviation
Al_2O_3	-	-
Ni	128.3	0.06
Glass	54.7	0.21
PU-1	125.3	0.04
Polished PU-1	99.0*	-
PU-2	121.0	0.07
Polished PU-2	60.0*	-
PVA	0	-
TR-1	55.7	0.69
TR-2	53.7	0.07

* Measured manually

PVA is hydrophilic polymer and has a zero contact angle. The water spread out immediately after it touched the surface of PVA, since it can form hydrogen bonds with water. It also has a porous structure in which water can easily be absorbed.

Glass, TR-1, and TR-2 were partially wettable. The water spread out and the contact angles were less than 90° (Figure 4.34). The main surface component of a glass slide is SiO_2. Water molecules can form hydrogen bonds with SiO_2 and therefore the surface of glass is

wettable. PET, the polymer component of TR-1 and TR-2 samples, can also accept hydrogen bonds from water.
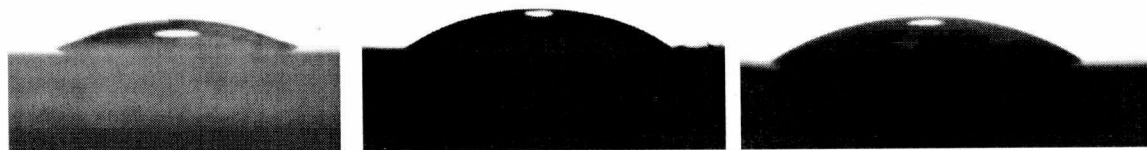
Figure 4.34 Contact angle measurements of glass, TR-1, and TR2 samples

Left: glass; middle; TR-1; right: TR-2

PU-1, PU-2, Al$_2$O$_3$, and Ni are all hydrophobic, with a contact angle that was larger than 90°. Water on Al$_2$O$_3$, Ni, PU-1, and PU-2 surfaces did not spread out (Figure 4.35). In order to increase the wettability of PU-1 and PU-2 surfaces, a polishing experiment was conducted as described in Chapter 2. After being polished, the contact angles of both PU-1 and PU-2 decreased (Figure 4.36). The polishing procedure changed the surface atomic arrangement and the surface roughness. The new-formed surfaces were less hydrophobic, but they still had the larger contact angles than the hydrophilic samples (Table 4.2).
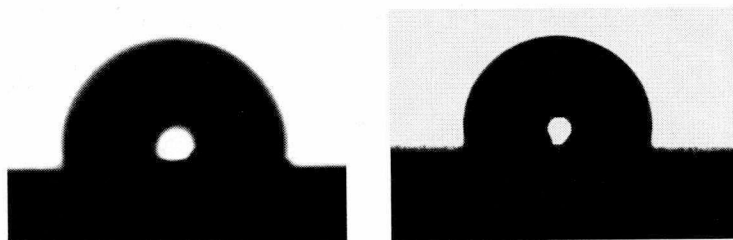
Figure 4.35 Contact angle measurements of polyurethane samples, left: PU-1; right: PU-2
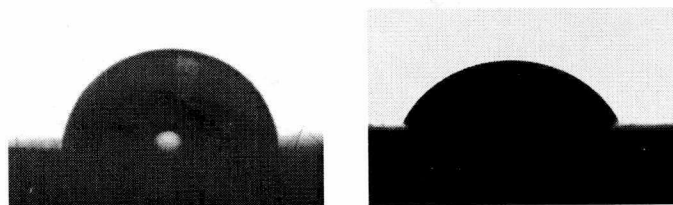
Figure 4.36 Contact angle measurements of polished polyurethane samples

Left: polished PU-1; right: polished PU-2

The best cell adhesion is usually achieved at intermediate values of surface wettability. This is supported by my observation that glass, TR-1, and TR-2 had a larger cell number than other samples. PU-1 and PU-2 are too hydrophobic in their unmodified state, but after polishing and UV light irradiation the surface wettabilty is increased.

After cell culture experiments, the contact angles of the samples were remeasured. The water spread out on the surface of all samples. The surfaces were all wettable. During the cell culture experiments, the samples were immerged in the culture media, which contains minerals, lipids, hormones, growth factors, and adhesion factors. The surfaces of the samples were coated with these polar molecules and dramatically improved the surface wettability.

4.7 Adhesion and proliferation

Motility-related processes depend on signal transduction related to the intracellular cytoskeleton. Signal transduction is regulated by signaling pathways governed by a variety of environmental stimuli, which is mediated by receptors in the plasma membrane that are linked to the cytoskeleton. Integrins, $\alpha\beta$ heterodimeric transmembrane proteins, bind the extracellular matrix. Cadherins, calcium-dependent transmembrane proteins, bind homotypically to their counterparts on adjacent cells (Figure 4.37, Lauffenburger et al. 2001).
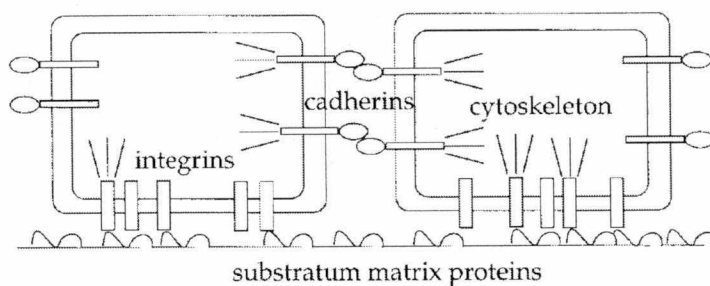
Figure 4.37 Schematic illustration of integrins in the plasma membrane that link to the cytoskeleton (Lauffenburger et al. 2001)

While the cell-cell adhesion on the matrix is receptor-mediated, the adhesion between the cells and the artificial materials is non-receptor-mediated. Cells and artificial materials adhere by weak chemical bonds such as hydrogen bonds, polar interactions, and electrostatic interactions between receptor molecules on the cell membrane and the chemical functional groups of the polymers. If cells cannot deposit their own ECM on the artificial surface in a short time (24-48 hours), they undergo apoptosis (Huang et al. 1998; Moiseeva 2001). Since the surface chemistry

is very important for cells to grow. Al_2O_3 and Ni do not provide a surface chemistry to which cells can anchor to and secrete ECM. Under this circumstance, cells undergo apoptosis. Other artificial matrix materials (glass slides, PU-1, PU-2, PVA, TR-1, and TR-2) do provide the surface chemistry so that the EMC secreted from the cells can, to some degree, anchor to. Cells were observed that could attach to the surface of these materials.

The pore size, pore structure, and porosity are very important for matrix scaffolds. Results showed that the open-pore polyurethane had more cells attached than the closed-pore polyurethane. The PVA samples in this study have a high porosity. PVA has more –OH groups and better wettabilty than polyurethane. However, results showed that less cells attached to the PVA than to the PU-1. The high porosity is a probable cause and the matrix should provide a high surface area for cell-polymer interactions in order for cells to spread out.

Cell adhesion and the cell behavior are summarized in Table 4.3. Under both concentrations (100,000 cell/ml and 200,000 cell/ml) cell culture gave the similar results.

Table 4.3 Comparison of Cell Adhesion And Cell Behavior (100,000 cell/ml)

Matrix	Cell Attachment[1]	Cell Clumping[2]	Cell Connectedness[3]	Cell Spreading[4]
Al2O3	0.5	0.0	0.5	0.0
Glass	3.5	4.5	4.5	4.5
Ni	0.1	0.0	0.1	0.0
PU1	2.0	2.0	2.0	3.0
PU2	1.5	1.5	2.0	2.0
PVA	2.5	2.5	2.0	3.0
TR1	3.0	4.5	4.0	4.5
TR2	3.5	4.5	4.5	4.5
Control	5.0	5.0	5.0	5.0

1. Cell attachment: the rank of the amount of the cells that attached to the matrix materials. The matrix with the most cells ranks 5.0. No cells ranks 0.0.
2. Cell clumping: the rank how cells clumped to each other. The matrix with the least clumped cells ranks 5.0. The matrix with most clumped cells ranks 0.0.
3. Cell connectedness: the rank of connectedness between the cells. Cells that were all connected with the least separation rank 5.0. Cells that were all separated rank 0.0.

4. Cell spreading: the rank of the distension of the cell spreading out. The material with the most spread out cells ranks 5.0. The material with the least spreading of the cells ranks 0.0.

For the statistic calculation, the hypothesis that "Cells cultured on matrix materials under comparison are normally distributed." was tested using non-parametric test – Kruskal-Wallis test. The data in ascending order and ranking is shown in Table 4.4 and Table 4.5.

Table 4.4 Order and Ranking of Data of Table 4.3 in Ascending Order

Data	0.0	0.0	0.0	0.0	0.1	0.1	0.5	0.5	1.5	1.5	2.0	2.0
Ranks	2.5	2.5	2.5	2.5	5.5	5.5	7.5	7.5	9.5	9.5	13.5	13.5
Data	2.0	2.0	2.0	2.0	2.5	2.5	3.0	3.0	3.0	3.5	3.5	4.0
Ranks	13.5	13.5	13.5	13.5	17.5	17.5	20.0	20.0	20.0	22.5	22.5	24.0
Data	4.5	4.5	4.5	4.5	4.5	4.5	4.5	4.5	5.0	5.0	5.0	5.0
Ranks	28.5	28.5	28.5	28.5	28.5	28.5	28.5	28.5	34.5	34.5	34.5	34.5

Table 4.5 Ranks of Data of Table 4.3 in Ascending Order

100,000 cell/ml	Cell Attachment	Cell Clumping	Cell Separation	Cell Spreading
Al_2O_3	7.5	2.5	7.5	2.5
Glass	22.5	28.5	28.5	28.5
Ni	5.5	2.5	5.5	2.5
PU1	13.5	13.5	13.5	20.0
PU2	9.5	9.5	13.5	13.5
PVA	17.5	17.5	13.5	20.0
TR1	20.0	28.5	24	28.5
TR2	22.5	28.5	28.5	28.5
Control	34.5	34.5	34.5	34.5
Sum ranks	$C_1=153.0$	$C_2=165.5$	$C_3=169.0$	$C_4=178.5$
Number of materials	$n_1=9$	$n_2=9$	$n_3=9$	$n_4=9$

The test statistic was calculated using the following formula:

$$\chi^2 = \frac{12}{N(N+1)}\left(\frac{C_1^2}{n_1} + \frac{C_2^2}{n_2} + \frac{C_3^2}{n_3} + \frac{C_4^2}{n_4}\right) - 3(N+1)$$

$N = n_1 + n_2 + n_3 + n_4 = 9 + 9 + 9 + 9 = 36$

$$\chi^2 = \frac{12}{36 \times 37}\left(\frac{153.0^2}{9} + \frac{165.5^2}{9} + \frac{169.0^2}{9} + \frac{178.5^2}{9}\right) - 3 \times 37$$

$$= 0.33$$

At 5% significance level, and with $v = c-1 = 3$, the χ^2 table (Appendix C) value is 7.81. Since χ^2 value of 0.33 does not exceed 7.81, the cells cultured on matrix materials under comparison are normally distributed.

From the experiments results, it could be observed that cells were growing on the different samples at different level.

Al_2O_3 and Ni showed poor cell adhesion and proliferation. These two samples are hydrophobic. PVA is total wettable. PU-1 and PU-2 are hydrophobic. Experiments showed that cells grew on these three, but cells were either formed clumps or were isolated on these samples. Results show that good cell adhesion and proliferation were observed on glass, TR-2, and TR-1. These three samples are partially wettable. The best cell adhesion was achieved at intermediate values of surface wettability in this research.

Chapter 5

Tribological performance of materials as scaffolds for cell growth:
Results and discussion of tribological tests

The scaffold matrix needs to have the mechanical properties of durability, load-bearing capacity, low friction and wear besides the compatibility for cell growth. Friction tests were conducted on the scaffold materials using both dry friction and lubricated friction methods.

The coefficient of friction is the resistance to motion between two contacting surfaces as those surfaces are moved relative to each other. If materials are non-lubricated (dry) and experience moderate pressures and velocities, Amonton's first law and Amonton's second law (see Chapter 1, Amontons 1699) apply: "The frictional force between two surfaces is proportional to the load that they carry and is not dependent on the apparent area between the two surfaces." When both surfaces are initially at rest, the static coefficient of friction is higher than the kinetic coefficient of friction. If the surface materials are well lubricated, Amonton's first and second laws do not apply. The friction coefficient depends upon many parameters including: temperature, surface roughness, contact area, load and pressure, lubricant and friction pairs, lubrication type and friction type.

A pin-on-disk mode, which is an ASTM accepted method to determine the friction coefficient (ASTM 1997), was used for friction tests. The applied force on the carriage was 5 mN and the test time was 10 minutes. The velocity was 1 mm/sec. Dry friction tests were conducted directly on the surface of the materials while lubricated friction tests were conducted in bovine serum solution (described in Chapter 2). Friction tests for cell culture materials were conducted immediately after the cell culture experiments.

5.1 Friction tests

Friction tests were conducted using UMT (Universal Micro-Tribotester). The setup condition of the machine is listed in Appendix D. and the data of the running time of the test, Fx (lateral force), Fz (vertical force), Ff (friction force), Fcoe (friction coefficient), and the MSE (mean standard error) are detailed in Appendix E.

Each test was repeated three times and the final friction coefficients were determined by averaging of the three friction coefficients. The MSEs were the average of the three MSE from the three tests. An example of data processing on the lubricated friction tests for PU-2 is shown in Table 5.1.

Table 5.1 Lubricated Friction Tests on PU-2

Test	Fx (mN)	MSE	Fz (mN)	MSE	Fcoe	MSE
1	0.10	0.14	4.94	0.39	0.46	0.14
2	0.16	2.49	4.95	0.45	0.49	0.14
3	0.14	2.53	4.95	0.45	0.50	0.15
Ave	0.13	1.72	4.95	0.43	0.48	0.14

Ni:

The friction coefficients of the dry, lubricated, and cell culture friction tests versus time are shown (Figure 5.1, Figure 5.2, Figure 5.3). The variation of friction over time represented the actual friction at each location. For example, the friction measurement of one stroke is shown in Figure 5.1: right. The variation indicates the surface condition of the sample surface. A higher surface roughness might be related to a higher friction.
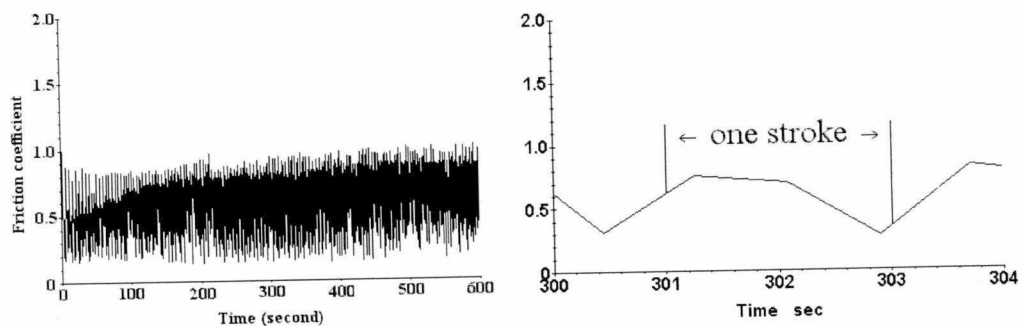
Figure 5.1 Dry friction test of Ni: left, the whole experiment; right, a few strokes
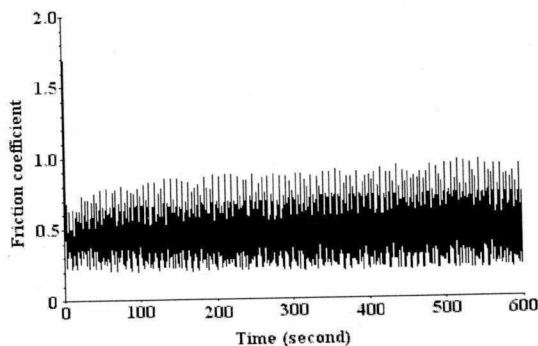
Figure 5.2 Lubricated friction test of Ni
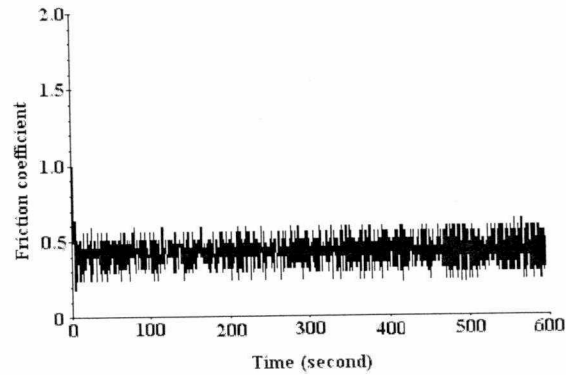
Figure 5.3 Cell culture friction test of Ni

The average friction coefficients and the MSE of the dry (dry), lubricated (lub), and cell culture (cell-cul) tests are listed in Table 5.2, and compared in Figure 5.4. Here the friction coefficients are the average of three measurements. Mean standard errors (MSEs) are the average of the three measurements. The software automatically gave the MSE of each experiment. As shown in Figure 5.4, the trend of reducing friction coefficient is evident.

Table 5.2 Average Friction Coefficients of All Tests on Ni

	Fcoe	MSE
Dry friction tests	0.61	0.28
Lubricated friction tests	0.47	0.24
Cell culture friction tests	0.34	0.14
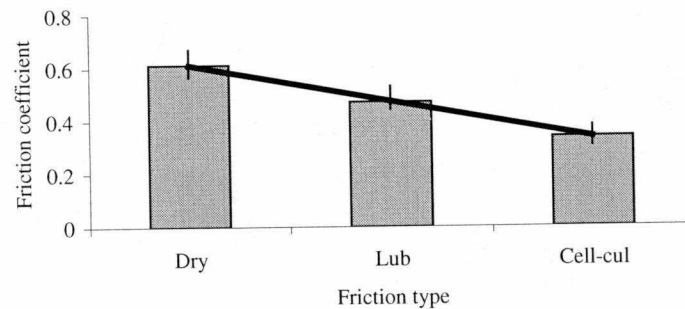
Figure 5.4 Comparison of coefficients of friction of different type of tests of Ni

The dry friction tests had the highest average friction coefficient (0.61) and the cell culture friction tests had the lowest average friction coefficient (0.34). The coefficient of dry friction was smaller at the beginning of the test and increased (Figure 5.1). Statistic calculation showed that the $p = 0.000$, which showed that there are significant differences among these three groups.

The Ni samples had lower friction coefficients at the beginning because Ni samples were soft and when the load was applied, substantial plastic deformation occurred which lowered the resistance. The lubricated Ni friction tests had the same trend in the tests but the change was smaller than that of the dry friction tests. The cell culture friction tests of Ni were the most constant of the three, having the smallest friction coefficient.

After the dry friction tests, the test areas of the Ni could be observed to be deformed (lower than the original surface). Adhesive wear also occurred during the dry friction tests. Mutual transfer of materials could also be observed, which included the transfer of the particulate material from one surface to another, particle growth by further repetitive transfer, and finally as loose debris. The grooves can be seen along the sliding direction (Figure 5.5: left). Because of the groove and debris, the friction coefficient increased with time.

When the BSA lubrication solution was dropped on the surface before the lubricated friction tests started, the lubricant solution gathered and formed a hemisphere. Since the Ni surface is hydrophobic, the pin is partially wettable, so when the test was ongoing, the fluid stayed on the surface. As the test continued, the hemisphere fluid started to extend, becoming flatter, because the weight of the fluid caused the infiltration of the fluid into the porous structure.

BSA contains many carboxyl and amine as well as disulfide loops groups (ref. Figure 2.1). Organic sulfur compounds are the traditional anti-wear additives as in rubber. Disulfides in general have lower bond energies than monosulfides and hence are considered to be better EP (extreme pressure) additives (Dorinson et al. 1985).

The friction between the two surfaces can lead to a mechanical activation of the surface that could produce 1) lattice and grain boundary effects, 2) catalytic activity of surfaces, 3) exoelectron emission, and 4) thermal excitation. Since low energy electrons were generated from rubbering of the surfaces, the material had positively charged areas. These areas chemsorbed negative ions and could undergo chemical reactions. For example, there is the interaction of disulphide with electrons:

$$R\text{-}S\text{-}SR + e \rightarrow RS^-$$
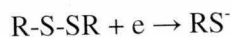
Adsorped friction polymers form a thin lubricated film and decrease both the friction coefficient and the wear. The friction coefficient increased with time, but the variation was smaller compared to that seen in dry friction tests. Although the friction coefficient decreased in the lubricated tests, grooves and the transfer of materials could still be observed on the surface, but less so (Figure 5.5: right).

Figure 5.5 Microscope image of Ni after the friction test

Left: dry friction test 20x; right: lubricated friction test, 20x

For the cell culture friction tests, the culture media played a larger role than the BSA solution. During the lubricated friction tests, the lubricant was added before the tests. The short reaction time limited reactions on the lubricant film before the friction tests. In the cell culture friction tests, the cell culture procedure changed the wettability of the matrix materials as described before. The surface of the Ni had been coated with protein molecules. The surface of the Ni changed to total wettability, and the lubricant extended and spread thoroughly on the Ni surface. Because of the modification of the surface during the cell culture, the surface was well protected. The friction coefficient was smaller after the cell culture and it did not increase during the whole test period.

Al_2O_3:

The surface of Al_2O_3 is rough because of the porous structure (see Figure 2.3). The pin could not move at the set velocity after the test began because of the roughness. Bulk Al_2O_3 is brittle. When stress was applied to Al_2O_3, cracks, instead of deformation, formed at the grain boundaries. As the stress continued, the Al_2O_3 started to break. The lack of plasticity in Al_2O_3 is due to the chemical bonds of Al_2O_3. In crystals and covalently bonded ceramics the bonding between atoms is specific and directional. Thus, when crystals of Al_2O_3 were stressed sufficiently, they exhibited brittle fracture due to a separation of electron-pair bonds without

subsequent reformation. No friction test results for Al_2O_3 were obtained because of this cracking of the materials.

Glass:

Friction tests of glass were conducted and the friction coefficients of dry, lubricated, and cell culture tests versus time are shown (Figure 5.6, Figure 5.7, Figure 5.8).
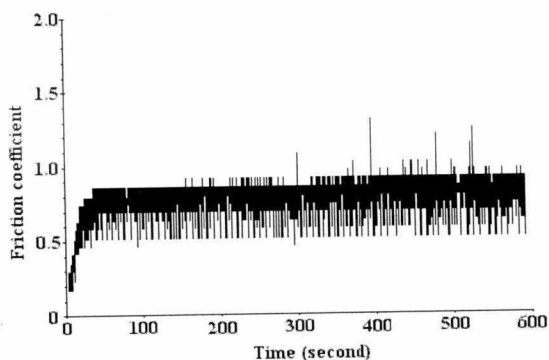
Figure 5.6 Dry friction test of glass

Figure 5.7 Lubricated friction test of glass
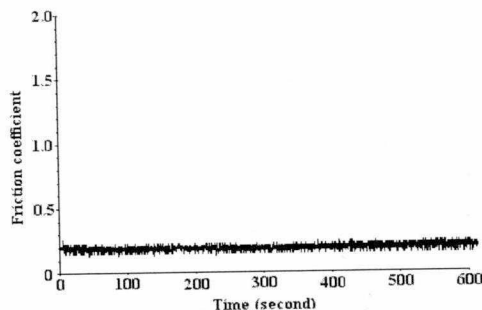
Figure 5.8 Cell culture friction test of glass

The average friction coefficients and the MSE of the tests are summarized in Table 5.3 and the friction coefficients are compared in Figure 5.9. As discussed in the previous section, the variation of friction is related to the surface contact condition.

Table 5.3 Average Friction Coefficients of All Tests on Glass

	Fcoe	MSE
Dry friction tests	0.73	0.26
Lubricated friction tests	0.45	0.17
Cell culture friction tests	0.22	0.08
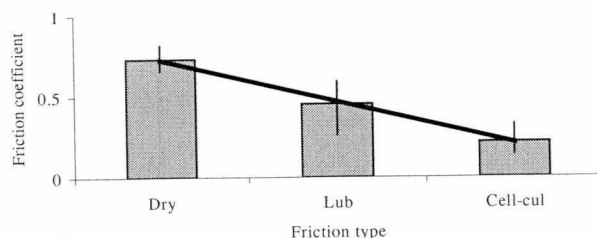
Figure 5.9 Comparison of coefficients of friction of different type of tests of glass

Glass is composed of SiO_2, CaO, and Na_2O and is brittle amorphous solid. Glass is bioactive and capable of direct chemical bonding with the host biological tissue. The results for the glass were similar to those for Ni. The dry friction tests had the highest average friction coefficient (0.73) and the cell culture friction tests had the lowest friction coefficient (0.22). Lubricated friction tests showed an average friction coefficient of 0.45. Statistic calculation showed that p = 0.000, which show that there are highly significant differences among the three groups tested.

When load was applied during the dry friction tests, the friction coefficient increased initially and held constant thereafter. Transfer of materials was observed and grooves were seen along the sliding direction (Figure 5.10: left).

The surface of glass has an intermediate surface wettability. During the lubricated friction tests, the lubricant solution was well spread over the surface. The proteins groups in the lubricant solution could easily attach to the O- on the glass surface and form a lubricant film which decreased the friction coefficient. Although the friction coefficient decreased, grooves and material transfer could still be observed. More debris was produced during the lubricated friction tests than the dry friction tests. The lubricant film formed on the surface was sheared and the BSA was dried because of the high temperature of the contacting surfaces during the friction tests.
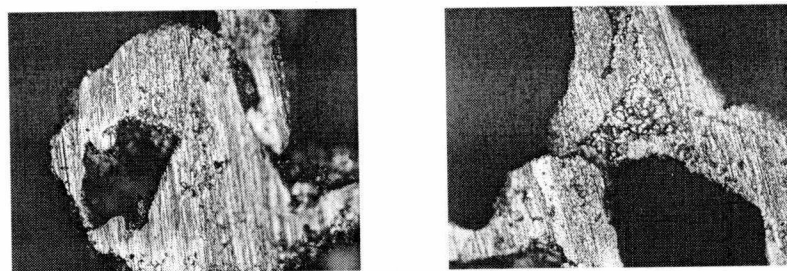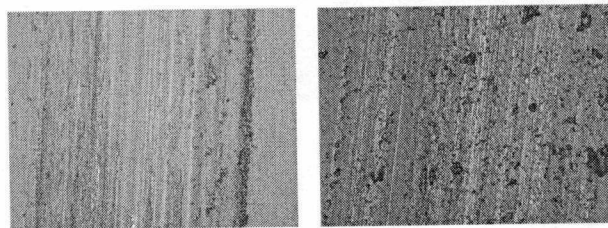

Figure 5.10 Microscope image of glass after the friction test:
Left: dry friction test, 20x; right: lubricated friction test, 20x

In the cell culture friction tests, the glass was coated with proteins from the media. This coating film was much thicker than the thin BSA film in the lubricated friction tests. The cell culture friction tests showed the lowest friction coefficients and the variation of the friction coefficient was also the smallest.

PVA:

Unlike metals and ceramics, friction on plastic polymers is more impacted by the experiment variables. Thermo properties, material transfer, microstructure, surface roughness, and the nature of the polymers can affect friction. The smoothness of molecular chains and a low surface energy associated with the weak intermolecular forces of a polymer will reduce friction.

Contact between a polymer and a metal is predominantly elastic. In this study, the contact of the PVA was partially elastic and partially plastic during the friction tests. The polymers showed a marked increase of flow stress with strain rate. Polymer operating limits are normally specified in terms of the pv factor, where p is the pressure and v is the velocity. The pv is related to temperature rise at the contact point.

Polymer friction can be attributed to two sources: deformation and adhesion. Polymers with branched carbon chains and polar polymers have higher friction coefficients due to greater adhesion. The primary mechanism postulated for polymer friction is the transfer mechanism. As the sliding started, polymers are transferred to the counter face. With further sliding, the transferred materials became oriented in the direction of sliding. Surface roughness helps to anchor the transferred layer. Later, transferred materials maybe removed as loose debris.

Friction tests of PVA were conducted and the friction coefficients of dry, lubricated, and cell culture tests versus time are shown (Figur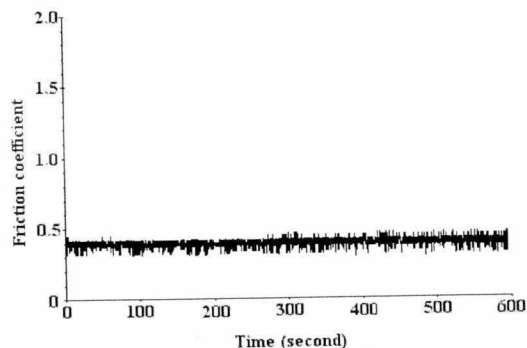e 5.11, Figure 5.12, Figure 5.13). The average friction coefficients and the MSE of the tests on PVA are summarized in Table 5.4 and the friction coefficients are compared (Figure 5.14).

Figure 5.11 Dry friction test of PVA

Figure 5.12 Lubricated friction test of PVA
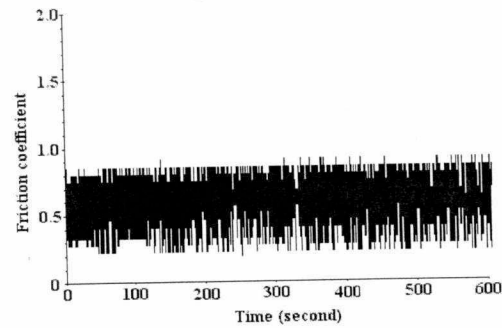
Figure 5.13 Cell culture friction test of PVA

Table 5.4 Average Friction Coefficients of All Tests on PVA

	Fcoe	MSE
Dry friction tests	0.37	0.27
Lubricated friction tests	0.56	0.28
Cell culture friction tests	0.55	0.28
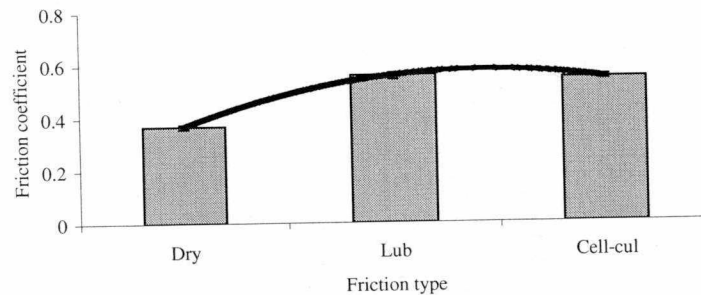
Figure 5.14 Comparison of coefficients of friction of different type of tests of PVA

The average dry friction coefficient (0.37) for PVA is the lowest of the three conditions. The variation of the friction coefficient of the dry friction is also the smallest. The average friction coefficients of lubricated friction tests (0.56) and the cell culture friction tests (0.55) are similar. Statistic calculation showed that $p = 0.422$, which showed that there were no significant differences among these groups.

Surface chemistry appears not to be a major factor during the PVA friction tests because there is a change in the mechanical properties of PVA when it is wet. When a thin sheet of PVA

is dry it is strong enough to bear some load, but once it is wet, it becomes softer. Its load-bearing capacity decreases. The lubricated and cell culture friction tests had wet surfaces and subsequently higher friction coefficients.

The wet PVA samples also experienced a high degree of deformation. As the load was applied, the sheet of PVA was thinned. The hardness of the holder needs to be considered. There were no running-in periods for PVA during the friction tests. When the pin was sliding on top of the PVA, it stretched and moved with the pin showing very little relative motion between the pin and the flat sample. The shear stress was concentrated at the contact point and, after the friction tests, it was observed that the spongy structure had become very thin. Transfer of material could be observed in both the dry friction tests and the lubricated friction tests (Figure 5.15).

Figure 5.15 Microscope image of PVA after the friction test

Left: dry friction test, 5x; right: lubricated friction test, 5x

PU:

Friction tests of PU-1 and PU-2 were conducted and the friction coefficients of dry, lubricated, and cell culture tests versus time are shown (Figure 5.16, Figure 5.17, Figure 5.18, Figure 5.19, Figure 5.20, Figure 5.21). The average friction coefficients and the MSE of the tests on PU-1 and PU-2 are summarized in Table 5.5 and the friction coefficients are compared (Figure 5.22, Figure 5.23).
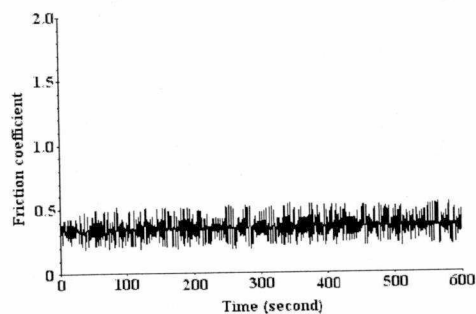

Figure 5.16 Dry friction test of PU-1

Figure 5.19 Dry friction test of PU-2
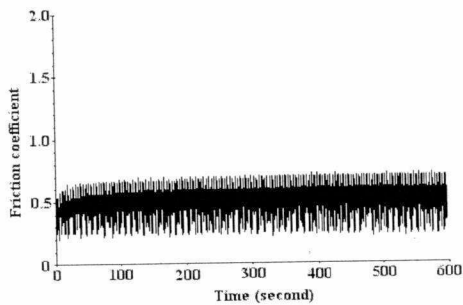
Figure 5.17 Lubricated friction test of PU-1
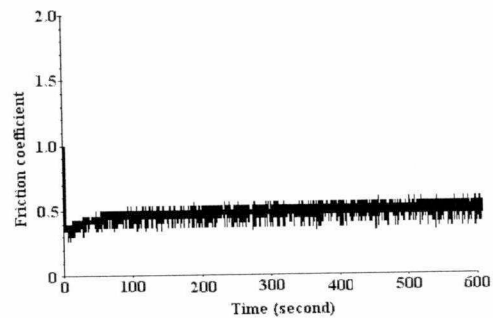
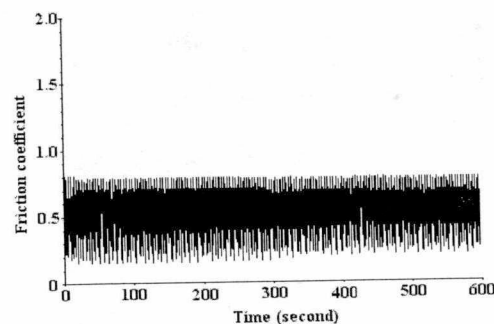**Figure 5.20 Lubricated friction test of PU-2**
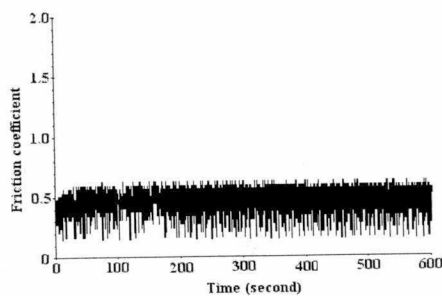
Figure 5.18 Cell culture friction test of PU-1
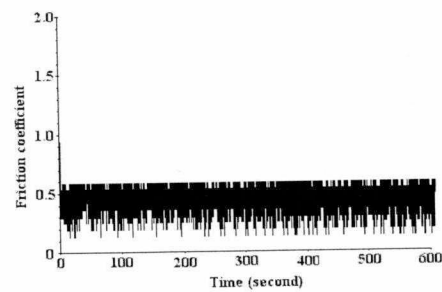
Figure 5.21 Cell culture friction test of PU-2

Table 5.5 Average Friction Coefficients of All Tests on PU-1 and PU-2

	PU-1		PU-2	
	Fcoe	MSE	Fcoe	MSE
Dry friction tests	0.30	0.09	0.19	0.10
Lubricated friction tests	0.52	0.25	0.48	0.15
Cell culture friction tests	0.50	0.21	0.48	0.20
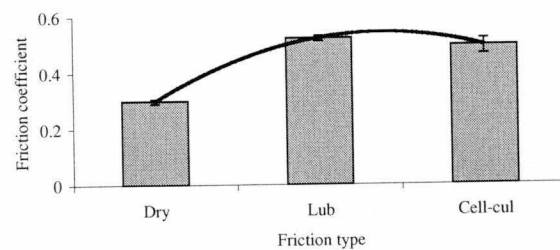
Figure 5.22 Comparison of coefficients of friction of different type of tests of PU-1
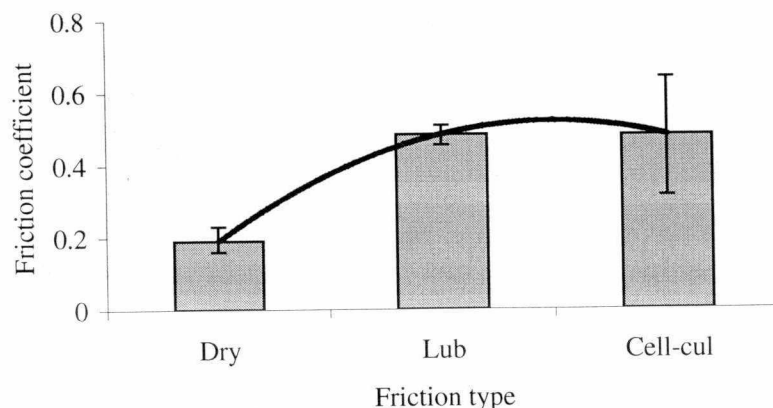
Figure 5.23 Comparison of coefficients of friction of different type of tests of PU-2

PU-1 and PU-2 had lower average dry friction coefficients (0.30 and 0.20) than that of the lubricated (0.52 and 0.48) and cell culture friction tests (0.50 and 0.48). The results of the lubricated and cell culture friction tests of PU-1 and PU-2 are similar. Statistic calculations of the p of tests of PU-1 and PU-2 are both 0.000, which showed that tests for PU-1 and PU-2 had significant differences among the groups tested.

PU-1 and PU-2 are both porous materials. During the lubricated and cell culture friction tests, the surfaces were wet and became softer. When load was applied to the wet surfaces more deformation occurred than for the dry friction samples. The deformation led to a higher friction under both the lubricated and cell culture friction tests.

Comparing the friction coefficients of PU-1 and PU-2, PU-1 had higher friction coefficients on all of the dry, lubricated, and cell culture friction tests. The surface chemistry is similar but the microstructures are different for PU-1 and PU-2. PU-1 has an open pore structure and has a higher porosity than PU-2. When load was applied on both of the samples, PU-1 had larger deformation than PU-2. This larger deformation resulted in higher friction coefficients of PU-1.

Because of the deformation, there were no running-in periods for all friction tests on the polyurethane samples. Transfer of the material could be observed for both of the dry friction and lubrication tests (Figure 5.24, Figure 5.25).

Figure 5.24 Microscope image of PU-1 after the friction test

Left: dry friction test; 10x; right: lubricated friction test, 10x
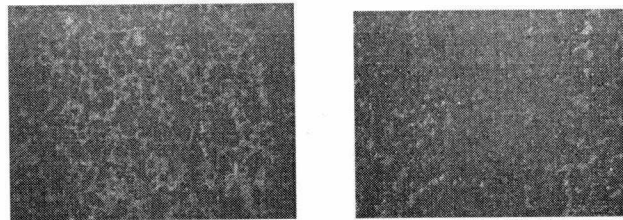
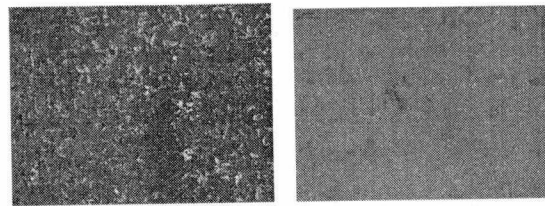**Figure 5.25 Microscope image of PU-2 after the friction test**

Left: dry friction test, 10x; right: lubricated friction test, 10x

Transparency materials:

TR-1 and TR-2 have the base material PET and coatings on both sides. Friction tests of TR-1 and TR-2 were conducted and the friction coefficients of dry, lubricated, and cell culture tests versus time are shown (Figure 5.26, Figure 5.27, Figure 5.28, Figure 5.29, Figure 5.30, Figure 5.31).
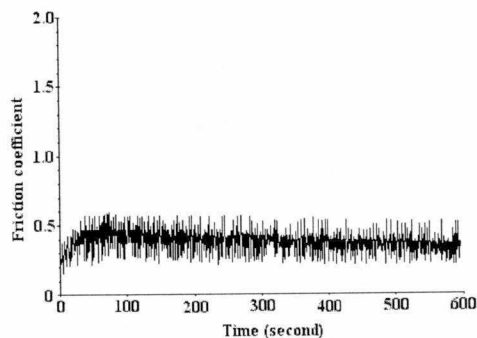
Figure 5.26 Dry friction test of TR-1
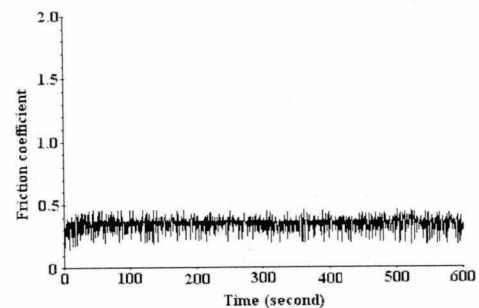
Figure 5.29 Dry friction test of TR-2
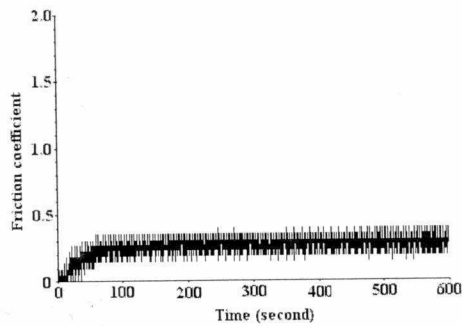
Figure 5.27 Lubricated friction test of TR-1
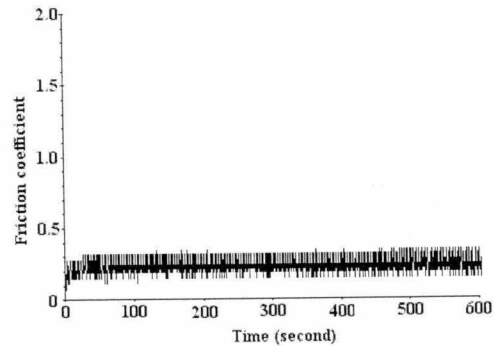
Figure 5.30 Lubricated friction test of TR-2
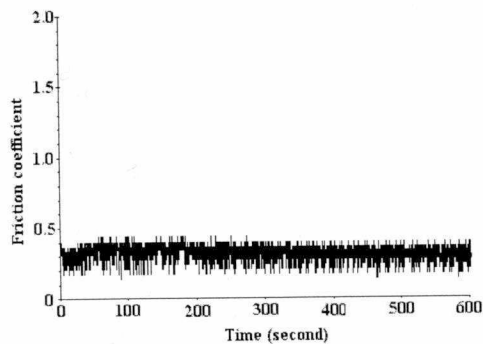
Figure 5.28 Cell culture friction test of TR-1
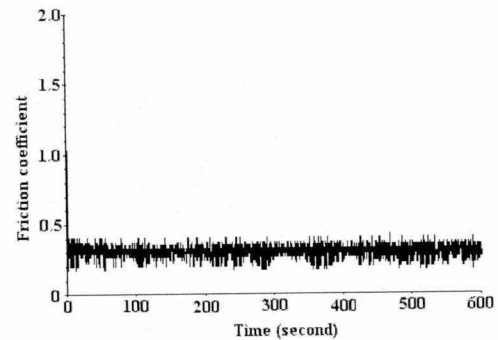
Figure 5.31 Cell culture friction test of TR-2

The average friction coefficients and the MSE of the tests on TR-1 and TR-2 are summarized in Table 5.6 and the friction coefficients are compared (Figure 5.32, Figure 5.33).
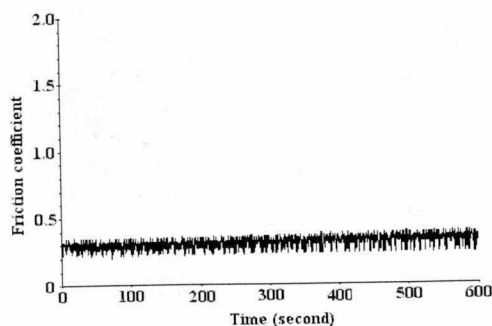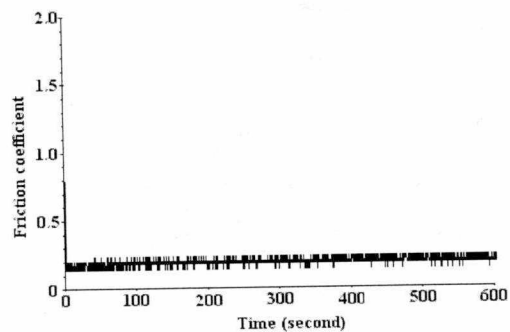
Table 5.6 Average Friction Coefficients of All Tests on TR-1 and TR-2

	TR-1		TR-2	
	Fcoe	MSE	Fcoe	MSE
Dry friction tests	0.41	0.14	0.35	0.10
Lubricated friction tests	0.28	0.16	0.26	0.09
Cell culture friction tests	0.31	0.13	0.31	0.13
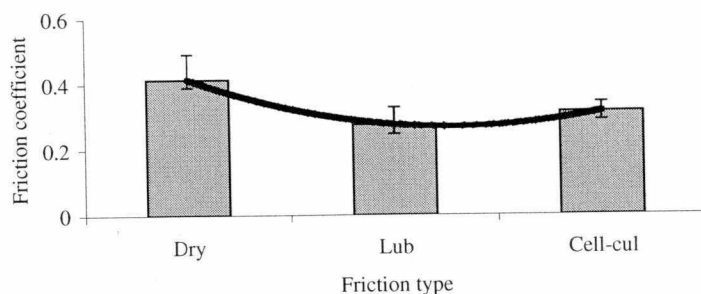
Figure 5.32 Comparison of coefficients of friction of different type of tests of TR-1
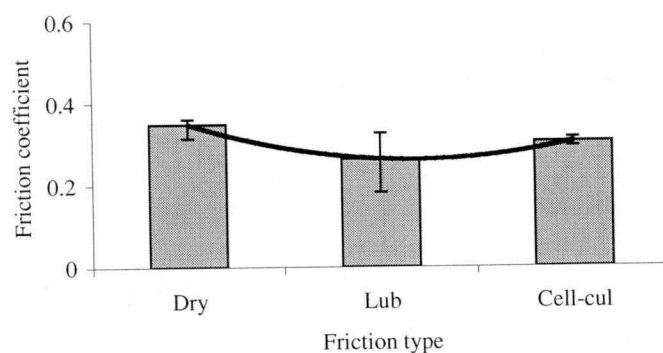
Figure 5.33 Comparison of coefficients of friction of different type of tests of TR-2

The results indicated that TR-1 and TR-2 had higher dry friction coefficients (0.41 and 0.35) than that of lubricated friction coefficients (0.28 and 0.26) and cell culture friction coefficients (0.31 and 0.31). Statistic calculations of p of the tests of TR-1 and TR-2 are both 0.000, which showed that there were highly significant differences among the groups of both TR-1 and TR-2.

Since TR-1 and TR-2 are thin film, the hardness of the bottom of the holder should be considered during the friction tests. The lubricant (BSA) decreased the friction coefficients. The lubricant molecules bonded to the surface of TR-1 and TR-2 and performed an anti-friction function. During the cell culture experiments, TR-1 and TR-2 were treated with ethanol which damaged the surface coatings. The TR-1 and TR-2 surfaces of the cell culture samples were not uniform because of the peeling of and folding over of the coatings. The cell culture friction tests showed higher average friction coefficients compared to the lubricated friction tests. TR-1 has a rougher surface profile and showed higher friction coefficients compared to TR-2.

The friction coefficient curves show that there were running-in periods for both of the dry friction tests because of the roughness of the coatings on the surfaces of TR-1 and TR-2. After the modification of the surface by the lubricant there were still running-in periods during the lubricated friction tests but with less variation. Since the cell culture experiment had modified the surface before the friction tests, no obvious running-in periods were observed during the tests. From the images after the friction tests, grooves and scratches, debris of the coatings, and the transfer of materials were observed in the cell culture friction tests (Figure 5.34, Figure 5.35).
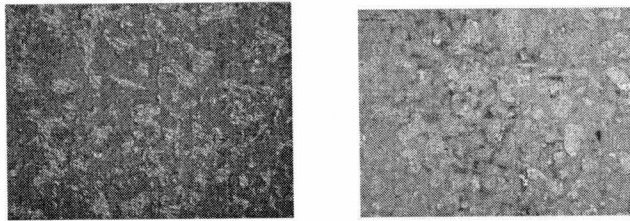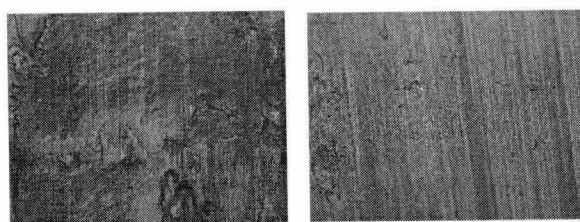

Figure 5.34 Microscope image of TR-1 after the friction test

Left: dry friction test; 20x; right: lubricated friction test, 20x
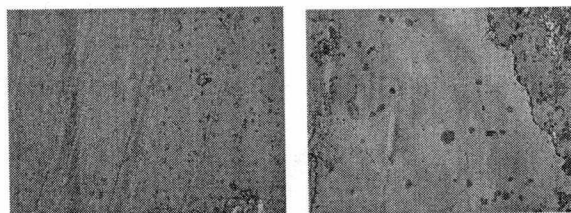
Figure 5.35 Microscope image of TR-2 after the friction test

Left: dry friction test, 10x; right: lubricated friction test, 20x

5.2 A cell-culture scaffold model of optimized material properties

Cells utilize several molecular mechanisms in adhering to other cells and to the extracellular matrix. The integrins and cadherins are proteins which are involved in cell-cell (cadherin) and cell-matrix (integrins) contacts.

The cadherins generally mediate homophilic interactions, whereas the integrins mediate heterophilic interactions. Both the cadherins and integrins act as transmembrane linkers and require extracellular divalent cations to function properly. Integrins link the cytoskeleton or they bind to the extracellular matrix (ECM). The integrin family of adhesion receptors is found throughout metazoan evolution (Hynes et al. 2000). Integrins are heterodidimeric transmembrane

receptors that bind through their globular head domain to components of ECM (Figure 5.36). Some integrins can also bind molecules present on the other cells such as bacterial polysaccharides, or viral coat proteins (Danen et al. 2003, Figure 5.36). The ECMs create and maintain a three-dimensional space for tissue formation, and they are used to guide tissue development in order to yield functional tissues (Putnam et al. 1996; Alberts et al. 2002).
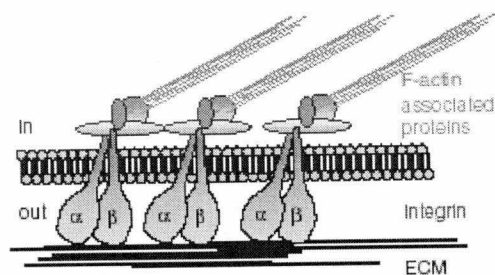
Figure 5.36 Schematic representation of a cell–matrix adhesion in which integrins connect the ECM with the actin cytoskeleton (Danen et al. 2003)

In this research, design is considered that the integrins from the cells bind to the biomaterials instead of the ECM excreted from the cell itself. The cells were seeded onto open, porous, exogenous matrices fabricated from biocompatible polymers. This matrix provides an adhesive substrate for the cells. Results showed that proper porosity is needed for this proper binding. PVA, polyurethane, Al_2O_3, and Ni were used as the macro-porous scaffold fabricated for providing strength and structural integrity. The matrix components of this artificial EMC resist the compressive forces on the matrix, while the porous structure provides tensile strength. Non-porous materials were also studied.

Chapter 6

Conclusions and future work

Current artificial joints implants are mainly metal-on-UHMWPE. The excessive wear debris from polyethylene leads to osteolysis. Fatigue, cement, and other different mechanisms lead to potential loosing of the prosthesis. Metal-on-metal artificial joints are considered as one of the alternatives for the generally used metal-on-UHMWPE bearings.

The results of materials tested: in this study - stainless steel, alumina (Al_2O_3), zirconia (ZrO_2), UHMWPE, and DLC thin film coated on stainless steel - showed that the DLC thin film coated stainless steel balls on stainless steel plate exhibited the lowest friction coefficient and the least wear. The tests of ceramic balls on stainless plate show a higher friction coefficient and visible wear with debris. Scratches, grooves, cracks, curliness, and material transfer can be observed in the wear area of stainless steel balls and ceramic balls, but not in the DLC thin film coated balls.

The diamond coatings and diamond-like coatings are chemically inert and impervious to acid and saline media and are mechanically hard, strong, and stiff (Neuville et al. 1997; Donnet et al. 1998). Carbon-based materials are highly biocompatible. Low friction and wear behavior in tests with DLC coated samples reflects the low friction attributes of the coating.

The conclusion of chapter 3 showed that it is becoming practical to coat materials with hard, smooth films of diamond and other hard carbon films. This research is preliminary. Coating materials other than stainless steel and, choosing friction pairs with different materials, should be done in the future.

Results from cell culture experiments showed that cells grew on some of the artificial matrix materials. Surface chemistry, microstructure and macrostructure of the matrix materials were all important factors. Glass and TR-2 have a higher confluency of cells than the others. Cells were observed on PVA, PU-1, PU-2, and TR-1 at different confluency.

Few cells were observed on Al_2O_3 and Ni. Al_2O_3 and Ni samples had few cells attached due to the surface chemistry and the structure. Because of their macropore structure, it is difficult for cells to migrate along the walls of the pores up onto the samples. Materials which provided basic similar surface chemistry, such as PU-1 and PU-2, showed a different cell adhesion ability because of their difference in microstructure. Open-pore structure demonstrated a better cell adhesion property compared with closed-pore structure. Proper porosity provided sufficient surface for cell-matrix interaction.

During the sterilization period, TR-1 and TR-2 coatings were partially peeled. Results showed that the areas with the coating had low confluency of cells and the areas where the coating had peeled off had much higher cell confluency. Glass, TR-1, and TR-2 are not porous matrix materials, but cells secreted ECM within a short time and could attach to the surface of these samples.

The dry, lubricated, and cell culture friction tests showed interesting results. For metal and ceramic samples, Ni and glass, dry friction was the highest friction coefficient. Lubricated friction and cell culture friction were lower respectively. TR-1 and TR-2 were also highest for dry friction but had a higher cell culture friction coefficient than a lubricated one. The porous polymers which are softer when wet showed higher friction during the lubricated and cell culture friction tests and deformation was the major factor. Clearly the cell's modification of material surfaces can have tribological impact in wear. Sometimes, the impact can be significant.

In this study, 3T3 cells were used. 3T3 cells may not make natural cartilage. Future experiments should use chondrocytes (articular cartilage cells). In this study both of the concentrations (100,000 cell/ml and 200,000 cell/ml) worked for cell culture. The pore size and porosity should be studied by synthesizing a series of open pore materials with different pore size and porosity and observing the cell adhesion on the series on different materials. Pore size and porosity also affect the mechanical properties. Some additional polymer materials, such as hyaluronic acid-based polymers, should be studied.

Cells respond to the surface chemistry, surface texture, and microstructure of the scaffolds. The mechanical influences can alter cells and cell growth. In this study, these factors were investigated. The shape and size of the cells are also factors for cell adhesion. The real fact is the combination of the complexity of these and many other factors. Recently, studies have largely focused on cartilage formation during fracture healing. Many studies are still in progress to investigate these factors that interact with each other. Further research could also investigate the role of blood vessels during the healing procedure.

References

- Acunas B., Rozanes I., Akpinar S., Tunaci A., Tunaci M., Acunas G. 1996. Palliation of malignant esophageal strictures with self-expanding nitinol stents: drawbacks and complications, Radiology, 199, 648-652.

- Akagi M., Nakamura T., Matsusue Y., Ueo T., Nishijyo K., Ohnishi E. 2000. The bisurface Total Knee Replacement: A unique design for flexion: four-to-nine-year follow-up study, J. Bone Joint Surg. Am., 82(11), 1626-1633.

- Alberts B., Bray B., Lewis J., Raff M., Roberts K., Watson J.D. 2002. Molecular biology of the cell, 4th edi., Garland Publishing, Inc. New York & London.

- Alberts B., Bray D., Lewis J., Raff M., Roberts K., Watson J.D. 1994. Molecular biology of the cell, 3rd edi., Garland Publishing.

- Alsberg E., Anderson K.W., Albeiruti A., Rowley J.A., Mooney D.J. 2002. Engineering growing tissues, Applied Biological Sciences, 99 (19), 12025–12030.

- Amontons G. 1699. De la ReÂ sistance CauseÂ e dans les Machines. MeÂmoires de l'AcadeÂmie Royale, A, 257-282.

- Andersen J. 2004. http://physics.about.com/mbiopage.htm.

- Anonymous 1955. Fretting and fretting corrosion, Lubrication, 41, 85-96.

- Armini, A.J., Bunker, S.N., Huntington D.M. 1998. Adherent alumina coatings by ion beam synthesis, Alternative bearing surfaces in Total Joint Replacement, ASTM STP 1346, J. J. Jacobs and T. L. Craig, Eds., American Society for Testing and Materials.

- Arthritis Foundation 2004. http://www.arthritis.org.

- Ashammakhi N., Ferretti P. 2003. Topics in tissue engineering, 1, e-book: www.tissue-engineering-oc.com

- Ashley-Ross M. 2003. www.wfu.edu/~rossma/bio322/joints.html.

- Association of Cancer of Online Resource 2004. Cartilage, http://www.acor.org/.

- ASTM-G99-95ael, Standard test method for wear testing with a pin-on-disk apparatus, in Annual Book of ASTM standards, American Society for Testing and Materials: Philadelphia.

- AZoM.com, Czernuszka J. 1996. Biomaterials under the microscope. Materials World, 4, 452-453.

- Barbour P.S.M., Barton D.C., Fisher J. 1995. The influence of contact stress on the wear of UHMWPE for total replacement hip prostheses, Wear, 181-183 (1), 250-257.

- Barrera D.A., Zylstra E., Lansbury P., Langer R. 1993. Synthesis and RGD peptide modification of a new biodegradable copolymer system: Poly (Lactic Acid-co-Lysine). J. of Amer. Chem. Soc., 115, 11010-11011.

- Barrett T.S., Stachowiak G.W., Batchelor A.W. 1992. Effect of roughness and sliding speed on the wear and friction of ultra-high molecular weight polyethylene, Wear, 153, 331-350.

- Begin-Colin S., Mocelin A., Stebut J.V., Bordi K., Mainard D. 1998. Al_2O_3 and Al_2O_3-TiN wear resistance in a simulated biological environment, J. mater. Sci., 33, 2837-2843.

- Bell E., Ehrlich P., Buttle D.J., Nakatsuji T. 1981. Living tissue formed in vitro and accepted as skin-equivalent of full thickness, Science, 221, 1052-1054.

- Berrien L.S.J. 1999. Studies of the effects of biochemical environments on the wear and damage of articular cartilage, Ph D. thesis of Virginia Polytechnic Institute.

- Bhushan B. 2002. Introduction to tribology, John Wiley & Sons, INC., New York.

- Biomet 2001. http://www.biomet.com/patients/bestimplant.html.

- Bisceglie V. 1933. Uber die antineoplastische immunitat; heterologe Einpflanzung von Tumoren in Huhner-embryonen. Ztschr. f. Krebsforsch, 40, 122-140.

- Blanchard C.R. 1995. Biomaterials: Body parts of the future, Technology Today, Southwest Research Institute, Fall 1995 issue.

- Blanchet T.A., Peterson S.L., Rosenberg K.D. 2002, Serum lubricant absorption by UHMWPE orthopaedic bearing implants, J. of Tribology, 124(1), 1-4.

- Booser R.E. 1984. Handbook of lubrication – Theory and practice of tribology, II, CRC Press, Inc.

- Bos O.J.M., Labro J.F.A., Fischer M.J.E., Witling, J., Janssen L.H.M. 1989. The molecular mechanism of the Neutral-to-Base transition of human serum albumin, J. Biol. Chem., 264, 953-959.

- Brown J.R. 1975. Structure of bovine serum albumin, Fed. Proc. 34, 591.

- Burke J.F., Yannas I.V., Quimby W.C., Bondoc C.C., Jung W.K. 1981. Successful use of a physiologically acceptable artificial skin in the treatment of extensive burn injury, Ann Surg, 194, 413-448.

- Campbell P., Ma S., Yeom B., McKellop H., Schmalzried T., Amstrutz H. 1995. Isolation of predominantly submicron-sized UHMWPE wear particles from periprosthetic tissues, J. Biomed. Mater. Res., 29, 127-131.

- Caplan A.I., Elyaderani M., Mochizuki Y., Wakitani S., Goldberg V.M. 1997. Principles of cartilage repair and regeneration, Clin. Orthop., 342, 254–269.

- Caprette D.R. 2000. www.ruf.rice.edu/~bioslabs/methods/microscopy/cellcounting.html

- Castleman L.S., Motzkin S.M., Alicandri F.P., Bonawit V.L. 1976. Biocompatibility of nitinol alloy as an implant material, J.Biomed.Mater.Res., 10, 695-731.

- Chan F.W., Bobyn J.D., Medley J.B., Krygier J.J., Yue S., Tanzer M.T. 1996. Engineering issues and wear performance of metal-metal hip implants, Clin. Orthop. 333, 96-107.

- Chick W.L., Like A.A., Lauris V. 1975. Beta cell culture on synthetic capillaries: an artificial endocrine pancreas, Science, 187, 847-848.

- Chu C.C., Williams D.F. 1983. The effect of gamma irradiation on the enzymatic degradation of polyglycolic acid absorbable sutures, Journal of Biomedical Materials Research, 17, 1029-1040

- Collier J. P., Surprenant V.A., Jensen R. E., Mayor M.B. 1991. Corrosion at the interface of cobalt-alloy heads on titanium-alloy stems, Clin. Orthop., 271, 305-312.

- Covert R.J. 2003. Durability evaluation of articular cartilage prostheses, PhD thesis of Georgia Institute of Technology.

- Danen E.H.J., Sonnenberg A. 2003. Integrins in regulation of tissue development and function, J. Patho, 200, 471-480.

- Dicarlo E.F., Bullough P.G. 1992. The biologic response to orthopedic implants and their wear debirs, Clin. Mater., 9, 235-260.

- Donnet C. 1998. Recent progress on the tribology of doped diamond-like and carbon alloy coatings: a review, Surface Coatings Technology, 100-101, 180-186.

- Dorinson A., Ludema K.C. 1985. Mechanics and chemistry in lubrication, Tribology series 9, Elsevier.

- Dowson D. 1979. History of tribology, New York, Longman, Inc.

- Dowson D. 1997. Progress in tribology: A historical perspective, new directions in tribology, Edi. Hutchings I.M., First World Tribology Congress, 8-12 Sept., London, 3-20.

- Dutta Roy T., Simon J., Ricci J.L., Rekow D.E., Thompson V.P., Parsons R.J. 2003. Performance of hydroxyapatite bone repair scaffolds created via three-dimensional fabrication techniques, Journal of Biomedical Materials Research Online, 1228 -1237.

- Eftekhar N.S. 1987. Long-term results of cemented total hip arthropoasty, Clin. Orthop. Rel. Res., 225, 207-217.

- Ekberg A. 1997. http://www.am.chalmers.se/~anek/research.

- Erdemir A., Eryilmaz O.L., Nilufer I. B., Fenske G.R. 2000. Synthesis of superlow-friction carbon films from highly hydrogenated methane plasmas, Surface and Coatings Technology, 133-134 (1-3), 448-454.

- Erdemir A., Nilufer I.B, Eryilmaz O.L., Beschliesser M., Fenske G. R. 1999. Friction and wear performance of diamond-like carbon films grown in various source gas plasmas, Surface and Coatings Technology, 120-121 (1-3), 589-593.

- Figge J., Rossing, T.H., Fencl, V. 1991. The role of serum-proteins in Acid-Base equilibria. J. Lab. Clin. Med., 117, 453-467.

- Flögel M. 2004. Introduction to glycococonjugates, http://www.pharma.hr/bmb/predavanja/Glycoconjugates/sld037.htm.

- Folkman J., Haudenschild C. 1980. Angiogenesis in vitro, Nature, 288, 551-556.

- Frank T., Willetts G.J., Cuschieri A. 1995. Detachable clamps for minimal access surgery, Proc. Inst. Mech. Eng., 209, 117-120.

- Freemont A.J., Denton J. 1991. Atlas of synovial fluid cytopathology, Kluwer Academic Publishers, Book series: Current histopathology, 18, Gresham GA.

- Freshney I.R. 2000. Culture of animal cells. 4th edi., John Wiley & Sons, Inc., New York.

- Friedli G.L. 1996. Interaction of deamidated soluble wheat protein (SWP) with other food proteins and metals, Ph D Thesis of the University of Surrey, England.

- Furey M.J. 1986. Tribology. In: Encyclopedia of Materials Science and Engineering, Edi. Bever M.B., Pergamon Press, Oxford, 5145-5157.

- Furey M.J., Burkhardt B.M. 1997. Biotribology: friction, wear, and lubrication of synovial joints, Lubrication Science, 9, 255-271.

- Gecheler K.E., Wacker R., Martini F., Hack A., Aicher W.K. 2003. Enhanced biocompatibility for SAOS-2 osteosarcoma cells by surface coating with hydrophobic epoxy resins, Cellular Physiology and Biochemistry, 13, 155-164.

- Gidling D.K., Reed A.M. 1979. Biodegradable polymers for use in surgery-polyglycolic/poly (latic acid) homo-and copolymers: 1, Polymer, 20, 1459-1464.

- Gilbert J.L., Buckley C.A. 1995. Mechanical-Electrochemical interactions during in vitro fretting corrosion tests of modular taper connections, Total Hip Revision Surgery, Edi. Galante J.O., Rosenberg A.G., Callaghan J.J., Raven Press, Ltd., New York.

- Gilbert J.L., Jacobs J.J. 1997. The mechanical and electrochemical processes associated with taper fretting crevice corrosion: a review, Modularity of orthopedic Implants, ASTM STP 1301, Edi. Marlowe D.E., Parr J.E., Mayor M.B., American Society for testing and Materials, 45-59.

- Goldberg J.R., Gilbert J.L. 1997. Electrochemical response of CoCrMo to high-speed fracture of its metal oxide using an electrochemical scratch test method, J. Biomed. Mater Res., 37, 421-431.

- Gottfried H.W., Gnann R., Brandle E., Bachor R., Gschwend J.E., Kleinschmidt K. 1997. Treatment of high-risk patients with subvesical obstruction from advanced prostatic carcinoma using a thermosensitive mesh stent, Br. J. Urol., 80, 623-627.

- Grande D.A., Breitbart A.S., Mason J., Paulino C., Laser J., Schwartz R.E. 1999. Cartilage tissue engineering: current limitations and solutions, Clin. Orthop., 367, S176–185.

- Griffith M., Seidenstein M., William D., Charnley J. 1978. Socket wear in Charnley low friction arthroplasty of the hip, Clin. Orthop., 137, 37-47.

- Gupta M.C., Deshmukh V.G. 1983. Radiation effects on polylatic acid, Polymer, 24, 827-830.

- Harris W.H. 1995. Problem in osteolysis, Clin. Orthop. Rel. Res. 311, 46-53.

- Hauck R.W., Lembeck R.M., Emslander H.P., Schomig A. 1997. Implantation of accuflex and strecker stents in malignant bronchial stenoses by flexible bronchoscopy, Chest, 112, 134-144.

- Hauert R. 2003. A review of modifies DLC coatings for biological applications, Diamond and Related Materials, 12, 583-589.

- He X.M., Carter D.C. 1992. Atomic structure and chemistry of human serum albumin, Nature, 358, 209-215.

- Herring M., Smith J., Dalsing M., Glover J., Compton R., Etchberger K., Zollinger T. 1994. Endothelial cell seeding of polytetrafluoroethylene femoral popliteal bypasses: The failure of low-density seeding to improve patency, J. Vasc. Surg., 20, 650-655.

- Hertling D., Kessler R.M., 1996. Management of common musculoskeletal disorders: Physical therapy principles and methods (3rd edi.), Philadelphia: Lippincott, 27-28.

- Hirayama K., Akashi S., Furuya M., Fukuhara, K.I. 1990. Rapid confirmation and revision of the primary structure of bovine serum albumin by ESIMS and FRIT-FAB LC/MS, Biochem. Biophys. Res. Commun., 173, 639-646.

- Hoeppner D.W., Chandrasekarn V. 1994. Fretting in orthopaedic implants: a review, Wear, 173,189-197.

- Hollister S.J. 2004. http://www.engin.umich.edu/class/bme456/index.htm.

- Homsy C.A., McDonald K.E., Akers W.W., Short C., Freeman B.S. 1968. Surgical suture-canine tissue interaction for six common suture types, J. Biomed. Mater. Res., 2, 215-230.

- Hu W.S., Peshwa M.V. 1991. Animal cell bioreactor – Recent advances and challenges to scale-up, Can. J. Chem. Eng., 69, 409–420.

- Huang S., Chen C.S., Ingber D.E. 1998. Control of cylin D1, p27(Kip1), and cell cycle progression in human capillary endothelial cells by cell shape and cytoskeletal tension, Mol. Biol. Cell, 9, 3179-3193.

- Hubbell J.A., Massia S.P., Drumheller P.D. 1992. Surface-grafted cell-binding peptides in tissue engineering of the vascular graft, Ann. N. Y. Acad. Sci., 665, 253-258.

- Hurricks P.L. 1970. The mechanism of fretting-A review, Wear, 15, 389-409.

- Hutchings I.M. 2002. Friction, Lubrication, and Wear of Artificial Joints, Professional Engineering Publishing.

- Hutmacher D.W. 2000. Scaffold in tissue engineering bone and cartilage, Biomaterials, 21(24), 2529-2543.

- Hynes R.O., Zhao Q. 2000. The evolution of cell adhesion. J. Cell Biol., 150, 89-96.

- Ijiri S., Yamamuro T., Nakamura T., Kotani S., Notoya K. 1994. Effect of sterilization on bone morphogenetic protein, Journal of Orthopaedic Research, 12(5), 628-636.

- Illingworth B., Tweden K., Schroeder R., Cameron J.D. 1998. In vivo efficacy of silver-coated (silzone) infection-resistant polyester fabric against a biofilm-producing bacteria, Staphylococcus Epidermidis, J. Heart Valve Dis., 7 (5), 524-530.

- Kaufman K. R., An K. 2003. Biomechanical principles and applications - Joint-articulating surface motion, Edi. Scheneck D.J., Bronzino J.D., CRC Press, 35-72.

- Kim B., Mooney D.J. 1998. Development of biocompatible synthetic extracellular matrices for tissue engineering, Trend Biotechnol, 16, 224-230.

- Klinge U., Klosterhalfen B., Conze J., Limberg W., Obolenski B., Öttinger A., Schumpelick V. 1988. Modified mesh for hernia repair that is adapted to the physiology of the abdominal wall, Eur. J. Surg., 164, 951-960.

- Kohn D.H., Dycheyne P. 1992. Medical and Dental Materials - Materials for bone, joint and cartilage replacement, Edi. Williams D.F., VCH Verlagsgesellschaft, FRG, 29-109.

- Kossovsky N., Mirra J.M. 1991. Biocompatibility and bioreactivity of arthroplastic materials, Hip Arthroplasty, 571-601, Edi. Amstutz H.C., New York, Churchill Livingstone.

- Kreighbaum E., Barthels K.M. 1985. Biomechanics, a qualitative approach for studying human movement, 2nd edi., Burgess Publishing Company, Minneapolis, Minnesota.

- Kreklau B., Sittinger M., Mensing M., Voigt C., Berger G., Gross U. 1999. Tissue engineering of biphasic joint cartilage transplants, Biomaterials, 20, 1743–1749.

- Kuznetsow A.N., Ebert B., Lassmann G., Shapiro A.B. 1975. Adsorption of small molecules to Bovine serum Albumin studied by the Spin-Probe method, Biochim. Biophys. Acta, 379, 139-146.

- Lambda N.M.K., Woodhouse K.A., Cooper S.L. 1998. Polyurethanes in Biomedical Applications, CRC Press.

- Langer R, Vacanti J.P. 1993. Tissue engineering, Science, 260, 920 –926.

- Langer R, Vacanti J.P. 1999. Tissue engineering: the challenges ahead, Sci Am, 280, 62-65.

- Lauffenburger D.A., Griffith L.G. 2001. Who's got pull around here? Cell organization in development and tissue engineering, PNAS, 98(8), 4282-4284.

- Laurencin 2001. http://laurencin.coe.drexel.edu.

- Lee S.W., Morillo C., Lira-Olivares J., Kim S.H., Sekino T., Niihara K., Hockey B.J. 2003. Tribological and microstructural analysis of Al_2O_3/TiO_2 nanocomposites to use in the femoral head of hip replacement, Wear, 255, 1040-1044.

- Lewis G. 1997. Polyethylene wear in total hip and knee arthroplasties, J. Biomed. Mater. Res. (Appl. Biomater.), 38, 55-75.

- Li S., Burstein A.H. 1994. Ultra-high molecular weight polyethylene. The material and its use in total joint implants, J Bone Joint Surg Am, 76, 1080-1090.

- Liang H., Shi B., Fairchild A., Cale A. 2004. Applications of plasma coatings in artificial joints: an overview, Vacuum, 73, 317-326.

- Liao Y.S., Mcnulty D., Hanes M. 2003. Wear rate and surface morphology of UHMWPE cups are effected by the serum lubricant concentration in a hip silulation test, Wear, 255, 1051-1056.

- Lin H., Garcia-Echeverria C., Asakura S., Sun W., Mosher D.F., Cooper S.L. 1992. Endothelial cell adhesion on polyurethanes containing covalently attached RGD-peptides, Biomaterials, 13, 905-914.

- Lin V.J.C., Koenig J.L. 1976. Raman studies of bovine serum albumin. Biopolymers, 15, 203-218.

- Liu G.J., Miyaji F., Kokubo T., Takadama H., Nakamura T., Murakami A. 1998. Apatite organicpolymer compositesprepared by a biomemetic process: improvement in adhesion of the apatite layer to the substrate by ultraviolet irradiation, Journal of Material Science: Materials in Medecine, 9(5), 285-290.

- Livermore J., Ilstrupand D., Morrey B. 1990. Effect of femoral head size on wear of the polyethylene acetabular component, J. Bone Joint Surg., 72-A(4), 518-528.

- Long M., Rack H. 1998. Review: titanium alloys in Total Joint Replacement - a materials science perspective, Biomaterials, 19, 1621-1639.

- Long M., Rack H.J. 1998. Titanium alloys in total joint replacement- a materials science perspective, Biomaterials, 19, 1621-1639.

- Lu S.B., Wang J.F., Guo J.F. 1986. Treatment of scoliosis with a shape-memory alloy rod, Chung Hua Wai Ko Tsa Chih, 24, 129-132.

- McGillivray R.T.A., Chung D.W., Davie, E.W. 1979. Biosynthesis of bovine plasma proteins in a cell-free system. Amino-terminal sequence of preproalbumin. Eur. J. Biochem, 98, 477-485.

- McIlwraith W.C. 2004. http://www.completerider.com/ucolorado/joints.html.

- McKee G.K. 1982. Total hip replacement – past, present and future, Biomaterials, 3, 130-135.

- McLaughlin J. 1994. 8-10 year results using the taperloc femoral component in uncemented total hip arthroplasty, Annual Meeting of the American Academy of Orthopedic Surgeons

- Metzger A., Restore Medical Inc. 2004. Polyethylene Terephthalate and the Pillar™ Palatal Implant: its historical usage and durability in medical applications, dentalimplants-usa.com.

- Mikos A.G., Bao Y., Cima L.G., Ingeber D.E., Vacanti J.P., Langer R.B. 1993. Preparation of poly(glycolic acid) bonded fiber structures for cell attachment and transplantation, J. Biomed Mater. Res., 27, 183-189.

- Moiseeva E.P. 2001. Adhesion receptors of vascular smooth muscle cells and their functions, Cardiovasc Res., 52, 372-386.

- Monteilh-Zoller M.K., Hermosura M.C., Nadler M.J.S., Scharenberg A.M., Penner R., Fleig A. 2003. TRPM7 provides an ion channel mechanism for cellular entry of trace metal ions, Journal of General Physiology, 121(1), 49-60.

- Mooney D.J., Mikos A.G. 1999. Growing new organs, Sci. Am., 280, 38-43.

- Mooney D.J., Vacanti J.P. 1993. Tissue engineering using cells and synthetic polymers, Transplant Rev., 7, 153–161.

- Mow V.C., Ratcliffe A. 1997. Basic orthopaedic biomechanics - Structure and function of articular cartilage and meniscus, Edi. Mow V.C.,Hayes W.C. , 2nd edi., Lippincott Williams & Wilkins Publishers.

- Mow V.C., Roth V., Armstrong C.G. 1980. Basic biomechanics of the skeletal system - Bimechanics of joint cartilage, Edi. Frankel V.H., Nordin M.A., Philadelphia, Lea & Febiger.

- Müller K.M., Dasbach G. 1994. The pathology of vascular grafts. In: The Pathology of Devices, edi., C.L. Berry, Springer Verlag, Berlin-Heidelberg. 273-306.

- Natures Health Products, Inc. 2004. http://www.coral1.com/syn.html

- Nerem R.M. 1991. Cellular engineering, Ann Biomed Eng., 19, 529 –545.

- Neuville S., Matthews A. 1997. Hard carbon coatings: The way forward, MRS Bull., 22(9), 22-26.

- Niihara K. 1991. New design concept of structural ceramics: ceramic nanocomposited, J. Jpn. Ceram. Soc., 99, 945-952.

- Nuttelman C.R., Mortisen D.J., Henry S.M., Anseth K.S. 2001. Attachment of fibronectin to poly(vinyl alcohol) hydrogels promotes NIH3T3 cell adhesion, proliferation, and migration, Journal of Biomedical Materials Research, 57 (2), 217-223.

- O'Neill C., Jordan P., Ireland G. 1986. Evidence for two distinct mechanisms of anchorage stimulation in freshly explanted and 3T3 swiss mouse fibroblasts, Cell, 44, 489-496.

- Oakes J. 1976. Thermally denatured proteins. J. Chem. Soc. Faraday I, 72, 228-237.

- Oatis C.A. 2004. Kinesiology - The mechanics & pathomechanics of human movement, Lippincott William & Wilkins.

- Overney R M. 2004. http://depts.washington.edu/nanolab/.

- Patterson J.E., Geller D.M. 1977. Bovine microsomal albumin: Amino terminal sequence of bovine proalbumin, Biochem. Biophys. Res. Commun., 74, 1220-1226.

- Peppas, N. A, Langer, R. 1994. New challenges in biomaterials, Science, 263, 1715–1720.

- Peters M.C., Isenberg B.C., Rowley J.A., Mooney D.J. 1998. Release from alginate enhances the biological activity of vascular endothelial growth factor, Journal of Biomaterials Science, Polymer Edi, 9(12), 1267-1278.

- Petrini P., Parolari C., Tanzi M.C. 2001. Silk fibroin-polyurethane scaffolds for tissue engineering, Journal of Materials Science: Materials in Medicine, 12 (10-12), 849-853.

- Pezzullo J.C. 2004. http://members.aol.com/johnp71/index.html#Reference

- Prokop D.J. 1997. Marrow stromal cells as stem cells for nonhematopoietic tissues, Science, 276, 71-74.

- Puolakkainen P.., Ranchalis J.E., Strong D.M., Twardzik D.R. 1983, The effect of sterilization on transforming growth factor B isolated from demineralized human bone, Transfusion, 33, 679-685.

- Putnam A.J., Mooney D.J. 1996. Tissue engineering using synthetic extracellular matrices, Nat. Med., 2, 824-826.

- Putnam A.J., Mooney D.J. 1996. Tissue engineering using synthetic extracellular matrices, Nature Medicine, 2 (7), 824-826.

- PVA Unlimited 2004. http://www.sponge-pva.com.

- Raimondi M.T., Boschetti F., Falcone L., Fiore G.B., Remuzzi A., Marinoni E., Marazzi M., Pietrabissa R. 2002. Mechanobiology of engineered cartilage cultured under a quantified fluid-dynamic environment, Biomechan. Model Mechanobiol., 1(1), 69-82.

- Rauber K., Franke C., Rau W.S., Syed A.S., Bensmann G. 1990. Peroral einfuhrbare endotracheale stutzgeruste aus der memory-legierung NiTi--Tierexperimentelle studie, Rofo. Fortschr. Geb. Rontgenstr. Neuen. Bildgeb. Verfahr, 152, 698-701.

- Reed R.G., Putnam, F.W., Peters T. Jr. 1980. Sequence of residues 400-403 of bovine serum albumin, Biochem. J., 191, 867-868.

- Ries M., Banks S., Sauer W., Anthony M. 1999. Abrasive wear simulation in total knee arthroplasty, 45th Annual Meeting, Orthopaedic research Society, Anaheim, CA.

- Risbud M., Ringe J., Bhonde R., Sittinger R. 2001. In Vitro expression of cartilage-specific markers by chondrocytes on a biocompatible hydrogel: implications for engineering cartilage tissue, Cell Transplantation, 10, 755-763.

- Ritter M.A., Worland R., Saliski J., Helphenstine J.V., Edmondson K.L., Keating E.M., Faris P.M., Meding J.B. 1995. Flat-on-flat, nonconstrained, compression molded polyethylene total knee replacement, Clinical Orthopedics and Related Research, 321, 79-85.

- Sarikaya M., Fong H., Frech D., Humbert R. 1999. Biomimetic assembly of nanostructured materials, Materials Science Forum, 293, 83-98.

- Schultz O., Sittinger M., Haeupl T., Burmester G.R. 2000. Emerging strategies of bone and joint repair, Arthritis Res. 2(6), 433-436.

- Service, R.F. 1995. Out of the Lab, Into the Body, Science, 270, 231.

- Shi B., Ajayi O.O., Fenske G., Erdemir A., Liang H. 2003. Tribological performance of some alternative bearing materials for artificial joints, Wear, 255, 1015-1021.

- Shi B., Fairchild A., Kleine Z., Kuhn T.B., Liang H. 2004. Effects of Surface Texturing on Cell Adhesion for Artificial Joints, MRS Symposium W Proceedings.

- Shi B., Liang H. 2001. Tribological applications of biomaterials: An overview, Scientia Sinica, Series A, 44, Supp., 297-306.

- Shier D., Butler J., Lewis R. 1999. Hole's human anatomy & physiology, 8th edition, WCB/McGraw-Hill, New York.

- Simon J., Dutta Roy T, Parsons J.R., Rekow R.E., Thompson V.P., Kemnitzer J., Ricci J.L. 2003. Engineered cellular response to scaffold architecture in a rabbit trephine defect, Journal of Biomedical Materials Research, 66A(2), 275 – 282.

- Simon M., Kaplow R., Salzman E , Freiman D. 1977. A vena cava filter using thermal shape memory alloy. Experimental aspects, Radiology, 125, 87-94.

- Skalak R., Fox C.F. 1988. Tissue engineering, Alan Liss, New York.

- Sodian R., Hoerstrup S.P., Sperling J.S., Daebritz S., Martin D.P., Moran A.M., Kim B.S., Schoen F.J., Vacanti J.P., Mayer, Jr. J.E. 2000. Early In Vitro experience of tissue-engineered trileaflet heart valves, Circulation,102, suppl III, 22-29.

- Spector M. 1992. Biomaterial failure, Orthop Clin North Am., 23(2), 211-217.

- SRI Consulting Business Intelligence 2004. www.sric-bi.com/Explorer/BM.shtml.

- Stachowiak G.W., Batchelor A.W., Griffiths L.J. 1994. Friction and wear changes in synovial joints, Wear, 171, 135-142.

- Stupp S.I. 2001. Biomaterials - Introduction for annual review of materials research, Annual Review of Materials Research, 31.

- Sutherland C.J., Wilde A.H., Borden L.S., Marks K.E. 1982. A ten-year follow-up of one hundred consecutive Muller curved-stem total hip-replacement arthroplasties, J. Bone joint Surg. A, 64(7), 970-982.

- Swanson S.A. 1980. Articular cartilage, Symp. Soc. Exp Biol, 34, 377-395.

- Temenoff J.S.; Mikos A.G. 2000. Review: tissue engineering for regeneration of articular cartilage, Biomaterials, 21, 431–440.

- Thomson J.A., Itskovitz-Eldor J, Shapiro S.S., Waknitz M.A., Swiergiel J.J., Marshall V.S., Jones J.M. 1998. Embryonic stem cell lines derived from human blastocysts, Science, 282, 1145-1147.

- Torrance A.A. 2004. http://www.mme.tcd.ie/~torrance.

- Tracey D. 2002. Functional Anatomy, anatomy.med.unsw.edu.au/teach/anat3131.

- Turell M., Wang A., Bellare A. 2003. Quantification of the effect of cross-path motion on the wear rate of ultra-high molecular weight polyethylene, Wear, 255, 1034-1039.

- University of Queensland 2004. http://www.cheque.uq.edu.au/research/bioengineering/ research/Metabolic_Engineering

- Vacanti J.P., Langer R. 1999. Tissue engineering: the design and fabrication of living replacement devices for surgical reconstruction and transplantation, Lancet. 354, S1, 132-134.

- Vacanti J.P., Morse M.A., Saltzman W.M., Domb A.J., Perez-Atayde A., Langer R. 1988. Selective cell transplantation using bioabsorbable artificial polymers as matrices, J. Pediatr. Surg. 23, 3-9.

- Vance R.J., Miller D.C., Thapa A., Haberstroh K. M., Webster T.J. 2003. Decreased fibroblast cell density on chemically degraded poly-lactic-co-glycolic acid, polyurethane, and polycaprolactone, Biomaterials, 25(11), 2095-2103.

- Vaxa International Inc. 1998. Get those joints jumping, vaxa.com/html/634.html.

- Vinard E., Eloy R., Descotes J., Brudon J., Guidicelli H., Magne J., Patra P., Berruet R., Huc A., Chauchard J. 1988. Stability of performances of vascular prostheses retrospective study of 22 cases of human implanted prostheses, J Biomed. Mater. Res., 22, 633-648.

- von Recum A.F. 1984. Applications and failure modes of percutaneous devices: A review, J. Biomed. Mater. Res., 18, 323-336.

- Vunjak-Novakovic G, Freed L, Biron R.J., Langer R. 1996. Effects of mixing on the composition and morphology of tissue-engineered cartilage, Am Inst Chem Eng J, 42, 850-860.

- Waigh T., McLeish T. 2004. Molecular biophysics, www.physics.leeds.ac.uk/pages/ MolecularBiophysics.

- Wang A. 2001. A unified theory of wear for ultra-high molecular weight polyethylene in multidirectional sliding, Wear, 248, 38-47.

- Wang A., Essner A., Polineni V.K., Sun D.C., Stark C., Dumbleton J.H. 1997. New Directions in Tribology - Lubrication and wear of Ultra-high Molecular Weight Polyethylene in total joint replacement, Edi. Hutchings I.M., World Tribology Congress, London, 443-458.

- Wang B., Sun D.C., Startk C., Dumbleton J.H. 1995. Orientation softening in the deformation and wear of Ultra-hogh molecular weight polyethylene, Wear, 181-183, 241-249.

- Waterhouse R.B. 1981. Fretting wear, Proc. Int. Conf. Of Wear of Materials, ASME, New York, 17-22.

- Waterhouse R.B. 1992. ASM handbook, 18, Friction, Lubrication and Wear technology - Fretting wear, ASM International, Materials Park, OH, 242-256.

- Wholey M.H., Wholey M., Bergeron P., Diethrich E.B., Henry M., Laborde J.C., Mathias K., Myla S., Roubin G.S., Shawl F., Theron J.G., Yadav J.S., Dorros G., Guimaraens J., Higashida R., Kumar V., Leon M., Lim M., Londero H., Mesa J., Ramee S., Rodriguez A., Rosenfield K. , Teitelbaum G., Vozzi C. 1998. Current global status of carotid artery stent placement, Cathet. Cardiovasc. Diagn., 44, 1-6.

- Williams J.A. 1994. Engineering tribology, Oxford Science Publications.

- www.argonne.gov, 2004.

- www.cetr.com, 2004.

- www.nikonusa.com, 2004

- www.olympusmicro.com, 2004.

- www.rame-hart.com, 2003

- www.utahhipandknee.com, 2004

- Yamamoto M., Tabata Yamamoto M., Tabata, Kawasaki H., Ikada Y. 2000. Promotion of fibrovascular tissue ingrowth into porous sponges by basic fibroblast factor, J. of Mater. Sci.: Mater. In Med., 11, 213-218.

- Zhou Y.S., Ohashi M., Ikeuchi K. 1997. Start up and steady state friction of alumina against alumina, Wear, 210, 112-119.

APPENDICES

Appendix A

Data of pin-on-disk friction tests of stainless steel ball on stainless steel ball

LABTECH NOTEBOOK

15 Hz Recip. Tester

The time is 09:37:14.69.

The date is 7-03-2001.

Elp Time seconds	TC #1 degs F	AvgPkLC Newtons	Fricoeff
0	72	0	0
5	72	0.1	0.002
10	72	8	0.159
15	72	3.8	0.077
20	72	4.7	0.093
25	72	5.1	0.101
...	...	...	...
...	...	...	...
...	...	...	...
...	...	...	...
...	...	...	...
...	...	...	...
3589	72	4.5	0.09
3594	72	4.6	0.092
3599	72	4.4	0.088
3604	72	4.4	0.089
3609	72	4.3	0.086

Appendix B

Analysis of variance of friction experiment results of balls on SS plate

A p-value less than 0.05 indicates that there is a significant difference somewhere among the various groups.

Enter your summary data here...

Group	N (count)	Mean	Std. Dev. ▼
1:	3	0.087	0.01915
2:	3	0.110	0.01850
3:	3	0.115	0.00966
4:	3	0.052	0.00384
5:	3	0.033	0.00218
6:			
7:			
8:			

ANOVA Table...

Source of Variation	Sum of Squares	d.f.	Variance	F	p
Between Groups:	0.0155	4	0.0039	23.5700	0.0000
Within Groups:	0.0016	10	0.0002		
Total:	0.0171	14			

Appendix C
Critical values for χ^2-distribution

One Tail Areas	0.20	0.10	0.05	0.01	0.001
$\nu=1$	1.64	2.71	3.84	6.63	10.83
2	3.22	4.61	5.99	9.21	13.82
3	4.64	6.25	7.81	11.34	16.27
4	5.99	7.78	9.49	13.28	18.47
5	7.29	9.24	11.07	15.09	20.52
6	8.56	10.64	12.59	16.81	22.46
7	9.80	12.02	14.07	18.48	24.32
8	11.03	13.36	15.51	20.09	26.12
9	12.24	14.68	16.92	21.67	27.88

Appendix D
Condition setup of UMT in friction tests

Takeoff:

Touch: -2 N

Carriage velocity (mm/sec): Far 1; Touch 0.5; Near 0.5

Accel/Deccel time: 0.05 sec

Autopilot:

Tolerance (mN): Positive 5; Negative 5

Filter size: 5

Loop count: 1

Landing:

Distance: 1mm

Velocity: 1mm/sec

Blackbox:

Channels: Fx, Fz, AE, R1, T, Z1, Z2

Save every Nth reading: 100 (for 10mins) 1 for 10 secs

Carriage:

Constant force: -5mN

Duration: 10mins

Spindle:

Continuous

Velocity: 60 rev/min

Direction: Counter clockwise

Slider:

Velocity: Manual

Position: Idle Initial 20

Velocity: 10mm/sec

Appendix E
Friction test data file of UMT

Radius=20

Velocity=60

Set Force=-5

Duration=551.9

Entry Count=24225

Fx	Fz	T	Z	È	AE	R1	Ff	COF
mN	mN	sec	mm	rev	Volt	KOhm	MN	
0.066	0.147	48.83	12.477	-305.899	0.002	-0.024	0.066	0.449
0.198	0.189	48.84	12.477	-305.899	0.002	-0.024	0.198	1.048
-0.066	0.147	48.86	12.477	-305.899	0.007	-0.024	0.066	0.449
0.154	0.231	48.89	12.477	-305.899	0.007	-0.024	0.154	0.667
...	...	...	...	...	...	...	...	...
...	...	...	...	...	...	...	...	...
...	...	...	...	...	...	...	...	...
0.066	-5.01	600.66	13.3328	-455.923	0.007	-0.024	0.066	0.013
-0.154	-4.884	600.68	13.331	-455.93	0.007	-0.024	0.154	0.031
0.066	-4.842	600.7	13.331	-455.936	-0.012	-0.024	0.066	0.014